

University of Alberta

*The Role of FAT/CD36 in Regulating Fatty Acid Oxidation in the Heart*

by

*Michael Elliot Kuang*



A thesis submitted to the Faculty of Graduate Studies and Research in partial fulfillment of the requirements for the degree of Master of Science

Department of *Pediatrics*

Edmonton, Alberta

*Fall, 2004*



Library and  
Archives Canada

Bibliothèque et  
Archives Canada

Published Heritage  
Branch

Direction du  
Patrimoine de l'édition

395 Wellington Street  
Ottawa ON K1A 0N4  
Canada

395, rue Wellington  
Ottawa ON K1A 0N4  
Canada

*Your file* *Votre référence*  
*ISBN: 0-612-95787-X*  
*Our file* *Notre référence*  
*ISBN: 0-612-95787-X*

The author has granted a non-exclusive license allowing the Library and Archives Canada to reproduce, loan, distribute or sell copies of this thesis in microform, paper or electronic formats.

L'auteur a accordé une licence non exclusive permettant à la Bibliothèque et Archives Canada de reproduire, prêter, distribuer ou vendre des copies de cette thèse sous la forme de microfiche/film, de reproduction sur papier ou sur format électronique.

The author retains ownership of the copyright in this thesis. Neither the thesis nor substantial extracts from it may be printed or otherwise reproduced without the author's permission.

L'auteur conserve la propriété du droit d'auteur qui protège cette thèse. Ni la thèse ni des extraits substantiels de celle-ci ne doivent être imprimés ou autrement reproduits sans son autorisation.

---

In compliance with the Canadian Privacy Act some supporting forms may have been removed from this thesis.

Conformément à la loi canadienne sur la protection de la vie privée, quelques formulaires secondaires ont été enlevés de cette thèse.

While these forms may be included in the document page count, their removal does not represent any loss of content from the thesis.

Bien que ces formulaires aient inclus dans la pagination, il n'y aura aucun contenu manquant.

# Canada

## **Dedication**

I would like to dedicate this to my family who have always supported me. I could not have done this without you all, thanks for being there for me.

## **Acknowledgements**

I would like to thank my supervisor Jason for taking me as a graduate student and I hope that I did not disappoint him. I want to especially thank those who contributed directly to this work, Cory, Amy and Suzanne. Finally, I would like to thank the entire Dyck lab, Teresa, Anita, Karalyn, Anna and Carrie, for helping every step of the way, providing support and a lively and entertaining place to work. Thanks everyone.

# TABLE OF CONTENTS

---

<b>Chapter 1: Introduction</b>	<b>1</b>
Fatty Acid Metabolism in the Healthy Heart	4
Carbohydrate Metabolism in the Healthy Heart	5
Crosstalk between Fatty Acid and Carbohydrate Metabolism	7
Malonyl CoA Fuel Sensing & Signaling Mechanism	9
A) Acetyl CoA Carboxylase	9
B) AMP-Activated Protein kinase	11
C) Malonyl CoA Decarboxylase	12
Fatty Acid and Glucose Oxidation in the Ischemic Heart	14
Fatty Acid Transport	17
Fatty Acid Transporters	18
A) Fatty Acid Binding Protein	18
B) Fatty Acid Transport Protein	18
C) Fatty Acyl CoA Synthetase	19
D) FAT/CD36	20
Translocation of FAT/CD36	22
FAT/CD36: Role in Regulating Fatty Acid Oxidation	23
FAT/CD36: The New Frontier	25
References	27
<b>Chapter 2: Materials and Methods</b>	<b>45</b>
Heart Perfusion	46
Measurement of Cardiac Function	46
Glucose Oxidation Rates	47
Palmitate Oxidation Rates	47
Calculation of Tricarboxylic Acid Cycle Activity	48
Measurement of ATP Levels	48
Cell Culture	49
Measurement of Fatty Acid Oxidation in Neonatal Rat	
Cardiac Myocytes	49
Triglyceride Measurement	50
Lipid Extraction for Thin Layer Chromatography	51

Western Blot Analysis	51
Perchloric Acid Extraction of Acetyl CoA & Malonyl CoA	52
Cell Transfection	52
Mitochondrial Staining	53
Statistical Analysis	53
<b>Chapter 3: FAT/CD36 Deficiency does not Energetically or Functionally Compromise Hearts Prior to or Following Ischemia</b>	<b>55</b>
<b>Introduction</b>	<b>56</b>
<b>Hypothesis</b>	<b>58</b>
<b>Materials and Methods</b>	<b>58</b>
<b>Mice</b>	<b>58</b>
<b>Heart Perfusion</b>	<b>59</b>
<b>Measurement of Cardiac Function</b>	<b>59</b>
<b>Glucose Oxidation Rates</b>	<b>59</b>
<b>Fatty Acid Oxidation Rates</b>	<b>59</b>
<b>Calculation of Tricarboxylic Acid Cycle Activity</b>	<b>59</b>
<b>Measurement of ATP Levels</b>	<b>59</b>
<b>Statistical Analysis</b>	<b>59</b>
<b>Results</b>	<b>60</b>
<b>Fatty Acid Oxidation Rates in Hearts Perfused with         0.4 mM Palmitate</b>	<b>60</b>
<b>Fatty Acid Oxidation Rates in Hearts Perfused with         1.2 mM Palmitate</b>	<b>60</b>
<b>Effects of Ischemia in Wild type and FAT/CD36 Deficient         Hearts</b>	<b>61</b>
<b>Oxidation Rates in Ischemic Hearts Perfused with         1.2 mM Palmitate</b>	<b>62</b>
<b>Discussion</b>	<b>63</b>
<b>Conclusion</b>	<b>68</b>
<b>References</b>	<b>69</b>
<b>Chapter 4: The Role of FAT/CD36 Overexpression on Rates of Fatty Acid Oxidation</b>	<b>81</b>

<b>Introduction</b>	<b>82</b>
<b>Hypothesis</b>	<b>85</b>
<b>Materials and Methods</b>	<b>85</b>
<b>Cell Culture</b>	<b>85</b>
<b>Adenovirus Construction</b>	<b>85</b>
<b>Adenovirus Infection of Neonatal Rat Cardiac Myocytes</b>	<b>85</b>
<b>Measurement of Fatty Acid Oxidation in Neonatal Rat Cardiac Myocytes</b>	<b>86</b>
<b>Triglyceride Measurement</b>	<b>86</b>
<b>Lipid Extraction for Thin Layer Chromatography</b>	<b>86</b>
<b>Thin Layer Chromatography</b>	<b>87</b>
<b>Western Blot Analysis</b>	<b>87</b>
<b>Statistical Analysis</b>	<b>88</b>
<b>Results</b>	<b>88</b>
<b>FACS Infection of Neonatal Rat Cardiac Myocytes</b>	<b>88</b>
<b>FAT/CD36 Infection of Neonatal Rat Cardiac Myocytes</b>	<b>88</b>
<b>Fatty Acid Oxidation in the Neonatal Rat Cardiac Myocytes</b>	<b>89</b>
<b>Rates of Palmitate Incorporation into Triglyceride</b>	<b>89</b>
<b>Rates of Palmitate Incorporation into Lipids</b>	<b>90</b>
<b>Rates of Fatty Acid Uptake into Neonatal Rat Cardiac Myocytes</b>	<b>90</b>
<b>Measurement of Triglyceride Pool in Neonatal Rat Cardiac Myocytes</b>	<b>91</b>
<b>Rates of Palmitate Incorporation into Neonatal Rat Cardiac Myocytes</b>	<b>91</b>
<b>Discussion</b>	<b>91</b>
<b>Conclusion</b>	<b>94</b>
<b>References</b>	<b>95</b>
<b>Chapter 5: Investigating Altered Signaling Mechanisms in the FAT/CD36 Deficient Mouse</b>	<b>108</b>
<b>Introduction</b>	<b>109</b>
<b>Hypothesis</b>	<b>110</b>

<b>Materials and Methods</b>	<b>110</b>
<b>Western Blot Analysis</b>	<b>110</b>
<b>Perchloric Acid Extraction of Acetyl CoA &amp; Malonyl CoA</b>	<b>110</b>
<b>Statistical Analysis</b>	<b>111</b>
<b>Results</b>	<b>111</b>
<b>Phospho-AMPK (Thr172) Levels in Reperfused FAT/CD36 KO and Wildtype Mouse Hearts</b>	<b>111</b>
<b>ACC Levels in Reperfused FAT/CD36 KO and Wildtype Mouse Hearts</b>	<b>112</b>
<b>MCD Levels in Reperfused FAT/CD36 KO and Wildtype Mouse Hearts</b>	<b>112</b>
<b>Malonyl CoA Levels in Reperfused FAT/CD36 KO and Wildtype Mouse Hearts</b>	<b>112</b>
<b>Acetyl CoA Levels in Reperfused FAT/CD36 KO and Wildtype Mouse Hearts</b>	<b>113</b>
<b>Peroxisome proliferator-activated receptor alpha (PPAR<sub>α</sub>) levels in FAT/CD36 KO and wildtype mouse hearts</b>	<b>113</b>
<b>Discussion</b>	<b>114</b>
<b>Conclusion</b>	<b>116</b>
<b>References</b>	<b>118</b>

<b>Chapter 6: Development of a New Model to Study Localization and Translocation of FAT/CD36</b>	<b>126</b>
<b>Introduction</b>	<b>127</b>
<b>Hypothesis</b>	<b>128</b>
<b>Materials and Methods</b>	<b>129</b>
<b>Cell Culture</b>	<b>129</b>
<b>Construction of CD36/DsRed2 Fusion Protein</b>	<b>129</b>
<b>Cell Transfection</b>	<b>129</b>
<b>Mitochondrial Staining</b>	<b>130</b>
<b>Confocal Laser Scanning Microscopy</b>	<b>130</b>
<b>Results</b>	<b>130</b>
<b>Transfection with DsRed2</b>	<b>130</b>
<b>Translocation of FAT/CD36-DsRed2 in response to insulin and AMPK stimulation</b>	<b>130</b>
<b>Colocalization of FAT/CD36 with the mitochondria</b>	<b>131</b>

<b>Colocalization of FAT/CD36 with GLUT 4</b>	<b>131</b>
<b>Discussion</b>	<b>132</b>
<b>References</b>	<b>135</b>
<b>Chapter 7: Conclusions and Future Directions</b>	<b>143</b>
<b>References</b>	<b>148</b>

## LIST OF TABLES

---

<b>Table 1.</b> List of immunoblotting antibodies	<b>36</b>
<b>Table 1-1.</b> Cardiac function in FAT/CD36 KO mouse hearts aerobically perfused with low levels of fatty acids	<b>74</b>
<b>Table 1-2.</b> Cardiac function in FAT/CD36 KO mouse hearts aerobically perfused with high levels of fatty acids	<b>75</b>
<b>Table 1-3.</b> Cardiac function in FAT/CD36 KO mouse hearts aerobically perfused with high levels of fatty acids and reperfused following ischemia	<b>76</b>

## LIST OF FIGURES

---

<b>Figure 3-1.</b> Palmitate oxidation in FAT/CD36 knockout (KO) and wildtype mouse hearts perfused with 0.4 mM palmitate	77
<b>Figure 3-2.</b> Palmitate oxidation (A), glucose oxidation (B) and TCA acetyl-CoA production (C) for the tricarboxylic acid cycle in from FAT/CD36 knockout (KO) and wild type mouse hearts perfused with 1.2 mM palmitate	78
<b>Figure 3-3.</b> Cardiac work (A) and % recovery of cardiac work (B) in FAT/CD36 knockout (KO) and wild type hearts	79
<b>Figure 3-4.</b> Palmitate oxidation rates (A), glucose oxidation rates (B) and TCA acetyl-CoA production (C) in FAT/CD36 knockout (KO) and wild type mouse hearts during reperfusion after ischemia	80
<b>Figure 4-1.</b> Expression of FACS in neonatal rat cardiac myocytes infected with GFP or FACS virus	99
<b>Figure 4-2.</b> Expression of FAT/CD36 in neonatal rat cardiac myocytes infected with GFP or CD36 virus	100
<b>Figure 4-3.</b> The effect of time on rates of fatty acid oxidation in neonatal rat cardiac myocytes	101
<b>Figure 4-4.</b> Rates of palmitate oxidation in neonatal rat cardiac myocytes	102
<b>Figure 4-5.</b> Rates of palmitate incorporation into triglyceride in neonatal rat cardiac myocytes	103
<b>Figure 4-6.</b> Rates of palmitate incorporation into lipids in neonatal rat cardiac myocytes	104

<b>Figure 4-7.</b> Rates of palmitate uptake in neonatal rat cardiac myocytes	<b>105</b>
<b>Figure 4-8.</b> Total triglyceride levels in neonatal rat cardiac myocytes	<b>106</b>
<b>Figure 4-9.</b> Rates of palmitate incorporation in neonatal rat cardiac myocytes	<b>107</b>
<b>Figure 5-1.</b> Phospho-AMPK (Thr172) levels in reperfused FAT/CD36 KO and wildtype mouse hearts	<b>120</b>
<b>Figure 5-2.</b> Actin levels in reperfused FAT/CD36 KO and Wildtype mouse hearts	<b>121</b>
<b>Figure 5-3.</b> ACC levels in reperfused FAT/CD36 KO and wildtype mouse hearts	<b>122</b>
<b>Figure 5-4.</b> MCD levels in reperfused FAT/CD36 KO and wildtype mouse hearts	<b>123</b>
<b>Figure 5-5.</b> Malonyl CoA and acetyl CoA levels in reperfused FAT/CD36 KO and wildtype mouse hearts	<b>124</b>
<b>Figure 5-6.</b> Peroxisome proliferator-activated receptor alpha (PPAR <sub>α</sub> ) levels in MHC-PPAR and PPAR KO mouse hearts and FAT/CD36 KO and wildtype mouse hearts	<b>125</b>
<b>Figure 6-1.</b> Confocal images of DsRed2 transfection in COS-7 and neonatal rat cardiac myocytes	<b>137</b>
<b>Figure 6-2.</b> Confocal images of FAT/CD36-DsRed2 transfection in COS-7 cells and neonatal rat cardiac myocytes	<b>138</b>

<b>Figure 6-3.</b> Confocal images of FAT/CD36-DsRed2 transfection in COS-7 Cells and FAT/CD36 translocation with insulin	<b>138</b>
<b>Figure 6-4.</b> Confocal images of FAT/CD36-DsRed2 transfection in neonatal rat cardiac myocytes and FAT/CD36 translocation with AICAR	<b>139</b>
<b>Figure 6-5.</b> Confocal images of FAT/CD36-DsRed2 transfection in neonatal rat cardiac myocytes and colocalization with mitochondria	<b>140</b>
<b>Figure 6-6.</b> Confocal images of FAT/CD36-DsRed2 transfection in neonatal rat cardiac myocytes and colocalization with mitochondria	<b>141</b>
<b>Figure 6-7.</b> Confocal images of FAT/CD36-DsRed2 and GLUT4-GFP transfection in neonatal rat cardiac myocytes	<b>142</b>

# **Chapter 1**

## **Introduction**

## **Introduction**

According to the Heart and Stroke Foundation of Canada, cardiovascular disease accounts for the deaths of more Canadians than any other disease. In 1998 (the latest year for which Statistics Canada has data), cardiovascular disease accounted for 79,389 Canadian deaths. Approximately, 35% of all male deaths in Canada in 1998 were due to heart disease, diseases of the blood vessels and stroke. For women, the toll was even higher, 38% of all female deaths in 1998 were due to cardiovascular disease.

Cardiovascular disease also has a significant economic impact in Canada, as measured by direct and indirect costs. Direct costs include the cost of physicians and other professionals, hospital and nursing home services, the cost of medications, home health care and other medical durables. Indirect costs include lost productivity that results from illness and death. According to Health Canada (1997), in 1995, \$7.3 billion or 17% of the total direct costs of illness, was spent on cardiovascular disease. In the same year, approximately \$12.3 billion, or 14.5% of total indirect costs of all disease categories, was lost due to cardiovascular disease. This percentage is greater than the individual costs associated with injuries, cancer or respiratory diseases. Therefore, because of the aging population in the 21<sup>st</sup> century, cardiovascular disease will become a more prevalent health risk. Thus, studies done in order to understand the pathogenesis of the disease state are necessary in order to improve treatment and prevent disease.

One avenue of research that has been explored in the pathogenesis of heart disease is metabolic disturbances, which can often result in energy depletion. The heart relies on adenosine triphosphate (ATP) as an energy source to drive contractile function.

ATP is synthesized by the metabolism of mainly carbohydrates and fat, and hydrolyzed to release its chemical energy. ATP can be used for a variety of intracellular processes, with most of the ATP being used for contractile function in the heart. Since the heart exhibits a high rate of ATP hydrolysis, ATP must be synthesized readily in order to avoid depletion of intracellular stores of ATP<sup>1</sup>. The lack of ATP within the heart would ultimately lead to deficient cardiac function. Reduced blood flow to the peripheral tissues results in the entire body being deprived of essential nutrients and oxygen.

Recently, it has been suggested that alterations in substrate preference of the heart may adversely affect cardiac efficiency, thereby disturbing contractile function (see <sup>2,3,4</sup> for reviews). Specifically, an imbalance between fatty acid oxidation and glucose oxidation may cause or contribute to the pathogenesis of ischemic cardiomyopathy, heart failure, hypertrophy, and dilated cardiomyopathy. The importance of substrate utilization has been elucidated by a variety of approaches<sup>5-7</sup>, including the use of metabolic modulators, which increase the efficiency by which energy production is coupled to contractile work. Several studies using the perfused rat heart model have shown that inhibition of fatty acid oxidation and increased glucose oxidation can increase the recovery of the working heart post-ischemia<sup>8,9</sup>. This improvement in ischemic heart recovery is due to enhanced coupling between glycolysis and glucose oxidation, which decreases lactate production and improves function post-ischemia. Therefore, metabolic modulation can improve cardiac function in some cases of heart disease in humans.

## Fatty Acid Metabolism in the Healthy Heart

ATP hydrolysis is required for 2 main functions in the heart: 1) to maintain contractile work, 2) as an energy source for ion pumps, in order to maintain ionic balance<sup>10</sup>. Therefore, it is essential to maintain a constant supply of ATP in order to sustain a healthy heart. In the healthy heart, ATP is primarily derived from carbohydrate and fatty acid metabolism. Carbohydrates are metabolized to produce ATP via glycolysis and glucose oxidation, whereas approximately 60-70% of ATP generation is derived from fatty acid oxidation in the mitochondria<sup>11</sup>.

The heart readily takes up fatty acids from the plasma and can subsequently be oxidized to produce ATP or be converted and stored as triglycerides<sup>12</sup>. Since the heart has extremely high energy demands, approximately 80% of the fatty acids taken up by the heart are oxidized and the remaining 20% is stored as triglycerides<sup>13</sup>. The plasma concentration of fatty acids can dramatically affect rates of fatty acid oxidation in the perfused heart<sup>14</sup>. Studies conducted on the perfused mouse heart have shown that by increasing the palmitate concentration in the perfusion buffer (from 0.4 mM to 1.2 mM palmitate), rates of palmitate oxidation increase concurrently<sup>15</sup>. This suggests that fatty acid metabolism in the heart is partially concentration dependent.

Inside the cardiomyocytes, long chain fatty acids are esterified by long-chain fatty acyl-CoA synthetases to form long chain fatty acyl CoA<sup>16</sup>. In order for long chain fatty acyl CoA to enter the mitochondria, it must be acted on by 3 enzymes in the carnitine shuttle (see <sup>17</sup> for review). First, carnitine palmitoyltransferase 1 (CPT 1), which lies on the outer membrane of the mitochondria, catalyzes the conversion of acyl CoA to

acylcarnitine<sup>18</sup>. Second, within the compartment between the inner and outer mitochondrial membranes, acylcarnitine is transported into the mitochondrial matrix through the inner membrane by carnitine acylcarnitine translocase<sup>19</sup>. Third, carnitine palmitoyltransferase 2 regenerates acyl CoA by catalyzing the exchange of carnitine for CoA. The released carnitine is recycled back into the compartment between the inner and outer mitochondrial membranes via carnitine acylcarnitine translocase, which insures that a sufficient amount of carnitine is available as a substrate for CPT 1. Since pharmacological inhibition of CPT 1 results in significantly decreased rates of fatty acid oxidation, CPT 1 plays an important role in the regulation of fatty acid oxidation in the heart<sup>8,12</sup>.

Fatty acid oxidation takes place in the mitochondrial matrix, which produces one acetyl CoA, one FADH<sub>2</sub> and one NADH for every turn through the  $\beta$ -oxidation spiral. Every successive turn of the beta-oxidation spiral cleaves 2-carbons off the fatty acyl CoA, which are used to produce acetyl CoA. The acetyl CoA is further metabolized within the Krebs cycle to produce additional NADH and FADH<sub>2</sub>. The NADH and FADH<sub>2</sub> formed from beta-oxidation are used as reducing equivalents in the electron transport chain to produce ATP.

## **Carbohydrate Metabolism in the Healthy Heart**

In the healthy heart, approximately 15% of total ATP produced is derived from glycolysis, glucose oxidation and lactate oxidation<sup>20</sup>. As in the case with fatty acid oxidation, glucose oxidation produces acetyl CoA, which feeds the tricarboxylic acid

cycle and produces reducing equivalents which drive ATP production. Although the endpoint is the same, the mechanisms by which ATP is derived from carbohydrates are vastly different from fatty acid metabolism. The mechanisms involved in this process are outlined below.

It has been shown that uptake of glucose in the heart is dependent on the transmembrane glucose gradient and the abundance of glucose transporters on the plasma membrane<sup>21</sup>. Two isoforms of the glucose transporter family have been identified on the myocardium: GLUT 1 and GLUT 4<sup>22,23</sup>. On a cellular level, GLUT 4 is localized to intracellular microsomal vesicles, and is translocated from these organelles to the plasma membrane upon insulin stimulation or ischemia<sup>24</sup>. Therefore, glucose transport is mediated by insulin and signaling mechanisms during ischemia.

Within the cytosol of the cardiomyocyte, it has been shown that glucose is phosphorylated by hexokinase to glucose-6-phosphate<sup>25</sup>. Since glucose-6-phosphate is impermeable to the plasma membrane, the conversion of glucose to glucose-6-phosphate inhibits the passage of glucose out of the cell. Therefore, a constant concentration gradient for glucose uptake is produced. Glucose-6-phosphate can either be used for glycogen synthesis or can enter the glycolytic pathway to produce pyruvate (see <sup>26</sup> for a review). In order to enter the glycolytic pathway, glucose-6-phosphate must first be converted to fructose-6-phosphate and fructose-6-phosphate is subsequently phosphorylated by phosphofructokinase I<sup>27</sup>. From one molecule of glucose, glycolysis produces 2 NADH, 4 ATP and 2 pyruvate, the latter of which can enter the mitochondria and undergo oxidation.

A key regulatory step in glucose oxidation occurs via the pyruvate dehydrogenase complex (PDH)<sup>28</sup>. The active form of PDH metabolizes pyruvate (from the glycolytic pathway or lactate derived pyruvate) to acetyl CoA and NADH. The acetyl CoA from glucose oxidation can enter the TCA cycle and further produce reducing equivalents to produce ATP in the electron transport chain. The PDH complex is tightly regulated by PDH kinase, which inactivates PDH via phosphorylation, and is reactivated by the dephosphorylation action of PDH phosphatase<sup>29</sup>. Although both fatty acid and glucose metabolism produce ATP via alternate pathways, there are points where the pathways intersect, which play a role in determining substrate preference.

### **Cross-Talk Between Fatty Acid and Carbohydrate Metabolism**

As stated above, the majority of the ATP produced in the heart is derived from oxidation of fatty acids and glucose. Both pathways produce acetyl CoA, which can enter the TCA cycle and ultimately lead to the production of ATP. In fatty acid oxidation, acetyl CoA is derived from  $\beta$ -oxidation of fatty acids, whereas in glucose oxidation, pyruvate is converted into acetyl CoA by the action of the PDH complex. The contribution of these pathways to ATP production can vary dramatically, and depends on many factors, including substrate availability to the heart. In situations where plasma fatty acid concentration is high, such as during myocardial ischemia, the fatty acid metabolic pathway is able to inhibit carbohydrate metabolism. As described by Randle, increases in fatty acid oxidation can inhibit glucose oxidation by what is now known as the Randle Cycle<sup>30</sup>. The Randle Cycle involves, fatty acid derived acetyl CoA directly

inhibiting the PDH complex and stimulation of pyruvate dehydrogenase kinase, which results in phosphorylation and inhibition of the PDH complex. In the Krebs Cycle, fatty acid derived acetyl CoA is combined with oxaloacetate and converted into citrate, which has been suggested to be transported out of the mitochondria via the citrate transporter. Therefore, high rates of fatty acid metabolism can inhibit glycolysis, since citrate has been shown to inhibit phosphofructokinase<sup>31</sup>, resulting in an accumulation of glucose-6-phosphate and hexokinase inhibition. These steps ultimately result in decreased total glucose uptake. Together, the effects of high rates of fatty acid oxidation effectively inhibits glucose utilization in the heart.

Recent evidence has suggested that reciprocal regulation of fatty acid oxidation by glucose oxidation also exists, mainly through changes in cytosolic concentrations of malonyl CoA, an endogenous inhibitor of CPT 1<sup>32</sup>. Malonyl CoA is produced in the cytosol by acetyl CoA carboxylase, which catalyzes the carboxylation of acetyl CoA to malonyl CoA<sup>33</sup>. Therefore, high concentrations of acetyl CoA can drive the reaction that produces increased amounts of malonyl CoA, thereby inhibiting the flux of fatty acids through CPT 1. It has been shown that stimulation of PDH with dichloroacetate (DCA), an inhibitor of PDH kinase<sup>34</sup>, can lead to an inhibition of fatty acid oxidation<sup>35</sup>. This is due to the conversion of mitochondrial produced acetyl CoA to acetylcarnitine, its transport into the cytoplasm by carnitine acetyl transferase, and its reversion to acetyl CoA by cytosolic carnitine acetyl transferase (see <sup>26</sup> for review). The excess of acetyl CoA in the cytoplasm can be carboxylated by acetyl CoA carboxylase, therefore, producing large amounts of malonyl CoA which will inhibit fatty acid oxidation via increased inhibition of CPT 1. Crosstalk between these metabolic pathways ensure that

energy substrates presented to the heart will be metabolized and provides an energy sparing mechanism due to the inhibition of either fatty acid or glucose metabolism.

### **Malonyl CoA Fuel-Sensing and Signaling Mechanism**

In the liver, malonyl CoA is both an intermediate in *de novo* synthesis of fatty acids and an allosteric inhibitor of CPT 1, which regulates fatty acid transport into the mitochondria<sup>36</sup>. In skeletal and cardiac muscle, where synthesis of fatty acids is minimal<sup>37</sup>, the main role of malonyl CoA is to regulate fatty acid uptake into the mitochondria. Studies have shown that malonyl CoA levels in the muscle can change dramatically within short periods of time. When there is a high energy demand, such as during exercise<sup>38</sup> or contractions<sup>39</sup>, malonyl CoA levels are diminished within minutes or seconds in the rat model. Moreover, during times of increased fatty acid oxidation, such as during fasting, malonyl CoA levels have been shown to drop by 80%<sup>40</sup>. This would relieve the inhibition on CPT 1 and allow fatty acids to enter the mitochondria, thereby increasing fatty acid oxidation and energy production. Conversely, during times of decreased fatty acid oxidation, such as upon insulin administration, malonyl CoA levels can increase 2-6 fold within 20 min<sup>41</sup>. These rapid changes in malonyl CoA levels are due to its tight regulation by several metabolic enzymes involved fuel sensing and signaling.

#### **A) Acetyl CoA Carboxylase (ACC)**

Immunological analysis<sup>42</sup> and cDNA cloning<sup>43</sup> have revealed that ACC exists as two isoforms, ACC $\alpha$  (265 kDa) and ACC $\beta$  (280 kDa). Structurally, both isozymes exhibit the same catalytic domain, but distribution differs according to their function.

ACC $\alpha$  is dominant in lipogenic tissues<sup>44</sup>, whereas ACC $\beta$  predominates in oxidative tissues such as the heart and skeletal muscle. Immunofluorescent microscopic analysis has suggested that ACC $\beta$  is localized to the mitochondria, using its extended N-terminus domain as an anchor to the mitochondrial membrane<sup>45</sup>.

ACC catalyzes the carboxylation of acetyl CoA to malonyl CoA<sup>46</sup>. It is this reaction that is important in the oxidation of fatty acids. In soleus muscle extracted from ACC knockout mice, rates of fatty acid oxidation increased 30% above control muscle and were not decreased by insulin<sup>47</sup>. Moreover, studies conducted on ischemic perfused rat hearts have shown that ACC is an important regulator of fatty acid oxidation<sup>48,49</sup>. An early study by Winder demonstrated that the concentration of malonyl CoA diminishes in rat muscle during exercise<sup>50</sup>. Electrical stimulation of muscle has also shown that a decrease in malonyl CoA is associated with a decrease in ACC $\beta$  activity<sup>51</sup>.

The activity of ACC $\beta$  has been shown to be regulated by glucose and insulin<sup>46</sup>, which has been suggested to be controlled by cytosolic concentrations of citrate (see<sup>52</sup> for review). The hypothesis states that citrate, which is a metabolite of pyruvate metabolism in the mitochondria, is transported out of the mitochondria and into the cytosol via citrate/malate exchanger and can allosterically activate ACC $\beta$ . This provides a novel mechanism by which the cell is able to control substrate utilization in response to substrate availability. Activity of ACC has also been shown to be under phosphorylation control via AMPK, which provides another form of regulation by which malonyl CoA production and fatty acid oxidation are controlled.

## B) AMP-Activated Protein Kinase (AMPK)

AMPK is a heterotrimeric kinase which consists of  $\alpha$ ,  $\beta$  and  $\gamma$  subunits, each of which have at least two isoforms. The  $\alpha$  subunit is the catalytic domain, the  $\gamma$  subunit is the site of AMP binding, whereas the  $\beta$  subunit acts as a scaffold on which the other subunits reside (see <sup>53</sup> for review). AMPK was originally identified in the liver<sup>54</sup>, but has more recently been identified in the heart<sup>55</sup>, where the  $\alpha 2$ ,  $\beta 2$ ,  $\gamma 1$  and  $\gamma 2$  subunits dominate. Since the expression pattern varies between tissues, it has been suggested that the distribution of the subunit isoforms relates to varying tissue functions<sup>56</sup>.

AMPK exists in an active and an inactive form. In its inactive form, the regulatory region on the  $\alpha$ -subunit inhibits the catalytic site. Upon AMP binding, the auto-inhibitory interaction between the regulatory and kinase domain is removed<sup>57</sup>. Binding of AMP is important as AMP-bound AMPK is a better substrate for AMPK-kinase (AMPKK) which phosphorylates and increases AMPK activity 3-fold<sup>58</sup>. It has been shown that AMPKK phosphorylates AMPK on the Thr172 residue<sup>59</sup>. Moreover, the Thr172 site is required for activity, such that when the site is mutated, AMPK activity is almost completely abolished<sup>60</sup>. Therefore, phosphorylation at the Thr172 is indicative of AMPK activity.

AMPK is a kinase that is activated by AMP, which suggests that AMPK is sensitive to the energy status of the cell. In fact, AMPK has been shown to activate in response to an increase in the AMP/ATP or creatine/creatine phosphate ratios<sup>61</sup>. AMPK is an important determinant of cellular metabolic processes since it shuts down energy consuming process and stimulates pathways which produce energy<sup>57</sup>. As described above, the 2 main substrates of the heart are glucose and fatty acids, both of which have been shown to be regulated by AMPK. A study on rat papillary muscles has shown that

translocation of GLUT 4, independent of insulin signaling, can be induced by a non-specific AMPK activator AICAR (5-aminoimidazole-4-carboxamide-1- $\beta$ -D-ribofuranoside)<sup>62</sup>. The increase in AMPK activity was accompanied by an increase in glucose uptake and increased levels of GLUT 4 in the sarcolemmal membrane. Subsequent studies showed that AMPK activation also leads to increased rates of glycolysis, which was shown to be mediated via phosphorylation of PFK 2, a key step in glycolysis<sup>63</sup>. Taken together, these steps provide mechanisms by which AMPK is able to activate metabolic pathways in order to produce ATP.

The role of AMPK in the regulation of fatty acid oxidation arises through its effect on regulating malonyl CoA levels. As stated above, ACC is a key regulator of malonyl CoA in the heart, thus, its activity is a determinant of malonyl CoA levels in the myocyte. It has been shown from heart tissue that AMPK can phosphorylate both forms of purified ACC *in vitro* at Ser79<sup>64</sup>. This phosphorylation is accompanied with a decrease in ACC activity. Therefore, during times of energy demand in the heart, AMPK is able to phosphorylate and inhibit ACC, thereby decreasing malonyl CoA levels in the cytosol. This relieves the inhibition on CPT 1 and fatty acid oxidation is able to increase. Despite the importance of malonyl CoA production in the heart, malonyl CoA levels are also regulated by its degradation as well.

### C) Malonyl CoA Decarboxylase (MCD)

Malonyl CoA decarboxylase decarboxylates malonyl CoA, producing acetyl CoA<sup>65,66</sup>. Currently, there are two MCD isoforms that have been identified from the

goose uropygial gland<sup>67</sup>. In the mammal, MCD was originally characterized in the rat liver<sup>68</sup>, and has more recently been also identified in the heart<sup>69</sup> and skeletal muscle<sup>66</sup>. Early studies have shown that 80% of MCD activity resides in the mitochondria, suggesting that MCD was intramitochondrial<sup>70</sup>. This would suggest that MCD would have no role in regulating cytoplasmic levels of malonyl CoA. Recently, MCD has been shown to reside in peroxisomes<sup>71</sup> and the cytoplasm<sup>72</sup>. This localization would provide an efficient mechanism by which MCD could degrade the cytosolic malonyl CoA which is in close proximity to the mitochondrial CPT 1. This would allow rapid disinhibition of CPT 1 and thus, increase fatty acid oxidation to occur when necessary.

Since MCD degrades an endogenous inhibitor of CPT 1, it is likely that MCD plays an important role in regulating fatty acid oxidation. It has shown that there is a switch in metabolic substrate preference between 1-day and 7-day rabbit hearts<sup>73</sup>. Specifically, there is a switch from a glycolytic fetal heart to a more oxidative heart, reliant on fatty acids. A study by Dyck et al<sup>74</sup> has shown that MCD is more active in 7-day old rabbit hearts. This suggests that MCD degradation of malonyl CoA plays a role in the switch from a fetal heart to adult heart metabolism. Taken together, these data suggest that malonyl CoA decarboxylase is an important regulator of fatty acid oxidation<sup>75</sup>. Therefore, malonyl CoA levels can be altered in order to stimulate or inhibit pathways according to substrate availability. Metabolic pathways that produce ATP can also be altered during ischemia.

## Fatty Acid and Glucose Oxidation in the Ischemic Heart

Contractile work of the heart depends on a constant supply of ATP. Aerobic synthesis of ATP depends on myocardial blood flow, oxygen supply and mitochondrial oxidative phosphorylation (see <sup>76</sup> for review). Ischemia most frequently occurs in coronary artery disease patients with deficiencies in coronary flow during times of increased contractile demand, such as exercise (see <sup>77</sup> for review). This is due to the presence of vascular lesions, which limit blood flow to the heart. Therefore, pathological conditions which limit oxygen supply, blood flow or oxidative metabolism can lead to an imbalance between energy supply and energy demand, leading to cardiovascular dysfunction.

In a normal healthy heart, glycolysis and glucose oxidation are tightly coupled, where pyruvate from glycolysis is metabolized in the mitochondria to carbon dioxide, water and ATP. Under aerobic conditions, glycolysis only contributes 10% of total ATP production in the heart<sup>20</sup>. However, during ischemia, oxygen is limiting which impairs aerobic metabolism of energy substrates, resulting in an increase in anaerobic metabolism (glycolysis) to compensate for the decrease in total ATP production<sup>78</sup>. This leads to the uncoupling of glycolysis from glucose oxidation which results in an increase in proton production<sup>79</sup>, since the metabolism of glycolytically derived ATP produces excess protons. Moreover, pyruvate (from glycolysis) cannot be further metabolized in the mitochondria, and the accumulated pyruvate is converted into lactate in a reaction which also reoxidizes NADH to  $\text{NAD}^+ + \text{H}^+$ .

The accumulation of protons becomes problematic when the cardiac myocyte attempts to expel the excess protons via  $\text{Na}^+/\text{H}^+$  exchange<sup>80</sup>, leading to  $\text{Na}^+$  accumulation and subsequent  $\text{Ca}^{2+}$  accumulation via  $\text{Na}^+/\text{Ca}^{2+}$  exchange, which can lead to calcium overload<sup>80</sup> and cell death (see<sup>53</sup> for review). In addition, proton accumulation can also result in decreased efficiency of the contractile proteins<sup>81</sup> and decrease cardiac efficiency (cardiac work/myocardial  $\text{O}_2$  consumption)<sup>82</sup>. Thus, high rates of glycolysis are detrimental to the ischemic heart, as a further uncoupling of glycolysis from glucose oxidation can occur. Moreover, inhibition of glycolysis has been shown to be beneficial to the reperfused ischemic heart<sup>83</sup>.

Upon reperfusion of the ischemic heart, flow is restored which washes out the metabolic byproducts, such as protons and lactate. In addition, the reperfused heart exhibits alterations in metabolism which are detrimental to functional recovery. Specifically, fatty acid oxidation quickly recovers and becomes the dominant energy substrate that replenishes ATP<sup>9</sup>, but glucose oxidation remains suppressed due to increased inhibition of PDH by fatty acid oxidation derived acetyl CoA, as described by the Randle Cycle. Rates of glycolysis during reperfusion remain high, resulting in an uncoupling of glycolysis from glucose oxidation and proton production<sup>82</sup>. These protons exert a negative influence on contractile function as energy is diverted from contractile function to maintenance of ionic balance. Therefore, metabolic strategies have been proposed to increase the coupling between glycolysis and glucose oxidation, in order to alleviate injury during reperfusion of an ischemic heart.

Several metabolic therapies have been proposed for the treatment of ischemic heart disease. These therapies generally focus on either: 1) inhibiting myocardial fatty

acid oxidation, thereby increasing the glucose flux through PDH, or 2) activating PDH and increasing glucose oxidation (see <sup>26</sup> for review). Both strategies ultimately improve coupling of glucose oxidation to glycolysis and thus, decrease the accumulation of protons and lactate.

One approach to stimulate glucose oxidation is to directly activate PDH, the rate-limiting enzyme in glucose oxidation. Dichloroacetate (DCA) has been shown in several studies to increase glucose oxidation by inhibiting PDH kinase, thereby relieving inhibition on PDH<sup>84</sup>. Moreover, DCA has been shown to inhibit fatty acid oxidation, most likely through the shuttling of acetyl CoA out of the mitochondria, and into the cytoplasm where it is converted into malonyl CoA by acetyl CoA carboxylase<sup>78</sup>. Studies conducted on ischemic working rat hearts have shown that treatment with DCA during reperfusion can significantly improve functional recovery of the heart<sup>85</sup>.

One approach to alter substrate utilization by decreasing fatty acid oxidation is to inhibit the transport of fatty acid into the mitochondria. This can be effectively accomplished through inhibition of CPT 1, the key step in mitochondria fatty acid transport. There are several pharmacological inhibitors, such as etomoxir, oxfenicine and perhexiline that have been studied. Studies have shown that oxfenicine can improve functional recovery of the ischemic heart during reperfusion<sup>86,87</sup>, and this beneficial effect is due to altered preference of fatty acid oxidation to glucose oxidation<sup>87</sup>.

More recently, an antianginal agent, trimetazidine, has been shown to be effective in inhibiting fatty acid oxidation and increasing glucose oxidation<sup>88</sup>. Trimetazidine inhibits the fatty acid  $\beta$ -oxidation enzyme 3-keto-acyl-CoA thiolase (3-KAT), thereby inhibiting fatty acid oxidation, indirectly increasing glucose oxidation<sup>88</sup>.

In working rat hearts subjected to low-flow ischemia, trimetazidine treatment resulted in 210% increase in glucose oxidation, which was accompanied by a 37% increase in the amount of active PDH<sup>88</sup>. Therefore, the antianginal activity may be due to a switch in substrate preference from mainly fatty acids to glucose.

## **Fatty Acid Transport**

Although regulation of fatty acid oxidation can be controlled at the level of the mitochondria, the entry of fatty acids into the myocyte may also be a major regulator of fatty acid oxidation. Fatty acids have been shown to enter the cardiac myocyte by 2 mechanisms: 1) via simple diffusion across the membrane<sup>89,90</sup>, and 2) via a protein-mediated process<sup>91</sup>. It was previously thought that fatty acids traverse the plasma membrane by simple diffusion alone. Uptake studies conducted on adipocytes<sup>92</sup> and fibroblasts<sup>93</sup> have shown that the uptake process is saturable. In addition, palmitate transport studies in heart giant vesicles<sup>94</sup>, have also shown that the transport process is saturable. The heart giant vesicles are ideal for studying transport as these vesicles are devoid of metabolism, and rates of fatty acid transport can be measured without interference from metabolism. This suggests that fatty acid transport can be limited, even though a fatty acid gradient across the membrane is maintained. The limiting aspect of fatty acid transport could be explained by the presence of a protein-mediated component presumably since fatty acid binding sites on the transporter can become fully saturated. Moreover, pharmacological inhibition of carrier-mediated membrane proteins results in significant decreases in palmitate transport by heart giant vesicles<sup>94</sup>. Therefore, a protein-

mediated component may be necessary in the uptake of fatty acids within a variety of cell types.

## **Fatty Acid Transporters**

### **A) Fatty Acid Binding Protein (FABP)**

Long chain fatty acid transport has been shown to involve a 40 kDa plasma membrane fatty acid binding protein (FABPpm). The involvement of FABPpm in fatty acid transport was originally described in hepatocytes<sup>95</sup> and adipocytes<sup>96</sup>, and more recently in cardiac myocytes<sup>97</sup>. Although the specific role of FABPpm in fatty acid transport has not been elucidated, its expression has been correlated with the oxidative capacity of certain types of muscle<sup>98</sup>. Thus far, it has only been shown that FABPpm plays a role in sarcolemmal fatty acid flux, and that palmitate binding to skeletal muscle plasma membrane fractions correlates with presence of FABPpm<sup>99</sup>. Therefore, more work has to be done on elucidating the specific role of FABPpm and its cooperativity with other putative fatty acid transporters.

### **B) Fatty Acid Transport Protein (FATP)**

FATP1 was first identified in the mouse adipocyte<sup>100</sup>, and has subsequently identified in humans as a 71 kDa transmembrane protein<sup>101</sup> expressed in skeletal muscle

and heart<sup>102</sup>. Another isoform, FATP6, has been shown to be a heart-specific FATP, and is the predominant FATP in the heart<sup>103</sup>. Uptake studies conducted on HEK 293 cells expressing FATP6 have shown that expression levels of FATP6 correlates with an increase in fatty acid uptake<sup>103</sup>. The same study also showed that FATP6 also partially colocalizes with another proposed fatty acid transport protein, FAT/CD36, in the mouse heart. This suggests that FAT/CD36 and FATP6 may work cooperatively in transporting fatty acids into the cell. Interestingly, there is evidence which suggests that FATP is actually a very-long chain acyl CoA synthetase, suggesting that it is not directly involved in fatty acid transport<sup>104</sup>. Taken together, these data suggest that FATP plays an important role in lipid transport and suggest some cooperative aspect with FAT/CD36 and FATP.

### C) Fatty Acyl CoA Synthetase (FACS)

FACS catalyzes the conversion of free fatty acids to long-chain acyl CoA esters by the addition of a hydrophilic CoA head-group. Long-chain acyl CoA esters play a central role in fatty acid elongation and  $\beta$ -oxidation. Suzuki et al<sup>105</sup> have cloned FACS from the rat liver and demonstrated that FACS1 is present in the heart and skeletal muscle. Further analysis of FACS has shown that it is present in the vesicular structures, similar to those of GLUT-4. In addition, FACS has also been shown to associate with the adipocyte plasma membrane, which suggests that FACS may be able to translocate from intracellular vesicles to the plasma membrane<sup>106</sup>. Moreover, studies by Luiken et al have shown that FACS1 expression correlates with muscle with high oxidative capacity<sup>107</sup>.

Taken together, these studies suggest that FACS may play an important role in uptake of fatty acids in the cell.

#### D) FAT/CD36

CD36 was first identified as a platelet integral membrane glycoprotein that bound to thrombospondin, and was classified as a thrombospondin receptor<sup>108</sup>. Thrombospondins are a family of extracellular proteins that have a role in cell-cell interaction<sup>109</sup>, apoptosis<sup>109</sup>, cell adhesion<sup>110</sup>, angiogenesis<sup>111</sup> and signal transduction<sup>112</sup> (see <sup>113</sup> for review). More recently, CD36 has been found to bind to low density lipoproteins<sup>114</sup>, *Plasmodium falciparum* malaria-parasitized erythrocytes<sup>115</sup>, retinal photoreceptors<sup>116</sup> and most important to metabolism, long-chain fatty acids<sup>117</sup>. Based on the latter observation, it has been suggested that CD36 is a fatty acid transporter, and has thus been named fatty acid translocase (FAT)<sup>118</sup>. FAT/CD36 belongs to the class B scavenger receptor family, which also includes the receptor for selective cholesterol ester uptake, scavenger receptor class B type I (SR-B1) (see <sup>119</sup> for review). FAT/CD36 has an apparent molecular weight of 53 kDa, but since it is heavily glycosylated, the molecular weight increases to 88 kDa<sup>117</sup>. The heavy glycosylation is thought to protect FAT/CD36 from proteinase-rich environments, found in areas of inflammation. Moreover, it has been shown that mutations of the amino acids in the glycosylated regions of the SR-B1 have resulted in a marked reduction in lipid transport capability<sup>120</sup>, suggesting that post-translational modification may play a role in the function of FAT/CD36. Structurally, there are 2 hydrophobic regions on FAT/CD36, corresponding to transmembrane domains, one

on the carboxyl-terminal and the other on the N-terminal. Therefore, the predicted orientation projects FAT/CD36 mainly residing extracellularly, with 2 short intracellular domains (see <sup>119</sup> for review).

FAT/CD36 has been identified in various tissues such as, adipocytes, platelets, skeletal muscle, intestine and the heart (see <sup>119</sup> for review). On a cellular level, FAT/CD36 colocalizes with caveolin in specialized plasma membrane microdomains known as caveolae<sup>121</sup>. These lipids structures are known scaffolds of concentrated signal transduction mediators, suggesting that FAT/CD36 may play a role in signal transduction. In fact, it has been shown that Src-related protein tyrosine kinases are physically associated with the surface antigen FAT/CD36 in human dermal microvascular endothelial cells<sup>112</sup>. In addition, FAT/CD36 is physically associated with the Fyn, Lyn, and Yes protein-tyrosine kinases in human platelets<sup>122</sup>, although these signaling cascades have not been identified in the heart.

In skeletal muscle, FAT/CD36 has been found to localize to intracellular microsomal vesicles<sup>123</sup> and caveolae membrane domains in the plasma membrane<sup>121</sup> which is homologous to the distribution of the glucose transporter GLUT 4<sup>124</sup>. Therefore it has been suggested that FAT/CD36 may colocalize with GLUT 4 in intracellular compartments and share similar cellular machinery involved in their recruitment to the plasma membrane. Interestingly, studies in skeletal muscle have shown that insulin stimulates the translocation of both FAT/CD36 and GLUT 4 from intracellular microsomes to the plasma membrane<sup>124</sup> (discussed below). Although it may be reasonable to propose that FAT/CD36 and GLUT 4 are colocalized in intracellular compartments, it has been demonstrated that FAT/CD36 and GLUT4 are not localized

together in skeletal muscle<sup>125</sup>. Due to this controversy, the question of whether FAT/CD36 and GLUT 4 are colocalized in the microsomal compartment remains unanswered.

### **Translocation of FAT/CD36**

It has been shown in studies using cardiac myocytes that GLUT 4 translocates from small tubulo-vesicular elements to the sarcolemmal membrane upon insulin stimulation<sup>126</sup>. Interestingly, studies have shown that FAT/CD36 is able to translocate from the intracellular compartments to the plasma membrane upon insulin stimulation<sup>124</sup>, exercise<sup>127</sup> and contraction<sup>128</sup>, in cardiac myocytes. This suggests a novel mechanism by which insulin may be able to regulate fatty acid uptake and oxidation. Insulin is generally thought to decrease fatty acid oxidation by increasing the amount of malonyl CoA in the cytosol of the cell<sup>129</sup>. Therefore, a decrease in the rate of fatty acid oxidation accompanied by an increase in fatty acid uptake, upon insulin stimulation, may provide a mechanism by which fatty acids are shuttled to triglyceride production and storage. This increase in triglyceride production could become detrimental to the heart, as triglyceride accumulation has been associated with a lipotoxic cardiomyopathy<sup>130</sup>. Interestingly, a more recent study showed that triglyceride production may protect against fatty acid-induced lipotoxicity in cultured cell lines<sup>131</sup>. This protection has been proposed to be due to channeling of free fatty acids away from an apoptotic-pathway, and towards inert triglyceride storage<sup>131</sup>. Therefore, controversy exists as to whether an increase in triglyceride formation would be beneficial or detrimental to the heart.

Luiken et al<sup>128</sup> demonstrated in cardiac myocytes that electrical stimulation also resulted in translocation of FAT/CD36 from the intracellular compartment to the plasma membrane. Interestingly, the increase in palmitate uptake by insulin treatment and electrical stimulation were additive, which suggests that there are two distinct pools of FAT/CD36, both of which are able to translocate to the membrane upon different stimuli<sup>123</sup>. Moreover, the stimulation induced increase in palmitate uptake, via FAT/CD36 translocation, is not inhibited by wortmannin, whereas the insulin induced uptake is decreased to basal levels, confirming that the effect of insulin is phosphatidylinositol-3 (PI-3) kinase dependent. On the other hand, contraction induced stimulation of FAT/CD36 translocation was shown to be mediated by AMPK<sup>128</sup>, which would suggest that the heart may be attempting to increase fatty acid metabolism during times of increased energy demand. In addition, AMPK-mediated translocation of FAT/CD36 suggests that the translocation process may be under phosphorylation control, although the direct mechanism has yet to be elucidated.

### **FAT/CD36: Role in Regulating Fatty Acid Oxidation**

The role of FAT/CD36 in fatty acid transport was uncovered mainly through studies conducted using the FAT/CD36 knockout (KO) mouse<sup>92</sup>. The FAT/CD36 KO mice contain a mutated allele, which exhibits a deletion of 30 amino acids which code for the N-terminal transmembrane domain of FAT/CD36. Therefore, the FAT/CD36 gene is effectively knocked out. Early studies examining palmitate transport into adipocytes from the FAT/CD36 KO mice showed that knockout mice exhibited lower levels of palmitate

uptake, as compared to wildtype (WT) adipocytes. Moreover, plasma analysis from FAT/CD36 KO and WT mice showed that FAT/CD36 KO mice exhibited significantly higher levels of plasma triglycerides and cholesterol<sup>92</sup>. The higher levels of plasma triglyceride are a consequence of decreased fatty acid uptake into tissues, since higher levels of fatty acid will be presented to the liver, resulting in increased plasma triglyceride. This suggests that FAT/CD36 is essential in the uptake of fatty acids and deficiency results in impaired fatty acid transport. Subsequent studies were conducted in order to examine fatty acid metabolism.

In order to examine further the role of FAT/CD36 in fatty acid transport and metabolism, transgenic mice overexpressing FAT/CD36 in muscle were generated<sup>132</sup>. Palmitate oxidation rates in perfused soleus muscle from the transgenic mice were significantly elevated compared to WT controls<sup>132</sup>. Contrasting the characteristics of the FAT/CD36 KO mouse, the FAT/CD36 overexpressor exhibited significantly lower levels of plasma triglycerides. This suggests that the increase in the expression of FAT/CD36 results in higher levels of fatty acid uptake from the plasma. These studies provide evidence for the importance of FAT/CD36 in fatty acid transport in adipocytes and skeletal muscle.

Studies have also been conducted investigating the role of FAT/CD36 in fatty acid oxidation in isolated adult rat cardiac myocytes. A study by Luiken et al<sup>133</sup> measured palmitate oxidation, in the presence or absence of sulfo-N-succinimidylolate (SSO), in quiescent and electrostimulated cardiac myocytes. SSO is a fatty acid derivative that specifically covalently modifies FAT/CD36, thereby disrupting its transport capability. Electrostimulation of the cardiac myocytes significantly increases palmitate oxidation,

with a parallel increase in palmitate transport, which is due to an increase in metabolic demand in response to increased contractile work<sup>133</sup>. Upon incubation with SSO, both quiescent and electrostimulated myocytes exhibited palmitate oxidation rates significantly below controls<sup>133</sup>, suggesting that contraction-induced increase in fatty acid uptake is FAT/CD36 mediated. This also suggests that FAT/CD36 may be rate-limiting in fatty acid oxidation. Before studies performed for this thesis, the role of FAT/CD36 in fatty acid oxidation in the intact working heart was unknown. Moreover, whether decreased rates of fatty acid oxidation in the working heart result in increased susceptibility to ischemic injury was unknown.

### **FAT/CD36: The New Frontier**

Although progress has been made to characterize FAT/CD36, there are many avenues of research that remain. It has been shown in several studies that FAT/CD36 is important in regulating uptake of fatty acids into various cell types<sup>94,133,134</sup>, but the role of FAT/CD36 in regulating fatty acid oxidation in the isolated working heart is unknown. Moreover, the question of whether the FAT/CD36 KO hearts are energetically compromised, suggesting that decreased rates of fatty acid oxidation in the working heart result in increased susceptibility to ischemic injury, has not been examined.

Investigation into alterations in signaling mechanisms involving energy metabolism in the FAT/CD36 KO mouse needs to be examined. Since AMPK, ACC and MCD all have been shown to be important in regulating fatty acid oxidation through malonyl CoA, it is not know whether FAT/CD36 deficient animals exhibit changes in

these metabolic proteins. It is possible that there is an upregulation in the expression of AMPK and ACC and a decrease in MCD expression, which would lead to a decrease in malonyl CoA levels that would be able to compensate for a hypothetical decrease in fatty acid oxidation rate due to diminished fatty acid uptake. This would be especially important in an ischemic heart, where inhibition of fatty acid oxidation has been shown to be beneficial to functional recovery<sup>8</sup>.

Further characterization of the function of FAT/CD36 is required. Although FAT/CD36 overexpression study has been conducted<sup>132</sup>, this study does not elucidate the role of FAT/CD36 expression alone, since other proteins involved in fatty acid transport, such as FACS, are present in the adult mouse. This is important since the hypothesis of whether FAT/CD36 and FACS cooperate in order to transport fatty acids across the membrane has been proposed. Therefore, a model where only FAT/CD36 and FACS are present in high levels must be used in order address this hypothesis.

The translocation of FAT/CD36, upon insulin and AMPK stimulation, has been studied by the use of membrane fractionation<sup>124,128</sup>, but the process has not been visualized or characterized. Therefore, an improved model is required in order to further examine the translocation process.

## References

1. Taegtmeyer H, King LM, Jones BE. Energy substrate metabolism, myocardial ischemia, and targets for pharmacotherapy. *Am J Cardiol.* 1998;82:54K-60K.
2. Lopaschuk GD, Rebeyka IM, Allard MF. Metabolic modulation: a means to mend a broken heart. *Circulation.* 2002;105:140-2.
3. Stanley WC, Chandler MP. Energy metabolism in the normal and failing heart: potential for therapeutic interventions. *Heart Fail Rev.* 2002;7:115-30.
4. Stanley WC. Introduction to special issue on myocardial energy metabolism in heart failure. *Heart Fail Rev.* 2002;7:113.
5. Haneda T, Ganz W, Burnam MH, Katz J. Metabolic effects of glucose-insulin-potassium in the ischemic myocardium. *Jpn Heart J.* 1978;19:376-82.
6. Broderick TL, Currie RW, Paulson DJ. Heat stress induces rapid recovery of mechanical function of ischemic fatty acid perfused hearts by stimulating glucose oxidation during reperfusion. *Can J Physiol Pharmacol.* 1997;75:1273-9.
7. Schaefer S, Ramasamy R. Glycogen utilization and ischemic injury in the isolated rat heart. *Cardiovasc Res.* 1997;35:90-8.
8. Lopaschuk GD, Wall SR, Olley PM, Davies NJ. Etomoxir, a carnitine palmitoyltransferase I inhibitor, protects hearts from fatty acid-induced ischemic injury independent of changes in long chain acylcarnitine. *Circ Res.* 1988;63:1036-43.
9. Lopaschuk GD, Saddik M. The relative contribution of glucose and fatty acids to ATP production in hearts reperfused following ischemia. *Mol Cell Biochem.* 1992;116:111-6.

10. Suga H. Ventricular energetics. *Physiol Rev.* 1990;70:247-77.
11. Saddik M, Lopaschuk GD. Myocardial triglyceride turnover and contribution to energy substrate utilization in isolated working rat hearts. *J Biol Chem.* 1991;266:8162-70.
12. Lopaschuk GD, Belke DD, Gamble J, Itoi T, Schonekess BO. Regulation of fatty acid oxidation in the mammalian heart in health and disease. *Biochim Biophys Acta.* 1994;1213:263-76.
13. Wisneski JA, Gertz EW, Neese RA, Mayr M. Myocardial metabolism of free fatty acids. Studies with <sup>14</sup>C-labeled substrates in humans. *J Clin Invest.* 1987;79:359-66.
14. Oram JF, Bennetch SL, Neely JR. Regulation of fatty acid utilization in isolated perfused rat hearts. *J Biol Chem.* 1973;248:5299-309.
15. Belke DD, Larsen TS, Lopaschuk GD, Severson DL. Glucose and fatty acid metabolism in the isolated working mouse heart. *Am J Physiol.* 1999;277:R1210-7.
16. Kornberg A, Pricer WE, Jr. Enzymatic synthesis of the coenzyme A derivatives of long chain fatty acids. *J Biol Chem.* 1953;204:329-43.
17. Calvani M, Reda E, Arrigoni-Martelli E. Regulation by carnitine of myocardial fatty acid and carbohydrate metabolism under normal and pathological conditions. *Basic Res Cardiol.* 2000;95:75-83.
18. Pande SV. A mitochondrial carnitine acylcarnitine translocase system. *Proc Natl Acad Sci U S A.* 1975;72:883-7.

19. Ramsay RR. The role of carnitine, the carnitine acyltransferases and the carnitine-exchange system [proceedings]. *Biochem Soc Trans.* 1978;6:72-6.
20. Itoi T, Lopaschuk GD. The contribution of glycolysis, glucose oxidation, lactate oxidation, and fatty acid oxidation to ATP production in isolated biventricular working hearts from 2-week-old rabbits. *Pediatr Res.* 1993;34:735-41.
21. Zaninetti D, Greco-Perotto R, Jeanrenaud B. Heart glucose transport and transporters in rat heart: regulation by insulin, workload and glucose. *Diabetologia.* 1988;31:108-13.
22. Doria-Medina CL, Lund DD, Pasley A, Sandra A, Sivitz WI. Immunolocalization of GLUT-1 glucose transporter in rat skeletal muscle and in normal and hypoxic cardiac tissue. *Am J Physiol.* 1993;265:E454-64.
23. Studelska DR, Campbell C, Pang S, Rodnick KJ, James DE. Developmental expression of insulin-regulatable glucose transporter GLUT-4. *Am J Physiol.* 1992;263:E102-6.
24. Sun D, Nguyen N, DeGrado TR, Schwaiger M, Brosius FC, 3rd. Ischemia induces translocation of the insulin-responsive glucose transporter GLUT4 to the plasma membrane of cardiac myocytes. *Circulation.* 1994;89:793-8.
25. Manchester J, Kong X, Nerbonne J, Lowry OH, Lawrence JC, Jr. Glucose transport and phosphorylation in single cardiac myocytes: rate-limiting steps in glucose metabolism. *Am J Physiol.* 1994;266:E326-33.
26. Stanley WC, Lopaschuk GD, Hall JL, McCormack JG. Regulation of myocardial carbohydrate metabolism under normal and ischaemic conditions. Potential for pharmacological interventions. *Cardiovasc Res.* 1997;33:243-57.

27. Beitner R, Haberman S, Cycowitz T. The effect of cyclic GMP on phosphofructokinase from rat tissues. *Biochim Biophys Acta*. 1977;482:330-40.
28. Hiltunen JK, Hassinen IE. Energy-linked regulation of glucose and pyruvate oxidation in isolated perfused rat heart. Role of pyruvate dehydrogenase. *Biochim Biophys Acta*. 1976;440:377-90.
29. Pettit FH, Pelley JW, Reed LJ. Regulation of pyruvate dehydrogenase kinase and phosphatase by acetyl-CoA/CoA and NADH/NAD ratios. *Biochem Biophys Res Commun*. 1975;65:575-82.
30. Randle PJ, Garland PB, Hales CN, Newsholme EA. The glucose fatty-acid cycle. Its role in insulin sensitivity and the metabolic disturbances of diabetes mellitus. *Lancet*. 1963;1:785-9.
31. Garland PB, Randle PJ, Newsholme EA. Citrate as an Intermediary in the Inhibition of Phosphofructokinase in Rat Heart Muscle by Fatty Acids, Ketone Bodies, Pyruvate, Diabetes, and Starvation. *Nature*. 1963;200:169-70.
32. Mills SE, Foster DW, McGarry JD. Interaction of malonyl-CoA and related compounds with mitochondria from different rat tissues. Relationship between ligand binding and inhibition of carnitine palmitoyltransferase I. *Biochem J*. 1983;214:83-91.
33. Wolpert JS, Ernst-Fonberg ML. A multienzyme complex for CO<sub>2</sub> fixation. *Biochemistry*. 1975;14:1095-102.
34. Browning M, Baudry M, Bennett WF, Lynch G. Phosphorylation-mediated changes in pyruvate dehydrogenase activity influence pyruvate-supported calcium accumulation by brain mitochondria. *J Neurochem*. 1981;36:1932-40.

35. Man KC, Brosnan JT. Inhibition of medium and short-chain fatty acid oxidation in rat heart mitochondria by dichloroacetate. *Metabolism*. 1982;31:744-8.
36. McGarry JD, Leatherman GF, Foster DW. Carnitine palmitoyltransferase I. The site of inhibition of hepatic fatty acid oxidation by malonyl-CoA. *J Biol Chem*. 1978;253:4128-36.
37. Awan MM, Saggerson ED. Malonyl-CoA metabolism in cardiac myocytes and its relevance to the control of fatty acid oxidation. *Biochem J*. 1993;295 ( Pt 1):61-6.
38. Winder WW, Arogyasami J, Barton RJ, Elayan IM, Vehrs PR. Muscle malonyl-CoA decreases during exercise. *J Appl Physiol*. 1989;67:2230-3.
39. Odland LM, Heigenhauser GJ, Lopaschuk GD, Spriet LL. Human skeletal muscle malonyl-CoA at rest and during prolonged submaximal exercise. *Am J Physiol*. 1996;270:E541-4.
40. McGarry JD, Mills SE, Long CS, Foster DW. Observations on the affinity for carnitine, and malonyl-CoA sensitivity, of carnitine palmitoyltransferase I in animal and human tissues. Demonstration of the presence of malonyl-CoA in non-hepatic tissues of the rat. *Biochem J*. 1983;214:21-8.
41. Saha AK, Kurowski TG, Ruderman NB. A malonyl-CoA fuel-sensing mechanism in muscle: effects of insulin, glucose, and denervation. *Am J Physiol*. 1995;269:E283-9.
42. Bianchi A, Evans JL, Iverson AJ, Nordlund AC, Watts TD, Witters LA. Identification of an isozymic form of acetyl-CoA carboxylase. *J Biol Chem*. 1990;265:1502-9.

43. Ahmad F, Ahmad PM, Pieretti L, Watters GT. Purification and subunit structure of rat mammary gland acetyl coenzyme A carboxylase. *J Biol Chem.* 1978;253:1733-7.
44. Kim KH. Regulation of mammalian acetyl-coenzyme A carboxylase. *Annu Rev Nutr.* 1997;17:77-99.
45. Abu-Elheiga L, Brinkley WR, Zhong L, Chirala SS, Woldegiorgis G, Wakil SJ. The subcellular localization of acetyl-CoA carboxylase 2. *Proc Natl Acad Sci U S A.* 2000;97:1444-9.
46. Hardie DG. Regulation of fatty acid synthesis via phosphorylation of acetyl-CoA carboxylase. *Prog Lipid Res.* 1989;28:117-46.
47. Abu-Elheiga L, Matzuk MM, Abo-Hashema KA, Wakil SJ. Continuous fatty acid oxidation and reduced fat storage in mice lacking acetyl-CoA carboxylase 2. *Science.* 2001;291:2613-6.
48. Kudo N, Barr AJ, Barr RL, Desai S, Lopaschuk GD. High rates of fatty acid oxidation during reperfusion of ischemic hearts are associated with a decrease in malonyl-CoA levels due to an increase in 5'-AMP-activated protein kinase inhibition of acetyl-CoA carboxylase. *J Biol Chem.* 1995;270:17513-20.
49. Saddik M, Gamble J, Witters LA, Lopaschuk GD. Acetyl-CoA carboxylase regulation of fatty acid oxidation in the heart. *J Biol Chem.* 1993;268:25836-45.
50. Winder WW, Arogyasami J, Elayan IM, Cartmill D. Time course of exercise-induced decline in malonyl-CoA in different muscle types. *Am J Physiol.* 1990;259:E266-71.

51. Duan C, Winder WW. Nerve stimulation decreases malonyl-CoA in skeletal muscle. *J Appl Physiol*. 1992;72:901-4.
52. Ruderman NB, Saha AK, Vavvas D, Witters LA. Malonyl-CoA, fuel sensing, and insulin resistance. *Am J Physiol*. 1999;276:E1-E18.
53. Sambandam N, Lopaschuk GD. AMP-activated protein kinase (AMPK) control of fatty acid and glucose metabolism in the ischemic heart. *Prog Lipid Res*. 2003;42:238-56.
54. Witters LA, Kemp BE. Insulin activation of acetyl-CoA carboxylase accompanied by inhibition of the 5'-AMP-activated protein kinase. *J Biol Chem*. 1992;267:2864-7.
55. Kudo N, Gillespie JG, Kung L, Witters LA, Schulz R, Clanachan AS, Lopaschuk GD. Characterization of 5'AMP-activated protein kinase activity in the heart and its role in inhibiting acetyl-CoA carboxylase during reperfusion following ischemia. *Biochim Biophys Acta*. 1996;1301:67-75.
56. Stapleton D, Mitchelhill KI, Gao G, Widmer J, Michell BJ, Teh T, House CM, Fernandez CS, Cox T, Witters LA, Kemp BE. Mammalian AMP-activated protein kinase subfamily. *J Biol Chem*. 1996;271:611-4.
57. Hardie DG, Hawley SA. AMP-activated protein kinase: the energy charge hypothesis revisited. *Bioessays*. 2001;23:1112-9.
58. Hawley SA, Selbert MA, Goldstein EG, Edelman AM, Carling D, Hardie DG. 5'-AMP activates the AMP-activated protein kinase cascade, and Ca<sup>2+</sup>/calmodulin activates the calmodulin-dependent protein kinase I cascade, via three independent mechanisms. *J Biol Chem*. 1995;270:27186-91.

59. Hawley SA, Davison M, Woods A, Davies SP, Beri RK, Carling D, Hardie DG. Characterization of the AMP-activated protein kinase kinase from rat liver and identification of threonine 172 as the major site at which it phosphorylates AMP-activated protein kinase. *J Biol Chem.* 1996;271:27879-87.
60. Stein SC, Woods A, Jones NA, Davison MD, Carling D. The regulation of AMP-activated protein kinase by phosphorylation. *Biochem J.* 2000;345 Pt 3:437-43.
61. Ponticos M, Lu QL, Morgan JE, Hardie DG, Partridge TA, Carling D. Dual regulation of the AMP-activated protein kinase provides a novel mechanism for the control of creatine kinase in skeletal muscle. *Embo J.* 1998;17:1688-99.
62. Russell RR, 3rd, Bergeron R, Shulman GI, Young LH. Translocation of myocardial GLUT-4 and increased glucose uptake through activation of AMPK by AICAR. *Am J Physiol.* 1999;277:H643-9.
63. Marsin AS, Bertrand L, Rider MH, Deprez J, Beauloye C, Vincent MF, Van den Berghe G, Carling D, Hue L. Phosphorylation and activation of heart PFK-2 by AMPK has a role in the stimulation of glycolysis during ischaemia. *Curr Biol.* 2000;10:1247-55.
64. Dyck JR, Kudo N, Barr AJ, Davies SP, Hardie DG, Lopaschuk GD. Phosphorylation control of cardiac acetyl-CoA carboxylase by cAMP-dependent protein kinase and 5'-AMP activated protein kinase. *Eur J Biochem.* 1999;262:184-90.
65. Kim YS, Kolattukudy PE. Purification and properties of malonyl-CoA decarboxylase from rat liver mitochondria and its immunological comparison

- with the enzymes from rat brain, heart, and mammary gland. *Arch Biochem Biophys*. 1978;190:234-46.
66. Alam N, Saggerson ED. Malonyl-CoA and the regulation of fatty acid oxidation in soleus muscle. *Biochem J*. 1998;334 ( Pt 1):233-41.
67. Courchesne-Smith C, Jang SH, Shi Q, DeWille J, Sasaki G, Kolattukudy PE. Cytoplasmic accumulation of a normally mitochondrial malonyl-CoA decarboxylase by the use of an alternate transcription start site. *Arch Biochem Biophys*. 1992;298:576-86.
68. Dyck JR, Berthiaume LG, Thomas PD, Kantor PF, Barr AJ, Barr R, Singh D, Hopkins TA, Voilley N, Prentki M, Lopaschuk GD. Characterization of rat liver malonyl-CoA decarboxylase and the study of its role in regulating fatty acid metabolism. *Biochem J*. 2000;350 Pt 2:599-608.
69. Goodwin GW, Taegtmeier H. Regulation of fatty acid oxidation of the heart by MCD and ACC during contractile stimulation. *Am J Physiol*. 1999;277:E772-7.
70. Kim YS, Kolattukudy PE. Malonyl-CoA decarboxylase from the mammary gland of lactating rat. Purification, properties and subcellular localization. *Biochim Biophys Acta*. 1978;531:187-96.
71. FitzPatrick DR, Hill A, Tolmie JL, Thorburn DR, Christodoulou J. The molecular basis of malonyl-CoA decarboxylase deficiency. *Am J Hum Genet*. 1999;65:318-26.
72. Sacksteder KA, Morrell JC, Wanders RJ, Matalon R, Gould SJ. MCD encodes peroxisomal and cytoplasmic forms of malonyl-CoA decarboxylase and is

- mutated in malonyl-CoA decarboxylase deficiency. *J Biol Chem.* 1999;274:24461-8.
73. Lopaschuk GD, Witters LA, Itoi T, Barr R, Barr A. Acetyl-CoA carboxylase involvement in the rapid maturation of fatty acid oxidation in the newborn rabbit heart. *J Biol Chem.* 1994;269:25871-8.
74. Dyck JR, Barr AJ, Barr RL, Kolattukudy PE, Lopaschuk GD. Characterization of cardiac malonyl-CoA decarboxylase and its putative role in regulating fatty acid oxidation. *Am J Physiol.* 1998;275:H2122-9.
75. Dyck JR, Cheng JF, Stanley WC, Barr R, Chandler MP, Brown S, Wallace D, Arrhenius T, Harmon C, Yang G, Nadzan AM, Lopaschuk GD. Malonyl Coenzyme A Decarboxylase Inhibition Protects the Ischemic Heart by Inhibiting Fatty Acid Oxidation and Stimulating Glucose Oxidation. *Circ Res.* 2004.
76. Brown GC. Control of respiration and ATP synthesis in mammalian mitochondria and cells. *Biochem J.* 1992;284 ( Pt 1):1-13.
77. Arvind K, Pradeepa R, Deepa R, Mohan V. Diabetes & coronary artery disease. *Indian J Med Res.* 2002;116:163-76.
78. Lopaschuk GD, Wambolt RB, Barr RL. An imbalance between glycolysis and glucose oxidation is a possible explanation for the detrimental effects of high levels of fatty acids during aerobic reperfusion of ischemic hearts. *J Pharmacol Exp Ther.* 1993;264:135-44.
79. Liu Q, Docherty JC, Rendell JC, Clanachan AS, Lopaschuk GD. High levels of fatty acids delay the recovery of intracellular pH and cardiac efficiency in post-

- ischemic hearts by inhibiting glucose oxidation. *J Am Coll Cardiol.* 2002;39:718-25.
80. Tani M, Neely JR. Role of intracellular Na<sup>+</sup> in Ca<sup>2+</sup> overload and depressed recovery of ventricular function of reperfused ischemic rat hearts. Possible involvement of H<sup>+</sup>-Na<sup>+</sup> and Na<sup>+</sup>-Ca<sup>2+</sup> exchange. *Circ Res.* 1989;65:1045-56.
81. Parsons B, Szczesna D, Zhao J, Van Slooten G, Kerrick WG, Putkey JA, Potter JD. The effect of pH on the Ca<sup>2+</sup> affinity of the Ca<sup>2+</sup> regulatory sites of skeletal and cardiac troponin C in skinned muscle fibres. *J Muscle Res Cell Motil.* 1997;18:599-609.
82. Liu B, Clanachan AS, Schulz R, Lopaschuk GD. Cardiac efficiency is improved after ischemia by altering both the source and fate of protons. *Circ Res.* 1996;79:940-8.
83. Finegan BA, Lopaschuk GD, Gandhi M, Clanachan AS. Inhibition of glycolysis and enhanced mechanical function of working rat hearts as a result of adenosine A1 receptor stimulation during reperfusion following ischaemia. *Br J Pharmacol.* 1996;118:355-63.
84. Baudry M, Kessler M, Smith EK, Lynch G. The regulation of pyruvate dehydrogenase activity in rat hippocampal slices: effect of dichloroacetate. *Neurosci Lett.* 1982;31:41-6.
85. McVeigh JJ, Lopaschuk GD. Dichloroacetate stimulation of glucose oxidation improves recovery of ischemic rat hearts. *Am J Physiol.* 1990;259:H1079-85.

86. Molaparast-Saless F, Liedtke AJ, Nellis SH. Effects of the fatty acid blocking agents, oxfenicine and 4-bromocrotonic acid, on performance in aerobic and ischemic myocardium. *J Mol Cell Cardiol.* 1987;19:509-20.
87. Higgins AJ, Morville M, Burges RA, Gardiner DG, Page MG, Blackburn KJ. Oxfenicine diverts rat muscle metabolism from fatty acid to carbohydrate oxidation and protects the ischaemic rat heart. *Life Sci.* 1980;27:963-70.
88. Kantor PF, Lucien A, Kozak R, Lopaschuk GD. The antianginal drug trimetazidine shifts cardiac energy metabolism from fatty acid oxidation to glucose oxidation by inhibiting mitochondrial long-chain 3-ketoacyl coenzyme A thiolase. *Circ Res.* 2000;86:580-8.
89. Storch J, Bass NM. Transfer of fluorescent fatty acids from liver and heart fatty acid-binding proteins to model membranes. *J Biol Chem.* 1990;265:7827-31.
90. DeGrella RF, Light RJ. Uptake of fatty acids by isolated heart myocytes. *Basic Res Cardiol.* 1985;80 Suppl 2:107-10.
91. Luiken JJ, Glatz JF, Bonen A. Fatty acid transport proteins facilitate fatty acid uptake in skeletal muscle. *Can J Appl Physiol.* 2000;25:333-52.
92. Febbraio M, Abumrad NA, Hajjar DP, Sharma K, Cheng W, Pearce SF, Silverstein RL. A null mutation in murine CD36 reveals an important role in fatty acid and lipoprotein metabolism. *J Biol Chem.* 1999;274:19055-62.
93. Ibrahimi A, Sfeir Z, Magharaie H, Amri EZ, Grimaldi P, Abumrad NA. Expression of the CD36 homolog (FAT) in fibroblast cells: effects on fatty acid transport. *Proc Natl Acad Sci U S A.* 1996;93:2646-51.

94. Luiken JJ, Turcotte LP, Bonen A. Protein-mediated palmitate uptake and expression of fatty acid transport proteins in heart giant vesicles. *J Lipid Res.* 1999;40:1007-16.
95. Stremmel W, Berk PD. Hepatocellular influx of [14C]oleate reflects membrane transport rather than intracellular metabolism or binding. *Proc Natl Acad Sci U S A.* 1986;83:3086-90.
96. Abumrad NA, Perkins RC, Park JH, Park CR. Mechanism of long chain fatty acid permeation in the isolated adipocyte. *J Biol Chem.* 1981;256:9183-91.
97. Sorrentino D, Stump D, Potter BJ, Robinson RB, White R, Kiang CL, Berk PD. Oleate uptake by cardiac myocytes is carrier mediated and involves a 40-kD plasma membrane fatty acid binding protein similar to that in liver, adipose tissue, and gut. *J Clin Invest.* 1988;82:928-35.
98. Bonen A, Luiken JJ, Liu S, Dyck DJ, Kiens B, Kristiansen S, Turcotte LP, Van Der Vusse GJ, Glatz JF. Palmitate transport and fatty acid transporters in red and white muscles. *Am J Physiol.* 1998;275:E471-8.
99. Turcotte LP, Swenberger JR, Tucker MZ, Yee AJ, Trump G, Luiken JJ, Bonen A. Muscle palmitate uptake and binding are saturable and inhibited by antibodies to FABP(PM). *Mol Cell Biochem.* 2000;210:53-63.
100. Schaffer JE, Lodish HF. Expression cloning and characterization of a novel adipocyte long chain fatty acid transport protein. *Cell.* 1994;79:427-36.
101. Hirsch D, Stahl A, Lodish HF. A family of fatty acid transporters conserved from mycobacterium to man. *Proc Natl Acad Sci U S A.* 1998;95:8625-9.

102. Van Nieuwenhoven FA, Willemsen PH, Van der Vusse GJ, Glatz JF. Co-expression in rat heart and skeletal muscle of four genes coding for proteins implicated in long-chain fatty acid uptake. *Int J Biochem Cell Biol.* 1999;31:489-98.
103. Gimeno RE, Ortegon AM, Patel S, Punreddy S, Ge P, Sun Y, Lodish HF, Stahl A. Characterization of a heart-specific fatty acid transport protein. *J Biol Chem.* 2003;278:16039-44.
104. Coe NR, Smith AJ, Frohnert BI, Watkins PA, Bernlohr DA. The fatty acid transport protein (FATP1) is a very long chain acyl-CoA synthetase. *J Biol Chem.* 1999;274:36300-4.
105. Suzuki H, Kawarabayasi Y, Kondo J, Abe T, Nishikawa K, Kimura S, Hashimoto T, Yamamoto T. Structure and regulation of rat long-chain acyl-CoA synthetase. *J Biol Chem.* 1990;265:8681-5.
106. Gargiulo CE, Stuhlsatz-Krouper SM, Schaffer JE. Localization of adipocyte long-chain fatty acyl-CoA synthetase at the plasma membrane. *J Lipid Res.* 1999;40:881-92.
107. Luiken JJ, Han XX, Dyck DJ, Bonen A. Coordinately regulated expression of FAT/CD36 and FACS1 in rat skeletal muscle. *Mol Cell Biochem.* 2001;223:61-9.
108. Asch AS, Barnwell J, Silverstein RL, Nachman RL. Isolation of the thrombospondin membrane receptor. *J Clin Invest.* 1987;79:1054-61.
109. Friedl P, Vischer P, Freyberg MA. The role of thrombospondin-1 in apoptosis. *Cell Mol Life Sci.* 2002;59:1347-57.

110. Roberts DD, Sherwood JA, Spitalnik SL, Panton LJ, Howard RJ, Dixit VM, Frazier WA, Miller LH, Ginsburg V. Thrombospondin binds falciparum malaria parasitized erythrocytes and may mediate cytoadherence. *Nature*. 1985;318:64-6.
111. Taraboletti G, Roberts D, Liotta LA, Giavazzi R. Platelet thrombospondin modulates endothelial cell adhesion, motility, and growth: a potential angiogenesis regulatory factor. *J Cell Biol*. 1990;111:765-72.
112. Bull HA, Brickell PM, Dowd PM. Src-related protein tyrosine kinases are physically associated with the surface antigen CD36 in human dermal microvascular endothelial cells. *FEBS Lett*. 1994;351:41-4.
113. Chen H, Herndon ME, Lawler J. The cell biology of thrombospondin-1. *Matrix Biol*. 2000;19:597-614.
114. Endemann G, Stanton LW, Madden KS, Bryant CM, White RT, Protter AA. CD36 is a receptor for oxidized low density lipoprotein. *J Biol Chem*. 1993;268:11811-6.
115. Ockenhouse CF, Tandon NN, Magowan C, Jamieson GA, Chulay JD. Identification of a platelet membrane glycoprotein as a falciparum malaria sequestration receptor. *Science*. 1989;243:1469-71.
116. Ryeom SW, Sparrow JR, Silverstein RL. CD36 participates in the phagocytosis of rod outer segments by retinal pigment epithelium. *J Cell Sci*. 1996;109 ( Pt 2):387-95.
117. Harmon CM, Abumrad NA. Binding of sulfosuccinimidyl fatty acids to adipocyte membrane proteins: isolation and amino-terminal sequence of an 88-kD protein implicated in transport of long-chain fatty acids. *J Membr Biol*. 1993;133:43-9.

118. Sfeir Z, Ibrahimi A, Amri E, Grimaldi P, Abumrad N. Regulation of FAT/CD36 gene expression: further evidence in support of a role of the protein in fatty acid binding/transport. *Prostaglandins Leukot Essent Fatty Acids*. 1997;57:17-21.
119. Febbraio M, Hajjar DP, Silverstein RL. CD36: a class B scavenger receptor involved in angiogenesis, atherosclerosis, inflammation, and lipid metabolism. *J Clin Invest*. 2001;108:785-91.
120. Vinals M, Xu S, Vasile E, Krieger M. Identification of the N-linked glycosylation sites on the high density lipoprotein (HDL) receptor SR-BI and assessment of their effects on HDL binding and selective lipid uptake. *J Biol Chem*. 2003;278:5325-32.
121. Lisanti MP, Scherer PE, Vidugiriene J, Tang Z, Hermanowski-Vosatka A, Tu YH, Cook RF, Sargiacomo M. Characterization of caveolin-rich membrane domains isolated from an endothelial-rich source: implications for human disease. *J Cell Biol*. 1994;126:111-26.
122. Huang MM, Bolen JB, Barnwell JW, Shattil SJ, Brugge JS. Membrane glycoprotein IV (CD36) is physically associated with the Fyn, Lyn, and Yes protein-tyrosine kinases in human platelets. *Proc Natl Acad Sci U S A*. 1991;88:7844-8.
123. Luiken JJ, Koonen DP, Willems J, Zorzano A, Becker C, Fischer Y, Tandon NN, Van Der Vusse GJ, Bonen A, Glatz JF. Insulin stimulates long-chain fatty acid utilization by rat cardiac myocytes through cellular redistribution of FAT/CD36. *Diabetes*. 2002;51:3113-9.

124. Luiken JJ, Dyck DJ, Han XX, Tandon NN, Arumugam Y, Glatz JF, Bonen A. Insulin induces the translocation of the fatty acid transporter FAT/CD36 to the plasma membrane. *Am J Physiol Endocrinol Metab.* 2002;282:E491-5.
125. Muller H, Deckers K, Eckel J. The fatty acid translocase (FAT)/CD36 and the glucose transporter GLUT4 are localized in different cellular compartments in rat cardiac muscle. *Biochem Biophys Res Commun.* 2002;293:665-9.
126. Slot JW, Geuze HJ, Gigengack S, James DE, Lienhard GE. Translocation of the glucose transporter GLUT4 in cardiac myocytes of the rat. *Proc Natl Acad Sci U S A.* 1991;88:7815-9.
127. Glatz JF, Bonen A, Luiken JJ. Exercise and insulin increase muscle fatty acid uptake by recruiting putative fatty acid transporters to the sarcolemma. *Curr Opin Clin Nutr Metab Care.* 2002;5:365-70.
128. Luiken JJ, Coort SL, Willems J, Coumans WA, Bonen A, van der Vusse GJ, Glatz JF. Contraction-induced fatty acid translocase/CD36 translocation in rat cardiac myocytes is mediated through AMP-activated protein kinase signaling. *Diabetes.* 2003;52:1627-34.
129. Gamble J, Lopaschuk GD. Insulin inhibition of 5' adenosine monophosphate-activated protein kinase in the heart results in activation of acetyl coenzyme A carboxylase and inhibition of fatty acid oxidation. *Metabolism.* 1997;46:1270-4.
130. Chiu HC, Kovacs A, Ford DA, Hsu FF, Garcia R, Herrero P, Saffitz JE, Schaffer JE. A novel mouse model of lipotoxic cardiomyopathy. *J Clin Invest.* 2001;107:813-22.

131. Listenberger LL, Han X, Lewis SE, Cases S, Farese RV, Jr., Ory DS, Schaffer JE. Triglyceride accumulation protects against fatty acid-induced lipotoxicity. *Proc Natl Acad Sci U S A*. 2003;100:3077-82.
132. Ibrahim A, Bonen A, Blinn WD, Hajri T, Li X, Zhong K, Cameron R, Abumrad NA. Muscle-specific overexpression of FAT/CD36 enhances fatty acid oxidation by contracting muscle, reduces plasma triglycerides and fatty acids, and increases plasma glucose and insulin. *J Biol Chem*. 1999;274:26761-6.
133. Luiken JJ, Willems J, van der Vusse GJ, Glatz JF. Electrostimulation enhances FAT/CD36-mediated long-chain fatty acid uptake by isolated rat cardiac myocytes. *Am J Physiol Endocrinol Metab*. 2001;281:E704-12.
134. Coburn CT, Knapp FF, Jr., Febbraio M, Beets AL, Silverstein RL, Abumrad NA. Defective uptake and utilization of long chain fatty acids in muscle and adipose tissues of CD36 knockout mice. *J Biol Chem*. 2000;275:32523-9.
135. Larsen TS, Belke DD, Sas R, Giles WR, Severson DL, Lopaschuk GD, Tyberg JV. The isolated working mouse heart: methodological considerations. *Pflugers Arch*. 1999;437:979-85.

## **Chapter 2**

### **Materials and Methods**

*Heart Perfusions-* Hearts from wild type and FAT/CD36 KO male mice, 10-12 weeks of age, were perfused in the working mode as described. Briefly, mice were anesthetized with 12 mg intraperitoneal injection of pentobarbitol sodium. Hearts were then excised and immediately immersed in ice cold Krebs-Henseleit bicarbonate solution containing 118.5 mM NaCl, 25 mM NaHCO<sub>3</sub>, 4.7 mM KCl, 1.2 mM MgSO<sub>4</sub>, 1.2 mM KH<sub>2</sub>PO<sub>4</sub>, 2.5 mM CaCl<sub>2</sub>, 0.5 mM EDTA, 5 mM [U-<sup>14</sup>C]glucose and either 0.4 mM or 1.2 mM [9, 10-<sup>3</sup>H] palmitate prebound to 3% fatty acid free bovine serum albumin, and 100 μU/mL insulin. The aorta was then cannulated and was subject to a Langendorff perfusion (at 60 mmHg) for 10 min. Upon cannulation of the pulmonary vein, the heart was switched from the Langendorff to the working mode. The left atrium was perfused at a preload pressure of 11.5 mmHg, and afterload was set at 50 mmHg. A 2.5 mL sample of perfusate was taken every 10 min. Hearts were either perfused aerobically for 30 min or aerobically for 30 min and then were subjected to 18 min of global no-flow ischemia followed by 40 min of aerobic reperfusion. At the end of the experiment, hearts were frozen in liquid nitrogen and stored at -80 °C.

*Measurement of Cardiac Function-* Heart rate and pressure measurements were recorded using a pressure transducer in the aortic outflow line (Harvard Apparatus). Data were collected using an MP100 system from AcqKnowledge (BIOPAC Systems, Inc.). Cardiac output and aortic flows were obtained by measuring the flow into the left atria and from the afterload line using Transonic flow probes. Cardiac work was calculated as the product of peak systolic pressure and cardiac output. Coronary flow was calculated from the difference of the cardiac output and aortic flows. Frozen hearts were powdered

and ~20 mg (wet weight) were dried at 60 °C overnight to remove all water (dry weight). The ratio of this sample (dry/wet weight) was used to calculate the total dry mass of the heart.

*Glucose Oxidation Rates-* Glucose oxidation rates were determined by measuring  $^{14}\text{CO}_2$  released from the metabolism of [U- $^{14}$ ]glucose, as described <sup>135</sup>. Briefly, released  $^{14}\text{CO}_2$  was trapped using 1 M hyamine hydroxide, and collected by continuously bubbling outflow gases from the perfusion apparatus through 15 mL of hyamine hydroxide. A 300  $\mu\text{L}$  sample of hyamine hydroxide was taken every 10 min. The  $^{14}\text{CO}_2$  trapped in the perfusion buffer was released by the addition of 9 N  $\text{H}_2\text{SO}_4$  to 1 ml of perfusion buffer in sealed test tubes. The flasks were shaken overnight and the released  $^{14}\text{CO}_2$  was trapped by the center well containing 300  $\mu\text{L}$  of hyamine hydroxide. Hyamine hydroxide samples were counted using CytoScint® scintillation cocktail (ICN). Total  $^{14}\text{CO}_2$  production was calculated by adding the values for  $^{14}\text{CO}_2$  obtained from the outflow gas and from the perfusion buffer.

*Palmitate Oxidation Rates-* Palmitate oxidation rates were measured from the release of  $^3\text{H}_2\text{O}$ , derived from the metabolism of [9, 10-  $^3\text{H}$ ]palmitate, as described <sup>135</sup>. Briefly,  $^3\text{H}_2\text{O}$  was separated from 9,10- $^3\text{H}$ ]palmitate by mixing 0.5 ml of the perfusion buffer samples with 1.88 ml of a 1:2 vol/vol ratio of chloroform and methanol. Next, 0.625 ml of chloroform was added, followed by the addition of 0.625 ml of 1.1 M KCl, dissolved in 0.9 M HCl. Samples were allowed to separate into polar and non-polar phases and the polar phase was removed. The polar phase was mixed with 1 ml chloroform, 1 ml

methanol, 0.9 ml of KCl:HCl mixture. Again, the polar and non-polar phases were allowed to form and a 0.5 ml aliquot of the polar phase was removed and counted for  $^3\text{H}$ .

*Calculation of Tricarboxylic Acid Cycle (TCA) Activity-* Contribution of both glucose and palmitate oxidation to the TCA cycle was calculated as the product of the respective rates of oxidation and the amount of acetyl-CoA derived from glucose and palmitate, respectively. A value of 2 acetyl CoA per molecule of glucose oxidized and 8 acetyl CoA per molecule of palmitate oxidized was used.

*Measurement of ATP Levels-* Frozen mouse heart tissue (20 mg) was homogenized in a 6% perchloric acid/0.5 mM EGTA solution. The homogenate was incubated on ice for 10 min and centrifuged at  $10000 \cdot g$  for 2 min. The supernatant was collected and ATP concentrations were determined by HPLC. Separation was performed on a Beckman System Gold with a UV detector 167. Each sample was run through a precolumn cartridge and a microsorb short-one column. A gradient was set up using buffer A, consisting of 0.2 M  $\text{NaH}_2\text{PO}_4$ , pH 5.0, and buffer B, consisting of 0.25 M  $\text{NaH}_2\text{PO}_4$  and acetonitrile, pH 5.0, at a ratio of 80:20 (v/v). Both buffers were filtered using Nylon-66 filter membrane (Pierce). Buffers were initially mixed at 97% buffer A and 3% buffer B and maintained for 2.5 min, and changed to 18% B for 5 min. The gradient was changed to 37% buffer B for 3 min and to 90% buffer B for 17 min. At 42 min, buffer B was returned to 3% over 0.5 min and at 50 min, equilibration was completed. Peaks were integrated by Beckman System Gold.

*Cell Culture.* Hearts from 2-day old neonatal rat pups were isolated and placed in ice-cold 1 x phosphate buffered saline (PBS) solution. After repeated rinsing, the atria were removed and the ventricles were minced with scissors. The minced tissue was washed 3 times in ice cold PBS solution and then placed in a T-25 cm<sup>2</sup> tissue culture flask containing 19.5 mL ice cold PBS, 0.025% DNase (w/v), 0.1% collagenase (w/v) and 0.05% trypsin (w/v). The tissue was digested on a rotary shaker at 37 ° C for 20 min. After digesting, the tissue was centrifuged at 114 x g for 1 min at 4 ° C in 20 mL of DF20 media, 20% fetal bovine serum and 50 µg/mL gentamicin. The supernatant was discarded and the pellet was subsequently digested with DNase/collagenase/trypsin buffer for an additional 20 min at 37 ° C. After the second digestion, 20 mL of DF20 media was added to the tissue and centrifuged at 114 x g for 1 min at 4 ° C. This step was repeated once more. After the final digestion, all the supernatant fractions were pooled and centrifuged at 300 x g for 7 min at 4 ° C. The resulting pellet was resuspended in 10 mL of plating media (DF20 media, 5% fetal bovine serum, 10% horse serum and 50 µg/mL gentamicin) and incubated at 37 ° C in a T-75 cm<sup>2</sup> flask for 60 min. After 60 min the supernatant was removed and placed into another T-75 cm<sup>2</sup> flask and incubated for another 60 min at 37 ° C. After serial plating, the resulting pellet was resuspended in plating media and plated in 35 mm<sup>2</sup> primaria dishes (Falcon) at a density of  $1.8 \times 10^6$  cells/plate.

*Measurement of Fatty Acid Oxidation in Rat Neonatal Cardiac Myocytes.* After 48 hrs of incubation, fatty acid oxidation rates were measured in isolated neonatal rat cardiac myocytes. Media of the myocytes was changed to a Krebs-Henseleit bicarbonate solution

containing 118.5 mM NaCl, 25 mM NaHCO<sub>3</sub>, 4.7 mM KCl, 1.2 mM MgSO<sub>4</sub>, 1.2 mM KH<sub>2</sub>PO<sub>4</sub>, 2.5 mM CaCl<sub>2</sub>, 0.5 mM EDTA, and 1.2 mM [9, 10- <sup>3</sup>H] palmitate prebound to 3% fatty acid free bovine serum albumin, which was also supplemented with L-carnitine (0.25 mM). Cardiac myocytes were incubated for 3 hrs at 37 ° C. After 3 hrs, 200 μL of the labeled media aliquoted into an eppendorff tube, placed in a scintillation vial. The scintillation vials, containing both the labeled media and eppendorff tube, was incubated for 24 hrs at 50 ° C. After 24 hrs, the eppendorff tube was removed from the scintillation vial and the latter was counted. The remaining media from the cardiac myocytes was removed and cells were scraped in 120 μL of buffer containing 20mM Tris-HCL, pH 7.4, 50mM NaCl, 50 mM NaF, 5mM Na pyrophosphate, 0.25 M sucrose, protease inhibitor cocktail #1 (Sigma P8340), phosphatase inhibitor cocktail (Sigma P2850) and 1M DTT. Cell lysates were sonicated and centrifuged for 8 min at 1000 x g in order to remove cell debris. The supernatant was aliquoted, frozen with liquid nitrogen and stored at -80 ° C. A protein assay (BioRad) was conducted on the cell lysates to determine protein content of the samples.

*Triglyceride Measurements.* Cardiac myocyte homogenates from fatty acid oxidation measurements were used to examine triglyceride content in the cells. Cell homogenates were assayed using the L-Type TG H kit (WAKO). Briefly, 80 μL of Enzyme Color A was added to 10 μL sample and mixed. The mixture was incubated for 5 min, then, Enzyme Color B was added to the mixture, followed by a 5 min incubation. Absorbance of the samples and standards were measured at 600/700 nm. Total triglyceride content was expressed as μg of triglyceride per μg of total protein.

*Lipid Extraction for Thin Layer Chromatography.* 90  $\mu\text{L}$  samples were taken from cardiac myocyte cell homogenates from fatty acid oxidation assay and aliquoted into glass tubes. 1 mL of methanol was added to the sample, followed by 500  $\mu\text{L}$  of chloroform. If the mixed sample was not monophasic, than methanol was added drop wise until sample was one phase. Next, 500  $\mu\text{L}$  of 1 M NaCl, which was slightly acidified with acetic acid, was added, followed by 1 mL of chloroform. This resulted in a biphasic sample consisting of organic and aqueous phases. The samples were centrifuged at 1000 rpm for 5 min to further separate the phases. After centrifugation, the organic phase (bottom) was collected carefully, without contamination from the upper aqueous phase, and the extraction protocol was repeated on the aqueous phase to further extract the lipids. The two organic phases were pooled in a glass tube and dried under a stream of  $\text{N}_2$ . The dried residue was dissolved in 200  $\mu\text{L}$  of 2:1 chloroform:methanol.

*Western Blot Analysis.* Heart tissue was homogenized in buffer containing 20 mM Tris-HCL, pH 7.4, 50 mM NaCl, 50 mM NaF, 5 mM Na pyrophosphate, 0.25 M sucrose, protease inhibitor cocktail #1 (Sigma P8340), phosphatase inhibitor cocktail (Sigma P2850) and 1M DTT. Protein was separated using SDS-PAGE and transferred to nitrocellulose membranes. Membranes were blocked with 5% milk in Tris-buffered-saline solution containing 0.1% Tween (TBST). Membranes were incubated with an antibody against the protein of interest, washed 3-times with TBST, then incubated with a secondary antibody (Santa Cruz biotechnologies) conjugated to horseradish peroxidase and washed 3-times TBST. Signals were visualized using the ECL detection system

(Amersham). Densitometric scans were taken with the GS-800 scanner and analyzed with Quantity One software.

*PCA Extraction of Acetyl CoA and Malonyl CoA.* Approximately 25 mg of powdered heart tissue from ischemic FAT/CD36 KO and wildtype mice were weighed out into cryovials. The heart tissue was transferred to Dounce homogenizers and homogenized in 6% perchloric acid. The homogenate was centrifuged at 3500 RPM for 10 min at 4°C. The samples were then analyzed with HPLC. Separation was performed on a Beckman System Gold with a UV detector 167. Each sample was run through a precolumn cartridge and a microsorb short-one column. A gradient was set up using buffer A, consisting of 0.2 M NaH<sub>2</sub>PO<sub>4</sub>, pH 5.0, and buffer B, consisting of 0.25 M NaH<sub>2</sub>PO<sub>4</sub> and acetonitrile, pH 5.0, at a ratio of 80:20 (v/v). Both buffers were filtered using Nylon-66 filter membrane (Pierce). Buffers were initially mixed at 97% buffer A and 3% buffer B and maintained for 2.5 min, and changed to 18% B for 5 min. The gradient was changed to 37% buffer B for 3 min and to 90% buffer B for 17 min. At 42 min, buffer B was returned to 3% over 0.5 min and at 50 min, equilibration was completed. Peaks were integrated by Beckman System Gold.

*Cell Transfection.* Both COS-7 cells and neonatal rat cardiac myocytes were used in transfection experiments. COS-7 cells were maintained in DMEM supplemented with 10% fetal bovine serum and cardiomyocytes were maintained in DMEM supplemented with insulin-transferrin-sodium selenite media supplement (ITS) (SIGMA) and AraC (SIGMA). COS-7 cells were transfected with 1 µg CD36/DsRed2 DNA using 3 µL

FuGENE 6 (ROCHE) and cardiomyocytes were transfected with 2 µg CD36/DsRed2 DNA using 6 µL FuGENE 6 according to the manufacturer's instructions. Cells were incubated in the transfection medium for 24 hours, after which medium was changed and cells were incubated for 24 hours in serum free medium.

*Mitochondrial Staining.* For cardiac myocyte staining, MitoTracker Green was diluted to a working concentration of 25 nM in 1 mL of prewarmed serum free DMEM. Neonatal rat cardiac myocytes were incubated for 30 min with the stain and replaced with prewarmed serum free DMEM after incubation.

*Statistical Analysis-* Data is expressed as mean  $\pm$  S.E. Comparisons between wild type and FAT/CD36 deficient hearts were performed using the unpaired Student's two-tailed t-test. Differences were judged to be significant when  $p < 0.05$ . When more than two groups were being analyzed, an unpaired ANOVA was conducted with a Student-Newmann-Keuls post test. Differences were judged to be significant when  $p < 0.05$ .

**Table 1. Immunblotting Protocol**

Protein	[1° Ab]	Incubation in 1° Ab (at 4 ° C)	[2° Ab]	Incubation in 2° Ab
CD36	1:5000	Overnight	GAM 1:2000	1 hour
Streptavidin labelled peroxidase	1:500	Overnight	Not required	Not required
MCD	1:1000	Overnight	GAR 1:2000	1 hour
FACS	1:5000	Overnight	GAR 1:10000	1 hour
Actin	1:250	Overnight	DAG 1:2000	1 hour
P-ACC	1:1000	Overnight	GAR 1:2000	1 hour
AMPK	1:1000	Overnight	GAR 1:2000	1 hour
P-AMPK	1:1000	Overnight	GAR 1:2000	1 hour
PPAR $\alpha$	1:500	Overnight	GAM 1:1000	1 hour

Goat-anti-mouse (GAR)

Donkey-anti-goat (DAG)

Goat-anti-mouse (GAM)

## Chapter 3

# **FAT/CD36 Deficiency does not Energetically or Functionally Compromise Hearts Prior to or Following Ischemia**

A portion of this chapter was published in the journal *Circulation*. (Kuang M, Febbraio M, Wagg C, Lopaschuk GD, Dyck JR. Fatty acid translocase/CD36 deficiency does not energetically or functionally compromise hearts before or after ischemia. *Circulation*. 2004 Mar 30;109(12):1550-7.)

**Acknowledgements:** Heart perfusions and measurements of palmitate and glucose oxidation were conducted by Cory Wagg. HPLC was conducted by Kenneth Strynadka

## Introduction

In adult cardiac myocyte the oxidation of fatty acids provides the majority of energy needed to support contractile function. Although the heart has the ability to store fatty acids, it has a limited capacity to maintain its high metabolic demand on endogenous sources alone and relies on continuous uptake from blood <sup>1</sup>. Despite the obvious importance of fatty acid uptake to the cardiac myocyte, controversy still exists with respect to the exact process by which fatty acids enter into cells. The two main mechanisms proposed for transport of fatty acids into cells are: 1) passive diffusion and/or 2) protein mediated transport <sup>2,3</sup>. Accumulating evidence supports a role for fatty acid translocase (FAT; also known as CD36 <sup>4</sup>) in protein mediated fatty acid uptake in cardiac myocytes.

FAT/CD36 is an 88 kD ditopic glycosylated protein that belongs to the class B family of scavenger receptors. This family also includes scavenger receptor class B type I (SR-BI), the receptor for selective cholesteryl ester uptake and lysosomal integral membrane protein II (LIMP-II) (see <sup>5</sup> for review). Studies utilizing a non-metabolizable fatty acid analog, BMIPP suggest that FAT/CD36 accounts for 50 - 80 % of the total fatty acid uptake by the heart <sup>6</sup>. Polymorphisms in human FAT/CD36 occur in Asian and African populations at a relatively high frequency, and there have been reports that these deficient individuals have reduced cardiac fatty acid uptake <sup>7-14</sup> and cardiac abnormalities. However, considerable controversy exists with respect to the potential involvement of FAT/CD36 deficiency in the development of hypertrophic cardiomyopathy <sup>7,15-19</sup> and it has not been directly proven whether patients with

FAT/CD36 deficiency have reduced cardiac fatty acid oxidation rates or energetically compromised hearts.

To understand better the effects of FAT/CD36 deficiency, a mouse model of FAT/CD36 deficiency has been developed <sup>20</sup>. A recent report by Irie et al <sup>21</sup> suggested that hearts from FAT/CD36 null mice were energetically deficient. However, involvement of FAT/CD36 in regulation of fatty acid oxidation rates was determined using isolated cardiac myocytes and thus, may be skewed by the fact that isolated cardiac myocytes do not perform significant amounts of contractile work and therefore, have very low rates of fatty acid oxidation. It has not yet been determined whether FAT/CD36-mediated fatty acid uptake can regulate fatty acid oxidation rates in the intact working heart. In addition, the ability of carbohydrate oxidation to compensate for changes in fatty acid oxidation, such that the energy status of the heart can be determined, also needs to be assessed to understand fully the impact of FAT/CD36 deficiency.

The report by Irie et al<sup>21</sup> also suggested that hearts from FAT/CD36 null mice were less tolerant to ischemia, primarily due to deficiency in fatty acid oxidation and decreased ATP supply. However, we have previously shown that excessively high fatty acid oxidation rates contribute to ischemic injury by inhibiting glucose oxidation <sup>22</sup>. As a result, it is possible that depressed fatty acid oxidation rates, as seen in FAT/CD36 KOs, may actually protect the heart from ischemic damage. Therefore, the question remains as to whether FAT/CD36 deficiency leads to energetically deficient hearts and/or whether an alteration in fatty acid oxidation, due to FAT/CD36 deficiency, is detrimental or beneficial to the ischemic heart.

Using isolated working hearts from wild type and FAT/CD36 null mice, we directly measured fatty acid oxidation rates in hearts perfused with both low and high levels of fatty acids. We also investigated the relationship between fatty acid oxidation and glucose oxidation rates in FAT/CD36 deficient hearts and determined whether FAT/CD36 deficiency was beneficial or detrimental to the ischemic heart.

## **Hypothesis**

We hypothesize that FAT/CD36 KO mouse hearts will exhibit low rates of palmitate oxidation, which will be compensated for by increased rates of glucose oxidation, as compared to the wildtype mouse hearts. Due to this switch in energy substrate utilization, the FAT/CD36 KO mouse hearts will demonstrate improved recovery of cardiac work after an ischemic insult, as compared to wildtype hearts. Therefore, we hypothesize that the FAT/CD36 KO mouse hearts are not energetically or functionally compromised, before or after ischemia, as compared to the wildtype mouse hearts.

## **Materials and Methods**

*Mice*- CD36 KO mice and a littermate control line were created as previously described<sup>20</sup>. Mice were backcrossed 6x to C57Bl/6. Mice were maintained in a fully accredited facility on a 12 hour dark/light schedule with ad libitum access to food and water. The University of Alberta adheres to the principles developed by the Council for International

Organizations of Medical Sciences for biomedical research involving animals and complies with National Institutes of Health animal care guidelines.

*Heart Perfusions-* As described in the Methods and Materials section.

*Measurement of Cardiac Function-* As described in the Methods and Materials section.

*Glucose Oxidation Rates-* As described in the Methods and Materials section.

*Palmitate Oxidation Rates-* As described in the Methods and Materials section.

*Calculation of Tricarboxylic Acid Cycle (TCA) Activity-* As described in the Methods and Materials section.

*Measurement of ATP Levels-* Frozen mouse heart tissue (20 mg) was homogenized in a 6% perchloric acid/0.5 mM EGTA solution. The homogenate was incubated on ice for 10 min and centrifuged at 10000 • g for 2 min. The supernatant was collected and ATP concentrations were determined by HPLC as described <sup>23</sup>.

*Statistical Analysis-* Data are expressed as mean  $\pm$  SEM. Comparisons between wild type and FAT/CD36 deficient hearts were performed using the unpaired Student's two-tailed t-test. Differences were judged to be significant when  $p < 0.05$ .

## Results

*Fatty Acid Oxidation Rates in Hearts Perfused Aerobically with 0.4 mM Palmitate* - To examine whether FAT/CD36 mediated fatty acid uptake is rate-limiting for fatty acid oxidation, the rates of palmitate oxidation in the intact working heart were measured. In the presence of low levels of fatty acids (0.4 mM palmitate), rates of fatty acid oxidation in wild type hearts paralleled rates seen in other studies<sup>24</sup>. Palmitate oxidation rates in FAT/CD36 KO hearts were significantly lower compared with those in wild type hearts (Figure 3-1), supporting a role for FAT/CD36 as a fatty acid transporter in cardiac myocytes. Importantly, this did not result in compromised cardiac function (Table 3-1). Heart rate, coronary flow, cardiac work and peak systolic pressure measurements were not significantly different between wild-type and FAT/CD36 KO hearts, and these values compared well with those published for wild type hearts in previous studies<sup>24</sup>.

*Fatty Acid Oxidation and Glucose Oxidation Rates in Hearts Perfused Aerobically with 1.2 mM Palmitate* - To determine if FAT/CD36 deficient hearts were energetically and/or functionally compromised during conditions where the heart relies heavily on fatty acid oxidation for ATP, wild type and FAT/CD36 KO hearts were perfused with a high concentration of palmitate (1.2 mM). Under these conditions, rates of palmitate oxidation in wild type hearts were 6-fold higher than rates measured in the presence of 0.4 mM palmitate. Interestingly, fatty acid oxidation rates in FAT/CD36 KO hearts perfused with 1.2 mM palmitate were also elevated about 6-fold, but remained significantly lower than those in the wild type hearts (Figure 3-2A). Since palmitate

oxidation was significantly decreased in FAT/CD36 KO hearts, we determined if an increase in glucose oxidation was compensating for the loss of palmitate-derived ATP. We found that the reduction in the rate of fatty acid oxidation was accompanied by a 3-fold increase in the rate of glucose oxidation in FAT/CD36 KO hearts (Figure 3-2B). In wild type hearts perfused with 1.2 mM palmitate, the majority of TCA cycle acetyl-CoA originated from palmitate (80%), and the remainder from glucose (20%) (Figure 3-2C). In contrast, FAT/CD36 KO hearts derived 62% of the total acetyl-CoA from glucose, and only 38% from palmitate (Figure 3-2C). Despite this dramatic switch in energy substrate utilization, the total amount of TCA cycle acetyl-CoA derived from both palmitate and glucose oxidation was similar in both wild type and FAT/CD36 KO hearts (Figure 3-2C), demonstrating that FAT/CD36 deficient hearts were not energetically compromised. In addition, as was the case when the hearts were perfused with 0.4 mM palmitate, there were either no changes or no negative effects of FAT/CD36 deficiency on heart rate, peak systolic pressure, coronary flow, cardiac output or cardiac work in hearts perfused with 1.2 mM palmitate, demonstrating that FAT/CD36 deficient hearts were also not functionally compromised.

*Effects of Ischemia on Wild type and FAT/CD36 Deficient Hearts* - In order to determine how altered energy substrate preference affects functional recovery from ischemia, wild type and FAT/CD36 KO hearts were subjected to 30 min of aerobic perfusion, 18 min of global no-flow ischemia, followed by 40 min of aerobic reperfusion. During the pre-ischemic aerobic period, FAT/CD36 deficient hearts exhibited significantly higher levels of cardiac work as compared to wild type hearts (Figure 3-3A). Although pre-ischemic

work in the FAT/CD36 KO hearts were significantly elevated, as compared to wildtype hearts, both the wildtype and FAT/CD36 KO hearts exhibited similar levels of cardiac work post-ischemia (Figure 3-3A). When expressed as a percent recovery of cardiac work the recovery of FAT/CD36 KO and wild type hearts were not significantly different (Figure 3-3B).

*Fatty Acid Oxidation and Glucose Oxidation Rates in Hearts Perfused Aerobically with 1.2 mM Palmitate after Ischemia-* A recent study suggested that FAT/CD36 KO hearts recovered poorly following ischemia, due to decreased fatty acid metabolism. To determine if this were the case, we directly examined energy metabolism during reperfusion in wild type and FAT/CD36 deficient hearts. Upon aerobic reperfusion after ischemia, fatty acid oxidation rates in FAT/CD36 KO hearts were significantly lower (37%), compared to wild type hearts (Figure 3-4A). However, similar to the pre-ischemic period, the decrease in fatty acid oxidation rates in FAT/CD36 deficient hearts was compensated by a 2-fold increase in the rate of glucose oxidation (Figure 3-4B). During reperfusion, wild type hearts derived 66% of TCA cycle acetyl-CoA from palmitate. In contrast, FAT/CD36 KO hearts derived only half as much TCA cycle acetyl-CoA from palmitate (36%). There was a concomitant increase in TCA cycle acetyl-CoA from glucose in hearts from FAT/CD36 KOs: 34% vs 64% of TCA cycle acetyl-CoA from glucose, in wild type and FAT/CD36 KO hearts, respectively. Despite the continued depressed rates of fatty acid oxidation in FAT/CD36 KO hearts during reperfusion, the total amount of acetyl-CoA derived from palmitate and glucose oxidation was similar in both wild type and FAT/CD36 KO hearts (Figure 3-4C). Furthermore, ATP levels

measured in hearts at the end of reperfusion were similar in both groups ( $10.9 \pm 1.2$  vs  $13.8 \pm 1.2$  nmol/g dry wt in wild type and FAT/CD36 KO hearts, respectively), confirming that FAT/CD36 KO hearts were not energetically deficient during reperfusion following ischemia.

## Discussion

FAT/CD36 has been proposed to be a major regulator of fatty acid uptake by hearts. Evidence in support of this includes studies utilizing the non-metabolizable fatty acid analog, BMIPP, in FAT/CD36 deficient humans and KO mice. These studies showed a decrease in fatty acid transport in heart <sup>25</sup>, but the importance of this in the intact functioning heart remains unknown. In this study we examined whether a decrease in FAT/CD36-mediated fatty acid uptake resulted in depressed rates of fatty acid oxidation in ex vivo working mouse hearts. Our data show that FAT/CD36-mediated fatty acid uptake accounts for 40-60% of fatty acid oxidation in the heart under conditions of low and high palmitate (Figures 1A and 2A). Under both conditions, rates of fatty acid oxidation were significantly decreased in FAT/CD36 KO hearts. Despite the decrease in fatty acid oxidation in FAT/CD36 deficient hearts perfused with 0.4 mM palmitate, cardiac work was not different from wildtype hearts (Table 1). However, at 1.2 mM palmitate, FAT/CD36 KO hearts exhibited increased levels of cardiac work compared to the wildtype hearts. Although the reason(s) for this increased function in FAT/CD36 KO hearts is not known, the ability of FAT/CD36 KO hearts to maintain and in fact, increase cardiac function, despite exhibiting depressed fatty acid oxidation rates is

most likely due to a compensatory increase in glucose oxidation rates, which maintained adequate TCA cycle ATP supply in the FAT/CD36 deficient hearts. Although we did not measure ATP levels in hearts prior to ischemia, total acetyl-CoA production was not different in the wildtype and FAT/CD36 deficient hearts, suggests that the ATP production in the two sets of hearts are similar prior to ischemia.

In stark contrast to the study of Irie et al<sup>21</sup> which showed general poor function of FAT/CD36 KO hearts, we found cardiac function to be significantly elevated in the FAT/CD36 KO hearts as compared to wild type hearts. One potential mechanism for the improved cardiac function of FAT/CD36 deficient hearts, supported by our data, is the observed increase in glucose oxidation rates, which would result in more acetyl-CoA per molecule of oxygen and subsequent increase in cardiac efficiency. In the present study, hearts were perfused with insulin. However, insulin did not appear to be present in the perfusate of the Irie et al<sup>21</sup> study, which may have inhibited glucose uptake<sup>26</sup>. In addition, since the concentration of insulin used in our study was super-physiological, it is possible that this high concentration of insulin may have beneficial effects on function by itself<sup>27</sup>. The presence of insulin in the perfusate may have increased cardiac glucose utilization, which could play a role in the improved performance observed in the FAT/CD36 KO hearts in this study.

Our data suggest that FAT/CD36 deficient hearts, regardless of fatty acid concentration, are not energetically or functionally compromised during basal conditions that do not stress the heart. Since it has been reported that FAT/CD36 deficiency is detrimental during ischemia<sup>21</sup>, we also subjected hearts to an 18 min of global no flow ischemia followed by 40 min of aerobic reperfusion. Again, in contrast to the study by

Irie et al <sup>21</sup>, we found that reperfused ischemic FAT/CD36 deficient and wild type hearts recovered to a similar degree (Figure 3). In this study, we confirmed that FAT/CD36 deficient hearts had significantly lower palmitate oxidation rates under these conditions but this did not affect functional recovery. In the Irie et al study <sup>21</sup>, the authors speculated that the inability of FAT/CD36 KO hearts to oxidize fatty acids resulted in an energetic deficient state, thereby compromising functional recovery. However, energy metabolism or energy status of the hearts during reperfusion was not measured in that study. Our data show that the loss of energy from decreased rates of palmitate oxidation was completely compensated by increased rates of glucose oxidation in FAT/CD36 deficient hearts. Following ischemia there is an overall decrease in oxidative metabolism for both wildtype and FAT/CD36 KO hearts. However, in the FAT/CD36 KO hearts, the relative contribution to overall acetyl-CoA production by glucose and fatty acids is not different between pre- and post-ischemic hearts. Furthermore, ATP levels at the end of reperfusion in FAT/CD36 KO and wild type hearts were similar (10.9±1.2 vs 13.8±1.2 nmol/g dry wt, respectively). Therefore, our results clearly show that FAT/CD36 deficient hearts are not energetically compromised during reperfusion and that the hypothesis of Irie et al <sup>21</sup> is not supported by measurements of energy metabolism and status.

The discrepancy between our data and that of Irie et al <sup>21</sup> may be explained by differences in the overall health of the hearts before experimentation. We noted, for example, the low end-diastolic pressures in the perfused hearts utilized in the Irie et al <sup>21</sup> study. A study by Larsen<sup>28</sup> has shown that end-diastolic pressure should match more closely to preload pressure. In the case of Irie<sup>21</sup>, the end-diastolic pressure is lower than

that of the preload pressure, which suggests that the hearts used in their study exhibited poor function before ischemia. This is consistent with the fact that their hearts were not able to tolerate more than 6 min of ischemia and that all hearts (wild type and FAT/CD36 KO) failed to function after 12 min of ischemia. In our study, hearts were able to recover to approximately 50 % of their pre-ischemic values after 18 min of ischemia, while 12 minutes of ischemia resulted in 100% recovery of all hearts (data not shown). Another explanation for the differences in our data may be the apparent absence of albumin in the fatty acid free perfusate used in the Irie et al<sup>21</sup> study. Hearts perfused without fatty acids and albumin were compared to hearts perfused with fatty acids and albumin. It has previously been shown that albumin protects the heart against ischemic injury, and that hearts perfused without albumin exhibit increased tissue edema<sup>27</sup>. Therefore, the absence of albumin in hearts perfused without fatty acids in the Irie et al<sup>21</sup> study could provide an alternate explanation for decreased function in the glucose perfused FAT/CD36 KO hearts reperfused following ischemia. It is not unreasonable to predict that the FAT/CD36 KO hearts perfused in the absence of fatty acids and albumin, as in the Irie et al<sup>21</sup> study, would be energetically deficient, but the effect cannot necessarily be related to absence of FAT/CD36 due to the artificial conditions used (i.e. the total lack of fatty acids as a major source of myocardial energy). Although FAT/CD36 is responsible for 40-60% of cardiac fatty acid uptake, other mechanisms provide the heart with the remainder, and this could be an important nutritional resource which provides protection. The total lack of a major source of myocardial energy supply in the Irie et al<sup>21</sup> study makes conclusions with regard to FAT/CD36 function impossible. It is important to note

that in the clinical situation of ischemia and reperfusion (i.e. post myocardial infarction or post-surgery) the heart is normally exposed to high levels of fatty acid <sup>29-31</sup>.

Irie et al <sup>21</sup> concluded that the poor functional recovery of FAT/CD36 deficient hearts upon reperfusion was due to a decrease in fatty acid transport and the subsequent drop in fatty acid oxidation and energy production. Therefore, they concluded, lack of palmitate was detrimental to the recovery of hearts during reperfusion. Contrasting this data, previous studies have shown that decreased fatty acid oxidation during reperfusion is actually beneficial to functional recovery of the heart <sup>32</sup>. Normally, acetyl-CoA derived from fatty acid oxidation stimulates PDH kinase, inactivates the PDH complex, and decreases the rate of glucose oxidation. Therefore, in situations where fatty acid oxidation is decreased, glucose oxidation increases during reperfusion, leading to improved functional recovery. Moreover, pharmacological inhibition of fatty acid oxidation (i.e. inhibition of carnitine palmitoyl transferase I) has also been shown to be beneficial to the reperfused ischemic heart <sup>33</sup>. Thus, our data with regard to FAT/CD36 KO hearts are more consistent than the Irie et al <sup>21</sup> study with what has previously been published.

One observation made in the Irie et al <sup>21</sup> study that cannot be attributed to perfusion conditions is that non-perfused FAT/CD36 KO hearts exhibited lower levels of ATP compared to the wildtype hearts. This decrease in ATP may reflect lower energy production *in vivo* due to decreased rates of fatty acid oxidation. However, there are no reports showing that the decrease in ATP affects function in FAT/CD36 KO hearts *in vivo*, nor do the decreases in ATP adversely affect function *in vitro* if hearts are adequately perfused. It is possible that the lower ATP levels produced in FAT/CD36 KO

hearts may only depress cardiac function when stressed by potentially injurious perfusions, which may rapidly deplete myocardial ATP. In this instance, hearts with a higher energy reserve (i.e. wildtype hearts) would be less susceptible to ischemic injury. Indeed, our study demonstrates that, when adequately perfused, the initial decrease in total ATP does not hinder cardiac function.

## **Conclusion**

We show that FAT/CD36 mediated fatty acid uptake is an important regulator of fatty acid oxidation in the heart. Hearts from FAT/CD36 KO mice exhibit 40-60% lower rates of palmitate oxidation, as compared to wild type hearts. However, regardless of whether perfused under aerobic conditions or during reperfusion following ischemia, FAT/CD36 deficient hearts are not functionally or energetically compromised. This is because glucose oxidation rates compensate for the depressed rates of fatty acid oxidation. Therefore, in contrast to the findings of Irie et al<sup>21</sup>, the loss of FAT/CD36 is not detrimental to the heart either in the absence or presence of ischemia.

## References

1. van der Vusse GJ, Glatz JF, Stam HC, Reneman RS. Fatty acid homeostasis in the normoxic and ischemic heart. *Physiol Rev.* 1992;72:881-940.
2. van der Vusse GJ, van Bilsen M, Glatz JF. Cardiac fatty acid uptake and transport in health and disease. *Cardiovasc Res.* 2000;45:279-93.
3. Luiken JJ, van Nieuwenhoven FA, America G, van der Vusse GJ, Glatz JF. Uptake and metabolism of palmitate by isolated cardiac myocytes from adult rats: involvement of sarcolemmal proteins. *J Lipid Res.* 1997;38:745-58.
4. Luiken JJ, Willems J, van der Vusse GJ, Glatz JF. Electrostimulation enhances FAT/CD36-mediated long-chain fatty acid uptake by isolated rat cardiac myocytes. *Am J Physiol Endocrinol Metab.* 2001;281:E704-12.
5. Febbraio M, Hajjar DP, Silverstein RL. CD36: a class B scavenger receptor involved in angiogenesis, atherosclerosis, inflammation, and lipid metabolism. *J Clin Invest.* 2001;108:785-91.
6. Brinkmann JF, Abumrad NA, Ibrahimi A, van der Vusse GJ, Glatz JF. New insights into long-chain fatty acid uptake by heart muscle: a crucial role for fatty acid translocase/CD36. *Biochem J.* 2002;367:561-70.
7. Tanaka T, Sohmiya K, Kawamura K. Is CD36 deficiency an etiology of hereditary hypertrophic cardiomyopathy? *J Mol Cell Cardiol.* 1997;29:121-7.
8. Hirooka K, Yasumura Y, Ishida Y, Komamura K, Hanatani A, Nakatani S, Yamagishi M, Miyatake K. Improvement in cardiac function and free fatty acid metabolism in a case of dilated cardiomyopathy with CD36 deficiency. *Jpn Circ J.* 2000;64:731-5.

9. Yoshizumi T, Nozaki S, Fukuchi K, Yamasaki K, Fukuchi T, Maruyama T, Tomiyama Y, Yamashita S, Nishimura T, Matsuzawa Y. Pharmacokinetics and metabolism of <sup>123</sup>I-BMIPP fatty acid analog in healthy and CD36-deficient subjects. *J Nucl Med.* 2000;41:1134-8.
10. Nakata T, Nakahara N, Sohmiya K, Okamoto F, Tanaka T, Kawamura K, Shimamoto K. Scintigraphic evidence for a specific long-chain fatty acid transporting system deficit and the genetic background in a patient with hypertrophic cardiomyopathy. *Jpn Circ J.* 1999;63:319-22.
11. Nishimura T. beta-Methyl-p-(<sup>123</sup>I)-iodophenyl pentadecanoic acid single-photon emission computed tomography in cardiomyopathy. *Int J Card Imaging.* 1999;15:41-8.
12. Nozaki S, Tanaka T, Yamashita S, Sohmiya K, Yoshizumi T, Okamoto F, Kitaura Y, Kotake C, Nishida H, Nakata A, Nakagawa T, Matsumoto K, Kameda-Takemura K, Tadokoro S, Kurata Y, Tomiyama Y, Kawamura K, Matsuzawa Y. CD36 mediates long-chain fatty acid transport in human myocardium: complete myocardial accumulation defect of radiolabeled long-chain fatty acid analog in subjects with CD36 deficiency. *Mol Cell Biochem.* 1999;192:129-35.
13. Fukuchi K, Nozaki S, Yoshizumi T, Hasegawa S, Uehara T, Nakagawa T, Kobayashi T, Tomiyama Y, Yamashita S, Matsuzawa Y, Nishimura T. Enhanced myocardial glucose use in patients with a deficiency in long-chain fatty acid transport (CD36 deficiency). *J Nucl Med.* 1999;40:239-43.
14. Watanabe K, Ohta Y, Toba K, Ogawa Y, Hanawa H, Hirokawa Y, Kodama M, Tanabe N, Hirono S, Ohkura Y, Nakamura Y, Kato K, Aizawa Y, Fuse I,

- Miyajima S, Kusano Y, Nagamoto T, Hasegawa G, Naito M. Myocardial CD36 expression and fatty acid accumulation in patients with type I and II CD36 deficiency. *Ann Nucl Med*. 1998;12:261-6.
15. Miyaoka K, Kuwasako T, Hirano K, Nozaki S, Yamashita S, Matsuzawa Y. CD36 deficiency associated with insulin resistance. *Lancet*. 2001;357:686-7.
  16. Asano Y, Ishii K, Sagiuchi T, Tokita N, Aoki Y, Woodhams R, Katsunuma E, Izumi T, Hayakawa K. [No 123I-BMIPP accumulation in the myocardium and type I CD36 deficiency in a patient with acute subendocardial infarction: a case report]. *Kaku Igaku*. 2002;39:29-35.
  17. Chiba H, Yanai H, Fujiwara H, Matsuno K, Kobayashi K. CD36 deficiency and insulin resistance. *Lancet*. 2001;358:243-4; author reply 244.
  18. Iizuka Y, Gotoda T, Ishibashi S, Yamada N. CD36 deficiency and insulin resistance. *Lancet*. 2001;358:243; author reply 244.
  19. Yanai H, Chiba H, Morimoto M, Jamieson GA, Matsuno K. Type I CD36 deficiency in humans is not associated with insulin resistance syndrome. *Thromb Haemost*. 2000;83:786.
  20. Febbraio M, Abumrad NA, Hajjar DP, Sharma K, Cheng W, Pearce SF, Silverstein RL. A null mutation in murine CD36 reveals an important role in fatty acid and lipoprotein metabolism. *J Biol Chem*. 1999;274:19055-62.
  21. Irie H, Krukenkamp IB, Brinkmann JF, Gaudette GR, Saltman AE, Jou W, Glatz JF, Abumrad NA, Ibrahimi A. Myocardial recovery from ischemia is impaired in CD36-null mice and restored by myocyte CD36 expression or medium-chain fatty acids. *Proc Natl Acad Sci U S A*. 2003.

22. Lopaschuk GD, Wambolt RB, Barr RL. An imbalance between glycolysis and glucose oxidation is a possible explanation for the detrimental effects of high levels of fatty acids during aerobic reperfusion of ischemic hearts. *J Pharmacol Exp Ther.* 1993;264:135-44.
23. Ally A, Park G. Rapid determination of creatine, phosphocreatine, purine bases and nucleotides (ATP, ADP, AMP, GTP, GDP) in heart biopsies by gradient ion-pair reversed-phase liquid chromatography. *J Chromatogr.* 1992;575:19-27.
24. Campbell FM, Kozak R, Wagner A, Altarejos JY, Dyck JR, Belke DD, Severson DL, Kelly DP, Lopaschuk GD. A role for peroxisome proliferator-activated receptor alpha (PPARalpha) in the control of cardiac malonyl-CoA levels: reduced fatty acid oxidation rates and increased glucose oxidation rates in the hearts of mice lacking PPARalpha are associated with higher concentrations of malonyl-CoA and reduced expression of malonyl-CoA decarboxylase. *J Biol Chem.* 2002;277:4098-103.
25. Coburn CT, Knapp FF, Jr., Febbraio M, Beets AL, Silverstein RL, Abumrad NA. Defective uptake and utilization of long chain fatty acids in muscle and adipose tissues of CD36 knockout mice. *J Biol Chem.* 2000;275:32523-9.
26. Soltys CL, Buchholz L, Gandhi M, Clanachan AS, Walsh K, Dyck JR. Phosphorylation of cardiac protein kinase B is regulated by palmitate. *Am J Physiol Heart Circ Physiol.* 2002;283:H1056-64.
27. Van Rooyen J, McCarthy J, Opie LH. Increased glycolysis during ischaemia mediates the protective effect of glucose and insulin in the isolated rat heart

- despite the presence of cardiodepressant exogenous substrates. *Cardiovasc J S Afr.* 2002;13:103-9.
28. Larsen TS, Belke DD, Sas R, Giles WR, Severson DL, Lopaschuk GD, Tyberg JV. The isolated working mouse heart: methodological considerations. *Pflugers Arch.* 1999;437:979-85.
  29. Oliver MF. Metabolic causes and prevention of ventricular fibrillation during acute coronary syndromes. *Am J Med.* 2002;112:305-11.
  30. Tornvall P, Olivecrona G, Karpe F, Hamsten A, Olivecrona T. Lipoprotein lipase mass and activity in plasma and their increase after heparin are separate parameters with different relations to plasma lipoproteins. *Arterioscler Thromb Vasc Biol.* 1995;15:1086-93.
  31. Stubbe I, Gustafson A, Nilsson-Ehle P. Alterations in plasma proteins and lipoproteins in acute myocardial infarction: effects on activation of lipoprotein lipase. *Scand J Clin Lab Invest.* 1982;42:437-44.
  32. Lopaschuk GD, Wall SR, Olley PM, Davies NJ. Etomoxir, a carnitine palmitoyltransferase I inhibitor, protects hearts from fatty acid-induced ischemic injury independent of changes in long chain acylcarnitine. *Circ Res.* 1988;63:1036-43.
  33. Lopaschuk GD, Spafford MA, Davies NJ, Wall SR. Glucose and palmitate oxidation in isolated working rat hearts reperfused after a period of transient global ischemia. *Circ Res.* 1990;66:546-53.

Table 1-1 Cardiac Function in FAT/CD36 Knockout Mouse Hearts Aerobically  
Perfused with Low Levels of Fatty Acids

	Wildtype (n=6)	FAT/CD36 Knockout (n=8)
Heart rate (beats•min <sup>-1</sup> )	261±49	271±63
Peak systolic pressure (mm Hg)	66±2	65±1
Coronary flow (ml•min <sup>-1</sup> )	2.3±0.4	4.2±1
Cardiac output (ml•min <sup>-1</sup> )	7.7±1	9.3±1
Cardiac Work (ml•mmHg•min <sup>-1</sup> •10 <sup>-2</sup> )	5.1±1	6.1±0.8

Functional parameters were measured in isolated working hearts from FAT/CD36 knockout and wildtype mice perfused with 5.5 mM glucose, 0.4 mM palmitate, 3% bovine serum albumin and 100 μU/mL insulin, at a 11.5 mmHg preload

Table 1-2 Cardiac Function in FAT/CD36 Knockout Mouse Hearts Aerobically  
Perfused with High Levels of Fatty Acids

	Wildtype (n=13)	FAT/CD36 Knockout (n=13)
Heart rate (beats•min <sup>-1</sup> )	246±10	275±7 *
Peak systolic pressure (mm Hg)	69±1	68±1
Coronary flow (ml•min <sup>-1</sup> )	2.9±0.3	3.9±0.5
Cardiac output (ml•min <sup>-1</sup> )	8.1±0.3	10±0.4 #
Cardiac Work (ml•mmHg•min <sup>-1</sup> •10 <sup>-2</sup> )	5.5±0.1	6.8±0.2 †

Functional parameters were measured in isolated working hearts from FAT/CD36 knockout and wildtype mice perfused with 5.5 mM glucose, 0.4 mM palmitate, 3% bovine serum albumin and 100 µU/mL insulin, at a 11.5 mmHg preload and 50 mmHg afterload.

\* significantly different from wildtype value.  $p < 0.05$

# significantly different from wildtype value.  $p < 0.005$

Table 1-3 Cardiac Function in FAT/CD36 Knockout Mouse Hearts Aerobically Perfused with High Levels of Fatty Acids and Reperfused Following Ischemia

	Wildtype (n=13)	FAT/CD36 Knockout (n=13)
Heart rate (beats•min <sup>-1</sup> )	211±13	245±10 *
Peak systolic pressure (mm Hg)	63±2	59±2
Coronary flow (ml•min <sup>-1</sup> )	2.9±0.4	4.2±0.9
Cardiac output (ml•min <sup>-1</sup> )	5.6±0.5	6.4±1

Functional parameters were measured in isolated working hearts from FAT/CD36 knockout and wildtype mice perfused with 5.5 mM glucose, 1.2 mM palmitate, 3% bovine serum albumin and 100 µU/mL insulin, at a 11.5 mmHg preload and 50 mmHg afterload. Hearts were perfused for a 30 min aerobic period, followed by 18 min global no flow ischemia and 40 min aerobic reperfusion.

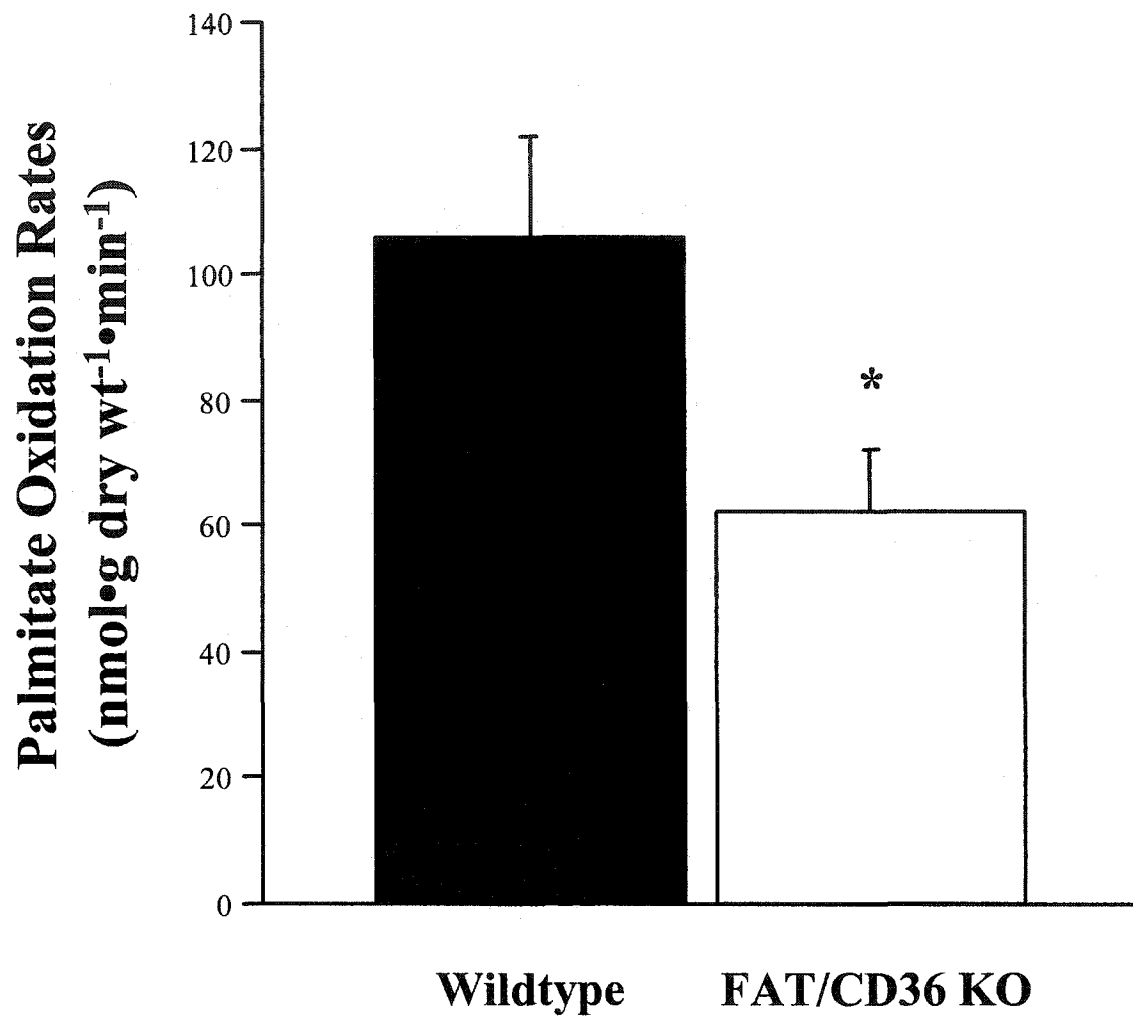


**Figure 3-1. Palmitate oxidation in FAT/CD36 knockout (KO) and wildtype mouse hearts perfused with 0.4 mM palmitate.** Values represent the mean  $\pm$  S.E. 8 KO and 6 wildtype mouse hearts for palmitate oxidation. \*, significantly different from wild type mouse hearts,  $P < 0.05$ .

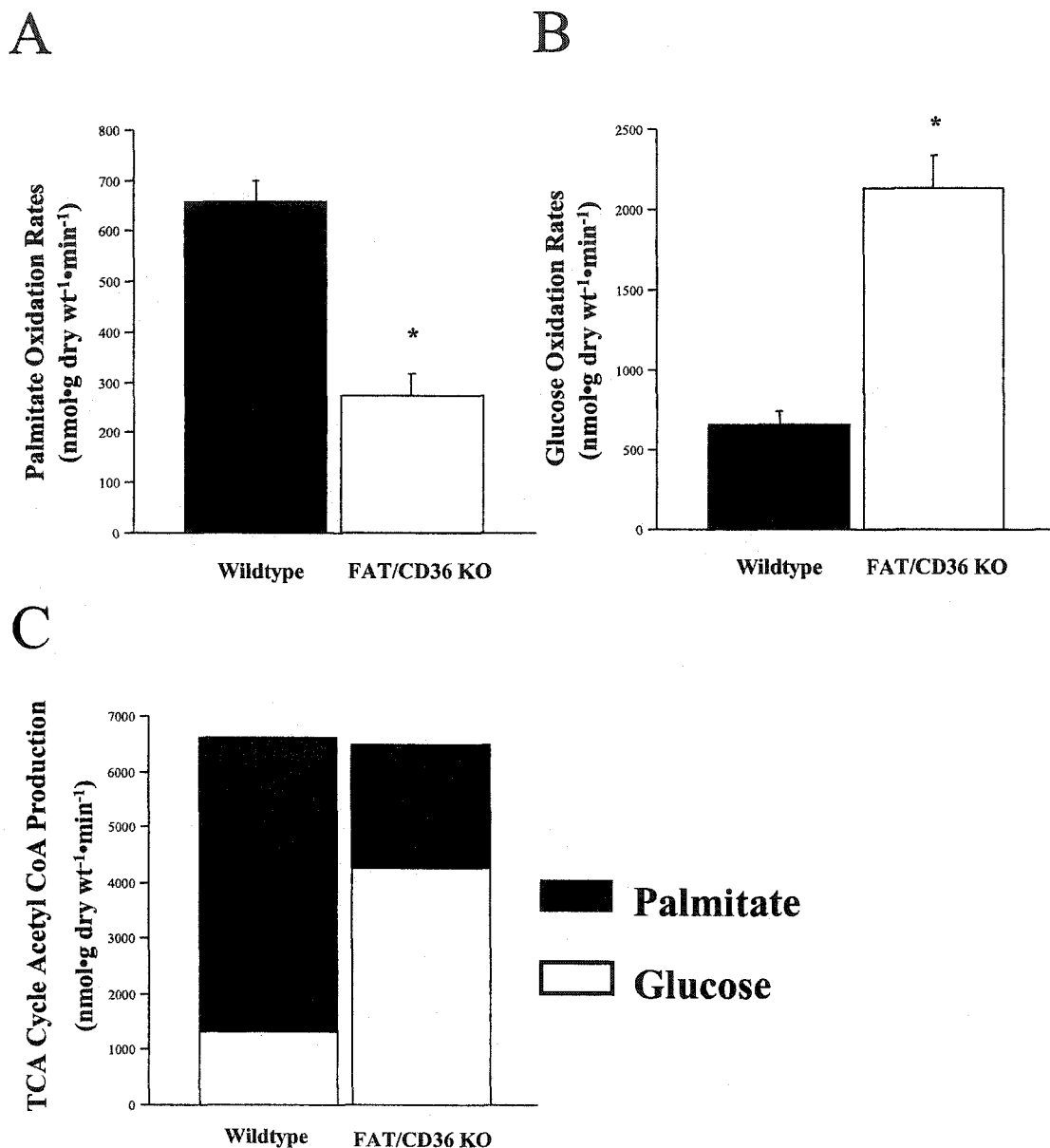


**Fig. 3-2. Palmitate oxidation (A), glucose oxidation (B) and tricarboxylic acid (TCA) acetyl-CoA production (C) for the TCA cycle in FAT/CD36 knockout (KO) and wildtype (WT) mouse hearts perfused with 1.2 mM palmitate.** Values represent the mean  $\pm$  S.E. 5 KO and 6 WT mouse hearts for palmitate oxidation; 8 KO and 7 WT mouse hearts for glucose oxidation. 13 KO and WT mouse hearts were used to calculate acetyl-CoA production from palmitate oxidation and glucose oxidation. TCA cycle activity was calculated from the rates of palmitate and glucose oxidation from A and B, using 8 mol of acetyl-CoA from every mol of palmitate oxidized and 2 mol of acetyl-CoA for every 1 mol of glucose oxidized. \*, significantly different from WT mouse hearts,  $p < 0.01$ .

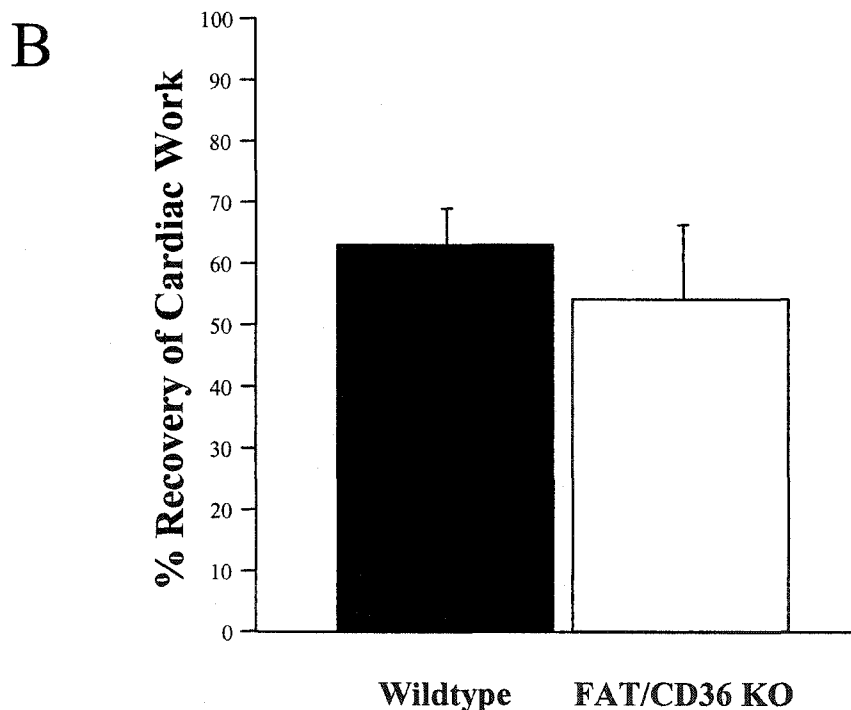
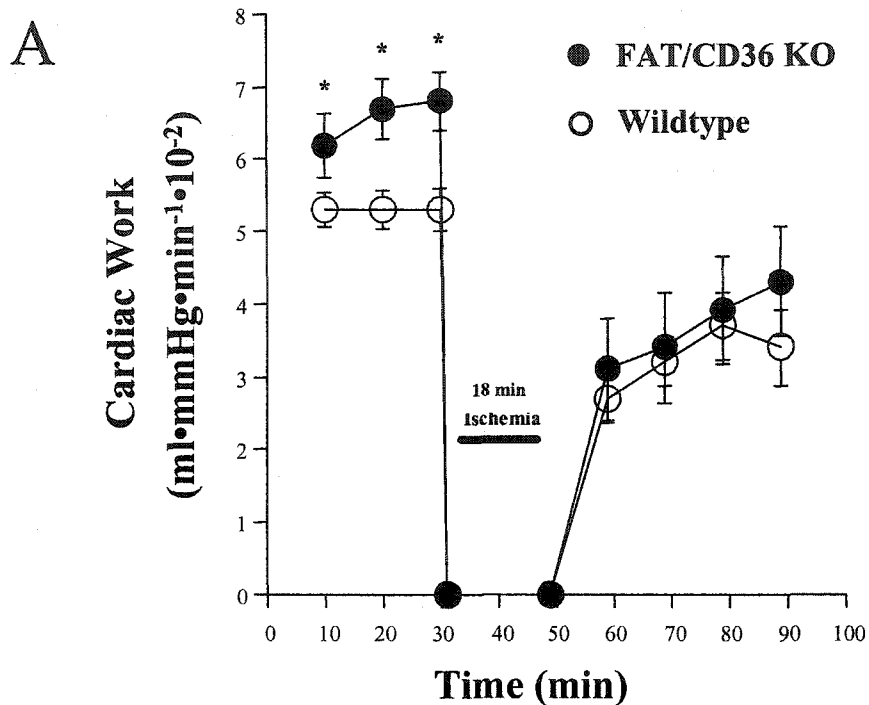


**Fig. 3-3. Cardiac work (A) and % recovery of cardiac work (B) in FAT/CD36 knockout (KO) and wildtype (WT) mouse hearts.** Cardiac work was calculated as a product of cardiac output and peak systolic pressure. Hearts perfused with 5.5 mM glucose, 1.2 mM palmitate, 3% BSA and 100  $\mu$ U/mL insulin were aerobically perfused for 30 min, followed by 18 min global no-flow ischemia and 40 min of aerobic reperfusion. \*, significantly different from WT values,  $p < 0.001$ . Recovery of cardiac function (measured after 40 min reperfusion) was calculated as a percentage of pre-ischemic values for the FAT/CD36 KO and WT mouse hearts

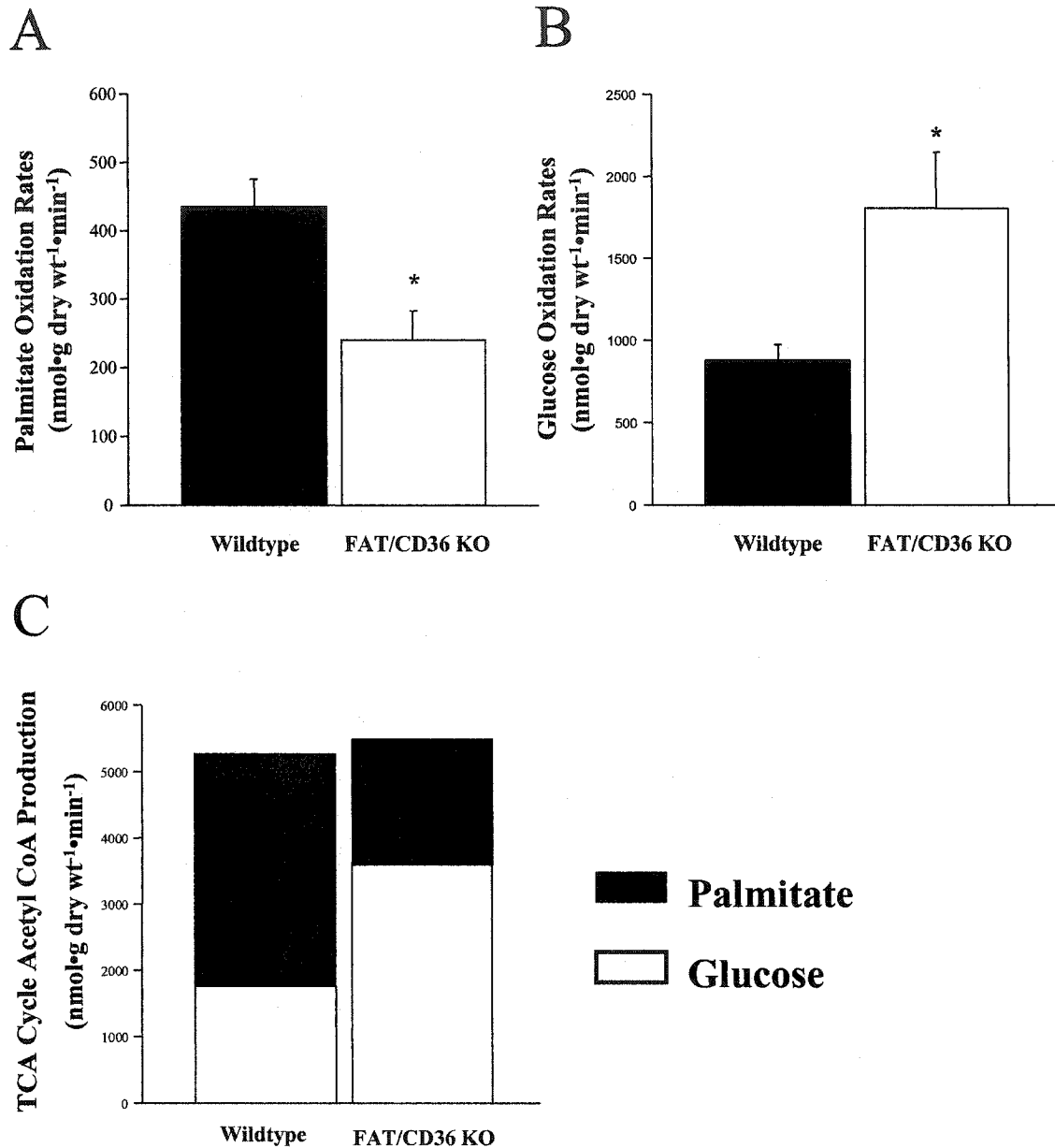


**Fig. 3-4. Palmitate oxidation (A), glucose oxidation (B) and tricarboxylic acid (TCA) acetyl-CoA production (C) for the TCA cycle in FAT/CD36 knockout (KO) and wildtype (WT) mouse hearts during reperfusion after ischemia.** Values represent the mean  $\pm$  S.E. 5 KO and 6 WT mouse hearts for palmitate oxidation; 8 KO and 7 WT mouse hearts for glucose oxidation. 13 KO and WT mouse hearts were used to calculate acetyl-CoA production from palmitate oxidation and glucose oxidation. TCA cycle activity was calculated from the rates of palmitate and glucose oxidation from A and B, using 8 mol of acetyl-CoA from every mol of palmitate oxidized and 2 mol of acetyl-CoA for every 1 mol of glucose oxidized. \*, significantly different from WT mouse hearts,  $p < 0.01$ .

## **Chapter 4**

# **The Role of FAT/CD36 and FACS in Cardiac Myocyte Fatty Acid Oxidation**

**Acknowledgements:** Neonatal cardiac myocytes were isolated by Suzanne Kovacic, and adenoviruses were constructed by Amy Barr

## Introduction

In adult cardiac myocytes the oxidation of fatty acids provides the majority of energy needed to support contractile function<sup>1</sup>. Although the heart has the ability to store fatty acids, it has a limited capacity to maintain its high metabolic demand on endogenous sources alone and relies on continuous uptake from blood<sup>2</sup>. Despite the obvious importance of fatty acid uptake to the cardiac myocyte, controversy exists with respect to the process by which fatty acids enter into cells. The two main mechanisms by which fatty acids are transported into cells are: 1) passive diffusion and/or 2) protein mediated transport<sup>3,4</sup>. Accumulating evidence supports a role for fatty acid translocase (FAT; also known as CD36<sup>5</sup>) in protein mediated fatty acid uptake in cardiac myocytes.

In studies using mice overexpressing FAT/CD36, palmitate oxidation rates in perfused soleus muscle from the overexpressors were significantly elevated, compared to WT controls<sup>6</sup>. Contrasting the characteristics of the FAT/CD36 KO mouse, the FAT/CD36 overexpressor exhibited significantly lower levels of plasma triglycerides, which suggests that the increase in the expression of FAT/CD36 results in higher levels of fatty acid uptake from the plasma. These studies provide evidence for the importance of FAT/CD36 in fatty acid transport in adipocytes and skeletal muscle. But the effect of FAT/CD36 overexpression on palmitate oxidation in the neonatal cardiac myocyte is currently unknown.

Studies have also been conducted investigating the role of FAT/CD36 in fatty acid oxidation in isolated adult rat cardiac myocytes. A study by Luiken et al<sup>5</sup> measured palmitate oxidation in the presence or absence of the FAT/CD36 inhibitor, sulfo-N-succinimidylolate (SSO) in quiescent and electrostimulated cardiac myocytes. The study

demonstrates that electrostimulation significantly increases palmitate oxidation, with a parallel increase in palmitate uptake. Upon incubation with SSO, both quiescent and electrostimulated myocytes exhibited palmitate oxidation rates significantly below controls<sup>5</sup>, suggesting that both basal and contraction-induced increase in fatty acid uptake is FAT/CD36 mediated. This also suggests that FAT/CD36 may be rate-limiting in fatty acid oxidation.

In cultured neonatal cardiac myocytes, treatment with fatty acid resulted in increased mRNA levels of FAT/CD36, heart-type fatty acid binding protein (H-FABP), fatty acyl CoA synthetase (FACS) and long-chain acyl-CoA dehydrogenase (LCAD) compared to cardiac myocytes exposed to glucose only<sup>7</sup>. This increase in the mRNA level of the proteins involved in fatty acid metabolism was accompanied by a 70% increase in rates of fatty acid oxidation<sup>7</sup>. The increase in gene expression was due to fatty acid activation of peroxisome proliferators-activated receptor  $\alpha$  (PPAR $\alpha$ ). The Van der Lee et al<sup>7</sup> study demonstrates that fatty acids can alter expression of FAT/CD36 and FACS, two proteins suggested to work in cooperation to promote fatty acid uptake into the cardiac myocyte<sup>8</sup>. However, the question of whether FAT/CD36 and FACS work in coordination to transport fatty acids remains unanswered.

FACS catalyzes the ligation of a fatty acid with coenzyme A which produces acyl CoAs<sup>9</sup>, which are substrates for energy metabolism and are required for synthesis of triglycerides and phospholipids (see <sup>10</sup> for review). Currently, five rat long-chain FACS isoforms have been cloned, each of which share common structural homology<sup>11</sup>. One isoform, FACS1, has been identified in the heart<sup>12</sup> and its expression has been shown to be induced by PPAR $\alpha$  ligands<sup>13,14</sup>. Since PPAR $\alpha$  ligands have been shown to increase

mRNA levels of genes involved in fatty acid metabolism<sup>7</sup>, FACS1 may play a role in fatty acid oxidation in the heart. Currently, it is not known if FAT/CD36 and FACS work coordinately to transport fatty acids into the cell.

A study by Van Nieuwenhoven et al have shown that FAT/CD36 and H-FABP exist in similar levels in the same tissues<sup>15</sup>. This is not unreasonable since a mechanism could exist where FAT/CD36 transports fatty acids into the cell and H-FABP binds the fatty acids, thereby maintaining the a concentration gradient of fatty acid across the membrane. These possible cooperative mechanisms may also exist in cardiac myocytes and can be examined. Schaffer and Lodish have proposed a model by which protein-mediated transport of long-chain fatty acids into the cell and activation by FACS1 are tightly coupled, thereby preventing the backflow of fatty acids across the membrane<sup>16</sup>. Studies on adipocytes have already shown that FACS and FATP work coordinately to increase fatty acid uptake<sup>17</sup>, suggesting that fatty acid uptake is tightly coupled with metabolism. Moreover, the same study also shows that FACS resides in the plasma membrane, much like FAT/CD36<sup>17</sup>. Therefore, it is not inconceivable that FACS1 may play a role in fatty acid metabolism, in coordination with FAT/CD36. In fact, a study by Luiken et al<sup>4</sup> have shown that long-chain fatty acid uptake and metabolism are tightly coupled by the conversion of fatty acids into acyl CoA by FACS1 in adult cardiac myocytes. In line with the previous study, a more recent study by Luiken et al<sup>8</sup> has shown that mRNA of FACS and FAT/CD36 increase in a linear fashion to the same degree upon muscle stimulation. Moreover, the increases in FAT/CD36 and FACS1 mRNA induced by muscle contraction are highly correlated. The coordinate increase in both FAT/CD36 and FACS1 may allow a greater rate of fatty acid transport into the cells during times of

energy demand. Despite this hypothesis, direct evidence demonstrating cooperation between FACS and FAT/CD36 in fatty acid metabolism has not been shown. Therefore, the purpose of this study was to coordinately express FACS and FAT/CD36 in neonatal rat cardiac myocytes and measure rates of palmitate uptake and utilization.

## **Hypothesis**

We hypothesize that FAT/CD36 and FACS cooperate in order to transport fatty acids across the plasma membrane. Therefore, we expect that the neonatal rat cardiac myocytes expressing FAT/CD36 or FACS alone will not exhibit higher rates of palmitate uptake. On the other hand, cardiac myocytes expressing both FAT/CD36 and FACS will exhibit significantly higher rates of palmitate uptake and utilization.

## **Methods and Materials**

*Cell Culture.* As described in the Methods and Materials section.

*Adenovirus Construction.* The adenoviruses were constructed as described for Ad.GFP<sup>18</sup>, Ad.FACS<sup>19</sup>, Ad.Null and Ad.CD36<sup>20</sup>.

*Adenovirus Infection of Rat Neonatal Cardiac Myocytes.* After 18 hours of culture, isolated neonatal rat cardiac myocytes were rinsed 2 times with Hank's Balanced Salt Solution (Gibco) and infected with 10 plaque forming units (PFU) of adenovirus, as follows:

Ad.Null + Ad.GFP, Ad.CD36 + Ad.GFP, Ad.Null + Ad.FACS, Ad.CD36 + Ad.FACS

Ad.Null – virus that encodes the vector for the CD36 virus

Ad.GFP – virus that encodes for green fluorescent protein

Ad.CD36 – virus that encodes for CD36

Ad.FACS – Virus that encodes for fatty acyl CoA synthetase

After infection, the media was changed to DMEM supplemented with ITS and a selective inhibitor of DNA synthesis, cytosine (BETA)-D-arabinofuranoside free base (AraC) (SIGMA), and cultured for an additional 48 hrs.

*Measurement of Fatty Acid Oxidation in Rat Neonatal Cardiac Myocytes.* As described in the Methods and Materials section.

*Triacylglyceride Measurements.* As described in the Methods and Materials section.

*Lipid Extraction for Thin Layer Chromatography.* 90  $\mu$ L samples were taken from cardiac myocyte cell homogenates from fatty acid oxidation assay and aliquoted into glass tubes. 1 mL of methanol was added to the sample, followed by 500  $\mu$ L of chloroform. If the mixed sample was not monophasic, than methanol was added drop wise until sample was one phase. Next, 500  $\mu$ L of 1 M NaCl, which was slightly acidified with acetic acid, was added, followed by 1 mL of chloroform. This resulted in a biphasic sample consisting of organic and aqueous phases. The samples were centrifuged at 1000 rpm for 5 min to further separate the phases. After centrifugation, the organic phase (bottom) was collected carefully, without contamination from the upper aqueous phase, and the extraction protocol was repeated on the aqueous phase to further extract the

lipids. The two organic phases were pooled in a glass tube and dried under a stream of N<sub>2</sub>. The dried residue was dissolved in 200  $\mu$ L of 2:1 chloroform:methanol.

*Thin Layer Chromatography.* Extracted lipids were loaded onto a Silica Gel G plate (FISHERbrand). The silica gel was placed in a TLC tank containing heptane:diisopropyl ether:acetic acid, at a ratio of 60:40:4, respectively. The plate was air dried and visualized with iodine vapors and TG segments were marked. The TLC plate was steamed in order to soften the silica and marked areas were scrapped and counted after addition of 5 mL of scintillation fluid (Cytoscint). The remainder of the TLC plate was scrapped and counted in order to determine lipid content, excluding TG.

*Western Blot Analysis.* Heart tissue was homogenized in buffer containing 20mM Tris-HCL, pH 7.4, 50mM NaCl, 50 mM NaF, 5mM Na pyrophosphate, 0.25 M sucrose, protease inhibitor cocktail #1 (Sigma P8340), phosphatase inhibitor cocktail (Sigma P2850) and 1M DTT. Protein was separated using SDS-PAGE and transferred to nitrocellulose membranes. Membranes were blocked with 5% milk in Tris-buffered-saline solution containing 0.1% Tween (TBST). Membranes were incubated with antibodies against FAT/CD36 (Cascade Bioscience) and FACS, washed 3-times with TBST, then incubated with a secondary antibody (See Antibody Table) conjugated to horseradish peroxidase and washed 3-times TBST. Signals were visualized using the ECL detection system (Amersham). Densitometric scans were taken with the GS-800 scanner and analyzed with Quantity One software.

*Statistical Analysis-* Multiple comparisons were calculated using an unpaired ANOVA was conducted with a Student-Newmann-Keuls post test. Differences were judged to be significant when  $p < 0.05$ .

## **Results**

*FACS Infection of Neonatal Rat Cardiac Myocytes.* Neonatal rat cardiac myocytes were infected with 10 PFU of FACS adenovirus. After 48 hours, all lysates were subject to immunoblot analysis against anti-FACS antibody (Figure 4-1A). Cells infected with Ad.FACS demonstrate a significant increase in FACS expression, as compared to Ad.GFP infected cells. The associated densitometric analysis demonstrates the overexpression of FACS in the Ad.FACS infected myocytes (Figure 4-1B).

*FAT/CD36 Infection of Neonatal Cardiac Myocytes.* Neonatal rat cardiac myocytes were infected with 10 PFU of Ad.CD36 adenovirus. After 48 hours, all lysates were subject to immunoblot analysis against anti-CD36 antibody (Figure 4-2A). Cells infected with Ad.CD36 demonstrate a significant increase in FAT/CD36 expression, as compared to Ad.Null infected cells. The associated densitometric analysis demonstrates the overexpression of FAT/CD36 in the Ad.CD36 infected myocytes (Figure 4-2B). There is no FAT/CD36 in the Ad.Null infected cells because we probed with a mouse specific FAT/CD36 antibody because the Ad.CD36 virus codes for a mouse isoform of FAT/CD36.

*Rates of Fatty Acid Oxidation in Neonatal Rat Cardiac Myocytes.* Rates of fatty acid oxidation were a function of specific activity of the non metabolized palmitate buffer. In order to establish linearity of our fatty acid oxidation assay, cardiac myocytes were incubated with 1.2 mM [<sup>3</sup>H]palmitate buffer for 0, 1.5, 3, 3.5 and 6 hours and rates of fatty acid oxidation were measured. The effect of time of incubation on rates of fatty acid oxidation is shown (Figure 4-3). Since fatty acid oxidation rates are linear at 3 hours of incubation with 1.2 mM [<sup>3</sup>H]palmitate, this incubation time was chosen for subsequent fatty acid oxidation assays. The mean rates of fatty acid oxidation, from six independent cardiac myocyte preparations, from each group were pooled and graphed. In figure 4-4, the Ad.Null/Ad.GFP infected group was normalized to 100 percent. Figure 4-4 demonstrates that cells expressing FAT/CD36 displayed marginally increased rates fatty acid oxidation, but did not reach statistical significance as compared to control (100 vs. 122±24). Moreover, cells expressing FACS also demonstrated slightly increased rates of fatty acid oxidation over control rates, but again, did not reach statistical significance (100 vs. 154±26). In cells infected with both FACS and FAT/CD36, the rates of fatty acid oxidation significantly increase above control rates (100 vs. 187±24).

*Rates of Palmitate Incorporation into Triglyceride.* Rates of labeled palmitate incorporation into triglyceride stores in neonatal cardiac myocytes are shown in Figure 4-5. In figure 4-5, the Ad.Null/Ad.GFP infected group was normalized to 100 percent. There are no significant differences between the Ad.Null/Ad.GFP control group and the experimental groups. Although the Ad.CD36/Ad.GFP group exhibits a trend for an increase in rates of triglyceride above the control, the values do not reach statistical

significance (100 vs.  $149 \pm 39$ ). Moreover, rates of triglyceride incorporation appear to be enhanced in the Ad.Null/Ad.FACS group, compared to both the Ad.Null/Ad.GFP and Ad.CD36/Ad.GFP groups, but again, they do not reach statistical significance ( $203 \pm 53$  vs. 100 and  $203 \pm 53$  vs.  $149 \pm 39$ , respectively).

*Rates of Palmitate Incorporation into Lipids.* Rates of labeled palmitate incorporation into lipids in neonatal rat cardiac myocytes are depicted in Figure 4-6. In Figure 4-6, the Ad.Null/Ad.GFP infected group was normalized to 100 percent. There is no significant difference in rates of palmitate incorporation into lipids between Ad.CD36/Ad.GFP and Ad.Null/Ad.GFP control ( $111 \pm 26$  vs. 100). Similarly, the Ad.Null/Ad.FACS and Ad.Null/Ad.GFP groups exhibited no significant difference in palmitate incorporation ( $145 \pm 23$  vs. 100). On the other hand, the Ad.CD36/Ad.FACS group exhibited significantly higher rates of palmitate incorporation into lipids, as compared to controls ( $219 \pm 43$  vs. 100, respectively).

*Rates of Fatty Acid Uptake into Neonatal Rat Cardiac Myocytes.* Rates of fatty acid uptake into neonatal rat cardiac myocytes are displayed in Figure 4-7. In figure 4-7, the Ad.Null and Ad.GFP infected group was normalized to 100 percent. Rates of fatty acid uptake in Ad.CD36/Ad.GFP and Ad.Null/Ad.FACS groups are not significantly different from control groups ( $107 \pm 9$  vs. 100 and  $139 \pm 9$  vs. 100, respectively). On the other hand, the Ad.CD36/Ad.FACS group exhibited significantly higher rates of fatty acid uptake, as compared to controls ( $168 \pm 20$  vs. 100).

*Measurement of Total Triglyceride Pool in Neonatal Rat Cardiac Myocytes.* In order to determine if either FAT/CD36 and/or FACS expression altered triglyceride pools, the total triglyceride pool was measured using the L-Type TG H kit (WAKO). Aliquots were taken from myocyte cell homogenates from fatty acid oxidation assay and assayed for total triglycerides. Total triglyceride pools in neonatal cardiac myocytes infected with specific viruses are depicted in Figure 4-8. There were no significant differences in the amount of total triglyceride in each experimental group of cardiac myocytes.

*Rates of Palmitate Incorporation in Neonatal Rat Cardiac Myocytes.* The total rate of palmitate utilization is shown in Fig. 4-9. There is no change in the amount of palmitate utilized by cells infected with Ad.CD36/Ad.GFP or Ad.Null/Ad.FACS alone, as compared to the control. However, when cells are infected with Ad.CD36 and Ad.FACS, there is an increase in palmitate utilization, specifically oxidation.

## **Discussion**

The relatively low levels of proteins involved in fatty acid uptake and metabolism render the neonatal rat cardiac myocyte an excellent model for the study of cooperation between FAT/CD36 and FACS in fatty acid uptake. Using this model, we are able to overexpress selected proteins in an environment where endogenous levels of these proteins are low. This allows us to elucidate the role of FAT/CD36 and FACS in fatty acid transport and metabolism. Despite the benefit of this model, the use of cardiac myocytes is limited by the fact that they are not performing sufficient amounts of

contractile work. Therefore, measurements of metabolism differ from those observed in the isolated working heart.

These are the first studies that demonstrate that FAT/CD36 or FACS alone is not adequate to significantly increase rates of fatty acid uptake in neonatal rat cardiac myocytes. However, when FAT/CD36 and FACS are expressed together, a significant increase in fatty acid uptake is observed. Expression of both FAT/CD36 and FACS, also resulted in a significant increase in rates of fatty acid oxidation and incorporation of palmitate into lipids, as compared to the Ad.Null/Ad.GFP group. This suggests that the increased levels of fatty acid that entered the myocytes were shuttled towards the mitochondria in order to be oxidized and directed towards lipid esterification.

In the present study, it appears that FAT/CD36 overexpression alone does not lead to increased rates of fatty acid oxidation. This is in direct contrast to a study by Ibrahimi et al<sup>6</sup>, which demonstrated that contracting muscle from FAT/CD36 transgenic mice exhibited significantly higher levels of fatty acid oxidation, as compared to controls. Although the reason(s) for this discrepancy is(are) unknown, the differences in the data may be due to the use of adult skeletal muscle in the Ibrahimi study versus the use of neonatal rat cardiac myocytes in the present study. Earlier studies have shown that the fetal heart relies mainly on glucose as an energy substrate<sup>21,22</sup>. Upon birth, the post-natal heart exhibits an enhanced ability to oxidize fatty acids<sup>23</sup>. In addition, it has been demonstrated that neonatal rat cardiac myocytes exhibit low levels of PPAR transcription factors, which are responsible for activating genes involved in fatty acid metabolism<sup>24,25,26</sup>. Taken together, these data suggest that the neonatal rat cardiac myocyte may exhibit hindered fatty acid metabolism as compared to adult soleus muscle,

since the expression of proteins involved in fatty acid transport, such as FACS and FATP, are diminished in neonatal rat cardiac myocytes. Therefore, fatty acid oxidation is able to increase in the adult soleus because other proteins involved in fatty acid transport are expressed, whereas expression of these proteins is lower in the neonatal rat cardiac myocyte. This further implicates the presence of a fatty acid transport complex, as being essential for fatty acid uptake.

The present study demonstrates that fatty acid uptake was only moderately increased when FAT/CD36 or FACS were expressed, suggesting that FAT/CD36 or FACS expression alone was not sufficient to increase the amount of fatty acid transported across the sarcolemmal membrane. However, when FAT/CD36 and FACS were coexpressed, there was a significant increase in the rate of palmitate transport across the membrane (Figure 4-7). This suggests that FAT/CD36 and FACS may work coordinately in order to transport fatty acids into the cell. This is in line with data from Luiken et al which suggest that fatty acid uptake and metabolism are tightly coupled in cardiac myocytes<sup>4</sup>. Although we cannot confirm this in the present study, it is not unreasonable to hypothesize that FACS associates with FAT/CD36 at the plasma membrane, in order to convert the incoming fatty acids into fatty acyl CoA esters. This concept is not unlike that of Van Nieuwenhoven et al<sup>15</sup>, where FAT/CD36 and H-FABP are coexpressed in the heart and skeletal muscle and their association has been shown in the mammary gland<sup>27</sup>, or that of Gimeno et al<sup>28</sup>, where FAT/CD36 has been shown to colocalize with FATP6. Therefore, it has already been shown that FAT/CD36 associates with proteins, H-FABP and FATP6, are involved in fatty acid transport across the sarcolemmal membrane, much like FACS.

In this study, we also demonstrate that the labeled palmitate that was transported into the myocytes and not oxidized was incorporated into lipids stores. The myocytes expressing FAT/CD36 alone do not exhibit a significant increase in lipid incorporation (Figure 4-6). On the other hand, myocytes expressing both FAT/CD36 and FACS exhibited significantly higher rates of lipid incorporation, as compared to FAT/CD36 and FACS expressed alone (Figure 4-6). Again, this supports the hypothesis that FACS and FAT/CD36 work in cooperation to transport fatty acids into the myocyte.

## **Conclusion**

Taken together, the data presented in this chapter suggest that FAT/CD36 and FACS are able to function in cooperation to transport fatty acids into neonatal cardiac myocytes. Although the mechanism by which this occurs remains unknown, it is likely that FAT/CD36 transports fatty acids across the plasma membrane, where FACS can activate the fatty acid by converting it into an acyl CoA. This would lead to formation of an acyl CoA sink which would maintain a fatty acid gradient and allow more fatty acids to be transported into the myocyte. The data suggest that FAT/CD36 and FACS are able to interact cooperatively and alter fatty acid uptake and metabolism in the neonatal rat cardiac myocyte. Further studies need to be conducted in order to investigate the role of expressing H-FABP and/or FATP on the uptake of fatty acids. This would determine whether FAT/CD36 is able to function in cooperation with H-FABP and/or FATP in the heart.

## References

1. Saddik M, Lopaschuk GD. Myocardial triglyceride turnover and contribution to energy substrate utilization in isolated working rat hearts. *J Biol Chem.* 1991;266:8162-70.
2. van der Vusse GJ, Glatz JF, Stam HC, Reneman RS. Fatty acid homeostasis in the normoxic and ischemic heart. *Physiol Rev.* 1992;72:881-940.
3. van der Vusse GJ, van Bilsen M, Glatz JF. Cardiac fatty acid uptake and transport in health and disease. *Cardiovasc Res.* 2000;45:279-93.
4. Luiken JJ, van Nieuwenhoven FA, America G, van der Vusse GJ, Glatz JF. Uptake and metabolism of palmitate by isolated cardiac myocytes from adult rats: involvement of sarcolemmal proteins. *J Lipid Res.* 1997;38:745-58.
5. Luiken JJ, Willems J, van der Vusse GJ, Glatz JF. Electrostimulation enhances FAT/CD36-mediated long-chain fatty acid uptake by isolated rat cardiac myocytes. *Am J Physiol Endocrinol Metab.* 2001;281:E704-12.
6. Ibrahim A, Bonen A, Blinn WD, Hajri T, Li X, Zhong K, Cameron R, Abumrad NA. Muscle-specific overexpression of FAT/CD36 enhances fatty acid oxidation by contracting muscle, reduces plasma triglycerides and fatty acids, and increases plasma glucose and insulin. *J Biol Chem.* 1999;274:26761-6.
7. van der Lee KA, Vork MM, De Vries JE, Willemsen PH, Glatz JF, Reneman RS, Van der Vusse GJ, Van Bilsen M. Long-chain fatty acid-induced changes in gene expression in neonatal cardiac myocytes. *J Lipid Res.* 2000;41:41-7.

8. Luiken JJ, Han XX, Dyck DJ, Bonen A. Coordinately regulated expression of FAT/CD36 and FACS1 in rat skeletal muscle. *Mol Cell Biochem.* 2001;223:61-9.
9. Kornberg A, Pricer WE, Jr. Enzymatic synthesis of the coenzyme A derivatives of long chain fatty acids. *J Biol Chem.* 1953;204:329-43.
10. Faergeman NJ, Knudsen J. Role of long-chain fatty acyl-CoA esters in the regulation of metabolism and in cell signalling. *Biochem J.* 1997;323 ( Pt 1):1-12.
11. Coleman RA, Lewin TM, Muoio DM. Physiological and nutritional regulation of enzymes of triacylglycerol synthesis. *Annu Rev Nutr.* 2000;20:77-103.
12. Memon RA, Fuller J, Moser AH, Smith PJ, Feingold KR, Grunfeld C. In vivo regulation of acyl-CoA synthetase mRNA and activity by endotoxin and cytokines. *Am J Physiol.* 1998;275:E64-72.
13. Schoonjans K, Staels B, Grimaldi P, Auwerx J. Acyl-CoA synthetase mRNA expression is controlled by fibric-acid derivatives, feeding and liver proliferation. *Eur J Biochem.* 1993;216:615-22.
14. Schoonjans K, Watanabe M, Suzuki H, Mahfoudi A, Krey G, Wahli W, Grimaldi P, Staels B, Yamamoto T, Auwerx J. Induction of the acyl-coenzyme A synthetase gene by fibrates and fatty acids is mediated by a peroxisome proliferator response element in the C promoter. *J Biol Chem.* 1995;270:19269-76.
15. Van Nieuwenhoven FA, Willemsen PH, Van der Vusse GJ, Glatz JF. Co-expression in rat heart and skeletal muscle of four genes coding for proteins implicated in long-chain fatty acid uptake. *Int J Biochem Cell Biol.* 1999;31:489-98.

16. Schaffer JE, Lodish HF. Expression cloning and characterization of a novel adipocyte long chain fatty acid transport protein. *Cell*. 1994;79:427-36.
17. Gargiulo CE, Stuhlsatz-Krouper SM, Schaffer JE. Localization of adipocyte long-chain fatty acyl-CoA synthetase at the plasma membrane. *J Lipid Res*. 1999;40:881-92.
18. He TC, Zhou S, da Costa LT, Yu J, Kinzler KW, Vogelstein B. A simplified system for generating recombinant adenoviruses. *Proc Natl Acad Sci U S A*. 1998;95:2509-14.
19. Kirshenbaum LA, Schneider MD. Adenovirus E1A represses cardiac gene transcription and reactivates DNA synthesis in ventricular myocytes, via alternative pocket protein- and p300-binding domains. *J Biol Chem*. 1995;270:7791-4.
20. Webb NR, de Beer MC, van der Westhuyzen DR, Kindy MS, Banka CL, Tsukamoto K, Rader DL, de Beer FC. Adenoviral vector-mediated overexpression of serum amyloid A in apoA-I-deficient mice. *J Lipid Res*. 1997;38:1583-90.
21. Fisher DJ, Heymann MA, Rudolph AM. Myocardial consumption of oxygen and carbohydrates in newborn sheep. *Pediatr Res*. 1981;15:843-6.
22. Fisher DJ, Heymann MA, Rudolph AM. Myocardial oxygen and carbohydrate consumption in fetal lambs in utero and in adult sheep. *Am J Physiol*. 1980;238:H399-405.
23. Werner JC, Sicard RE, Schuler HG. Palmitate oxidation by isolated working fetal and newborn pig hearts. *Am J Physiol*. 1989;256:E315-21.

24. Gilde AJ, van der Lee KA, Willemsen PH, Chinetti G, van der Leij FR, van der Vusse GJ, Staels B, van Bilsen M. Peroxisome proliferator-activated receptor (PPAR) alpha and PPARbeta/delta, but not PPARgamma, modulate the expression of genes involved in cardiac lipid metabolism. *Circ Res.* 2003;92:518-24.
25. Sato O, Kuriki C, Fukui Y, Motojima K. Dual promoter structure of mouse and human fatty acid translocase/CD36 genes and unique transcriptional activation by peroxisome proliferator-activated receptor alpha and gamma ligands. *J Biol Chem.* 2002;277:15703-11.
26. Holst D, Luquet S, Nogueira V, Kristiansen K, Leverve X, Grimaldi PA. Nutritional regulation and role of peroxisome proliferator-activated receptor delta in fatty acid catabolism in skeletal muscle. *Biochim Biophys Acta.* 2003;1633:43-50.
27. Spitsberg VL, Matitashvili E, Gorewit RC. Association and coexpression of fatty-acid-binding protein and glycoprotein CD36 in the bovine mammary gland. *Eur J Biochem.* 1995;230:872-8.
28. Gimeno RE, Ortegon AM, Patel S, Punreddy S, Ge P, Sun Y, Lodish HF, Stahl A. Characterization of a heart-specific fatty acid transport protein. *J Biol Chem.* 2003;278:16039-44.

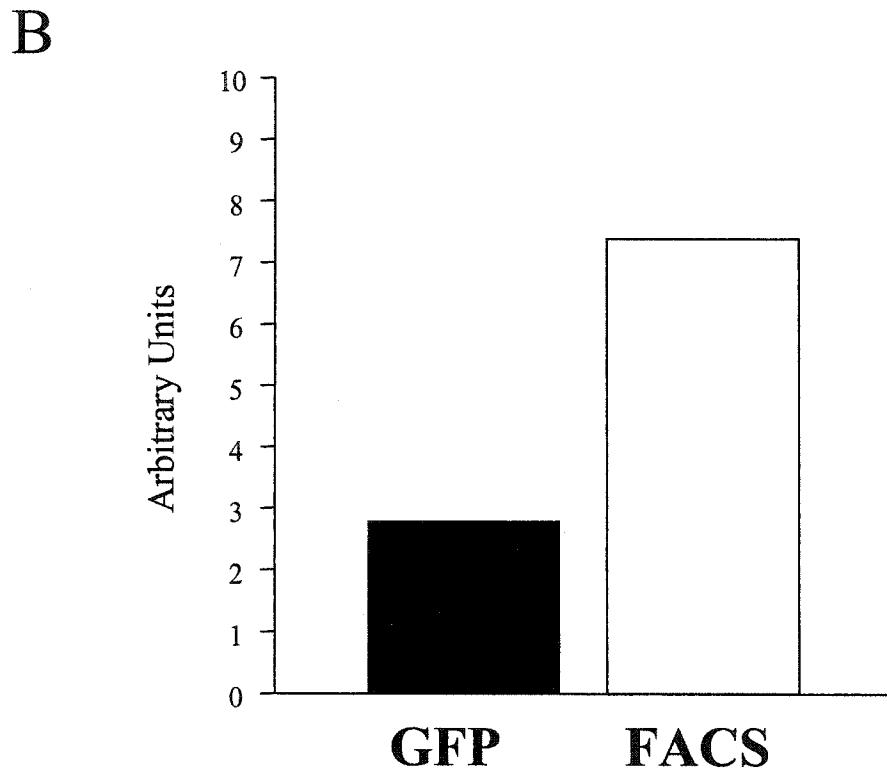
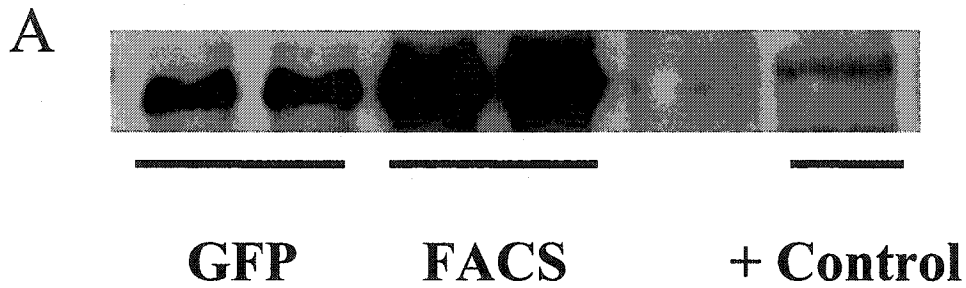
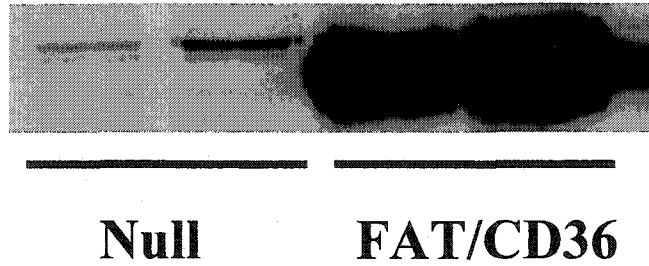


**Fig. 4-1. Expression of FACS in cardiac myocytes infected with GFP or FACS virus.** Western blot of homogenates from cardiac myocytes infected with GFP or FACS virus and probed with FACS antibody (A). Included is the associated densitometric analysis of the Western blot (B). Western blot protocol was conducted as described in “Methods and Materials” section.

**A**



**B**

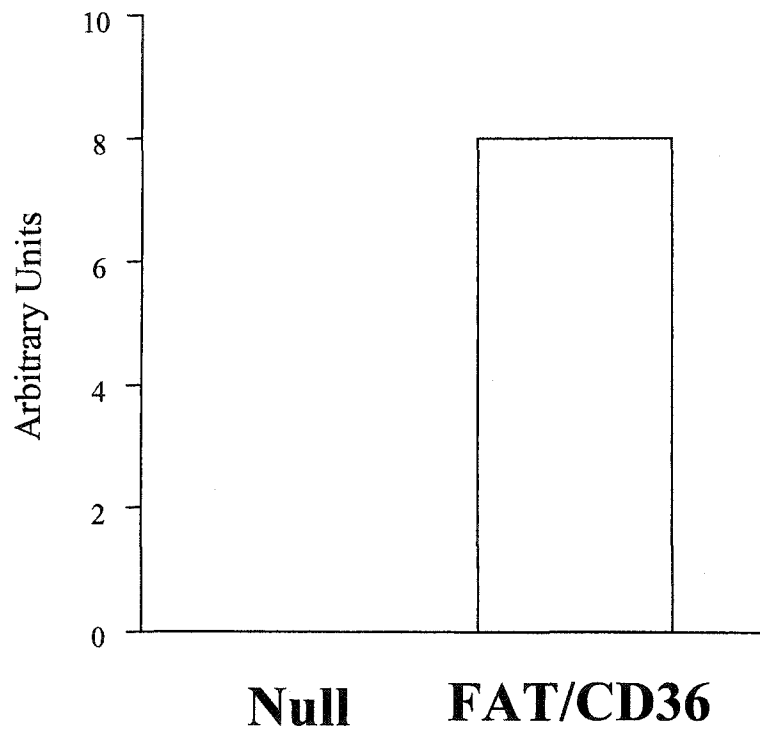


**Fig. 4-2. Expression of FAT/CD36 in cardiac myocytes infected with GFP or CD36 virus.** Western blot of homogenates from cardiac myocytes infected with GFP or CD36 virus and probed with FAT/CD36 antibody (A). Included is the associated densitometric analysis of the Western blot (B). Western blot protocol was conducted as described in “Methods and Materials” section.

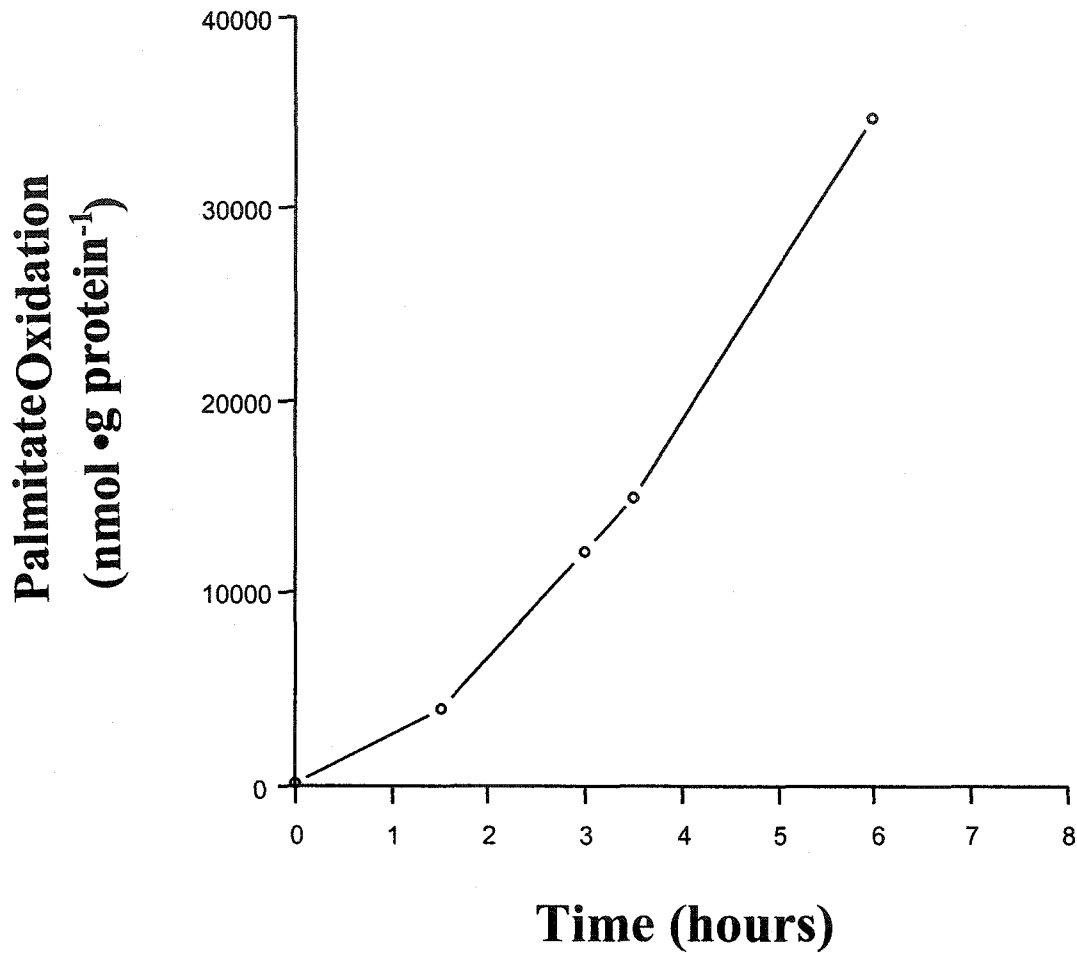


Fig. 4-3. **The effect of time on rates of fatty acid oxidation in cardiac myocytes.** Palmitate oxidation was calculated as function of  $^3\text{H}_2\text{O}$  production and was quantified as described in "Methods and Materials". Rates of palmitate oxidation are expressed as nmol of palmitate oxidized per gram protein. Values are the mean of one sample in duplicate per time interval.

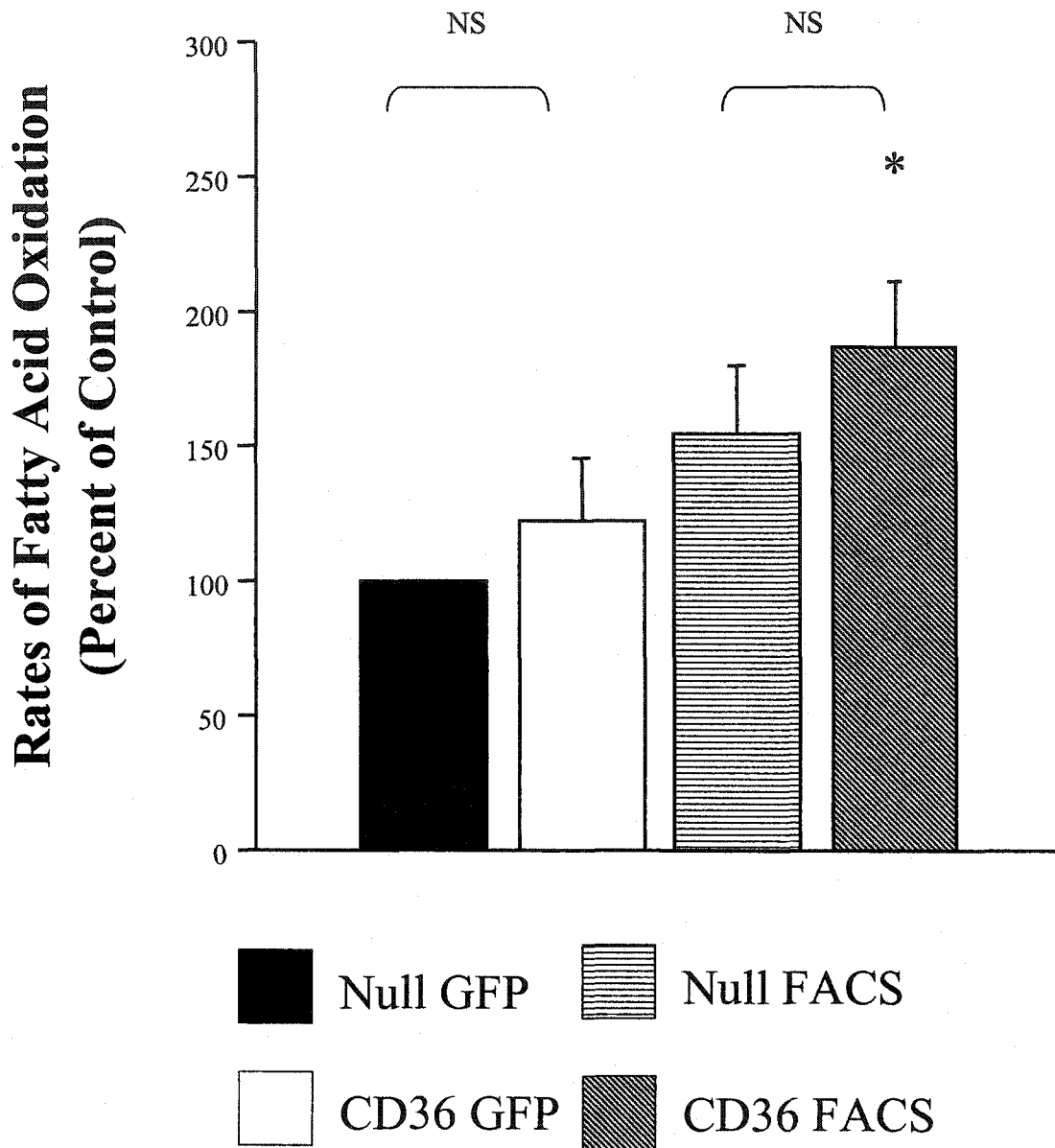


Fig. 4-4. Rates of palmitate oxidation in neonatal rat cardiac myocytes. Palmitate oxidation were calculated as a function of the amount of palmitate oxidized per gram cell mass per minute and expressed as a percent of control (Null GFP). Cell mass was calculated as a mean of eighteen pellets from neonatal cardiac rat myocyte cell homogenates. Data are means  $\pm$  S.E. of six experiments carried out with six different cardiomyocyte cell preparations. \*, signifies significantly different from Null GFP infected cardiac myocytes,  $p < 0.05$ . NS, signifies not significant.

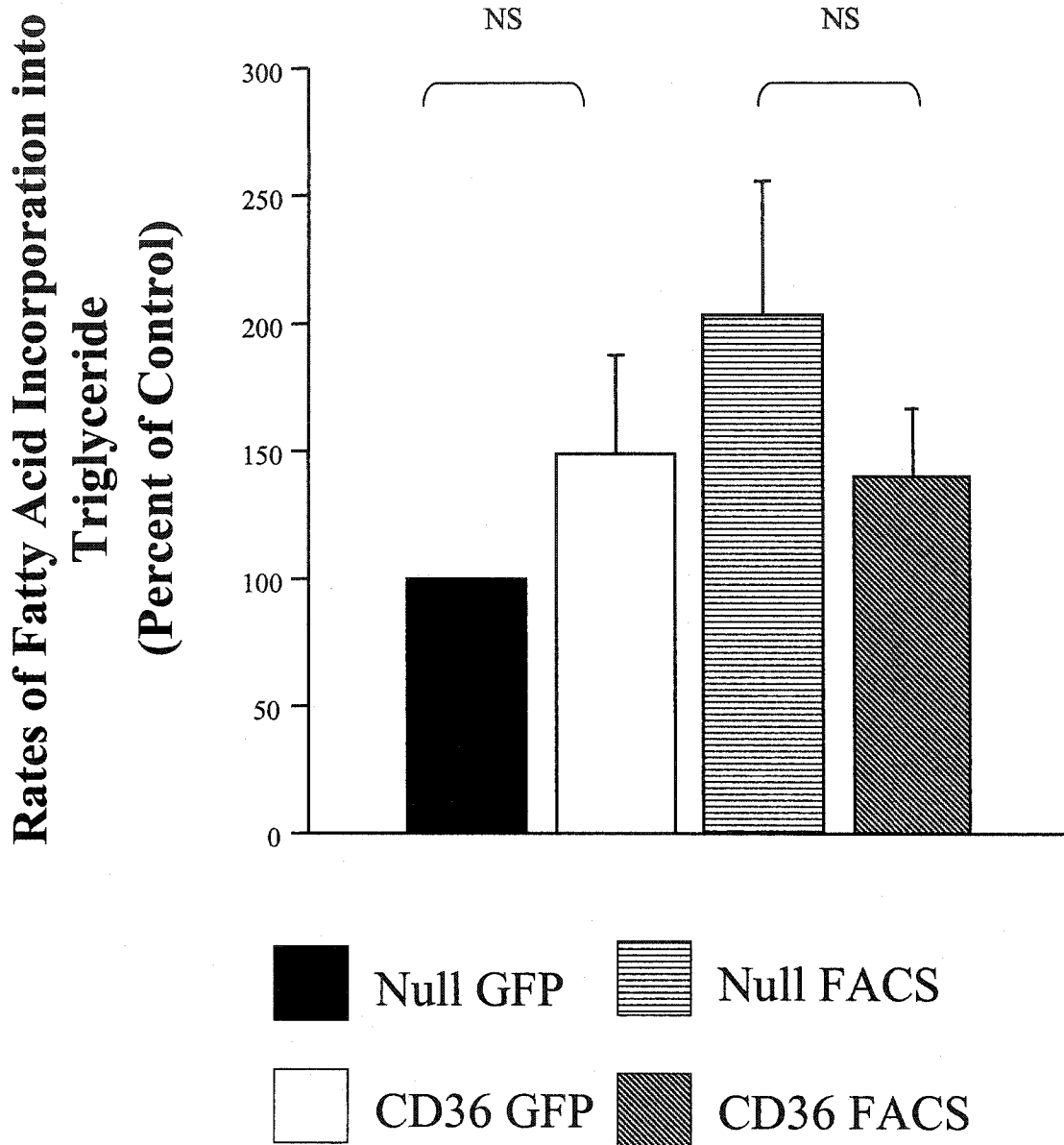


Fig. 4-5. **Rates of palmitate incorporation into triglycerides in neonatal rat cardiac myocytes.** Palmitate incorporation into triglycerides was calculated as a function of the amount of palmitate incorporated per gram cell mass per minute and expressed as a percent of control (Null GFP). Cell mass was calculated as a mean of eighteen pellets from neonatal cardiac rat myocyte cell homogenates. Data are means  $\pm$  S.E. of six experiments carried out with six different cardiomyocyte cell preparations. NS, signifies not significant.

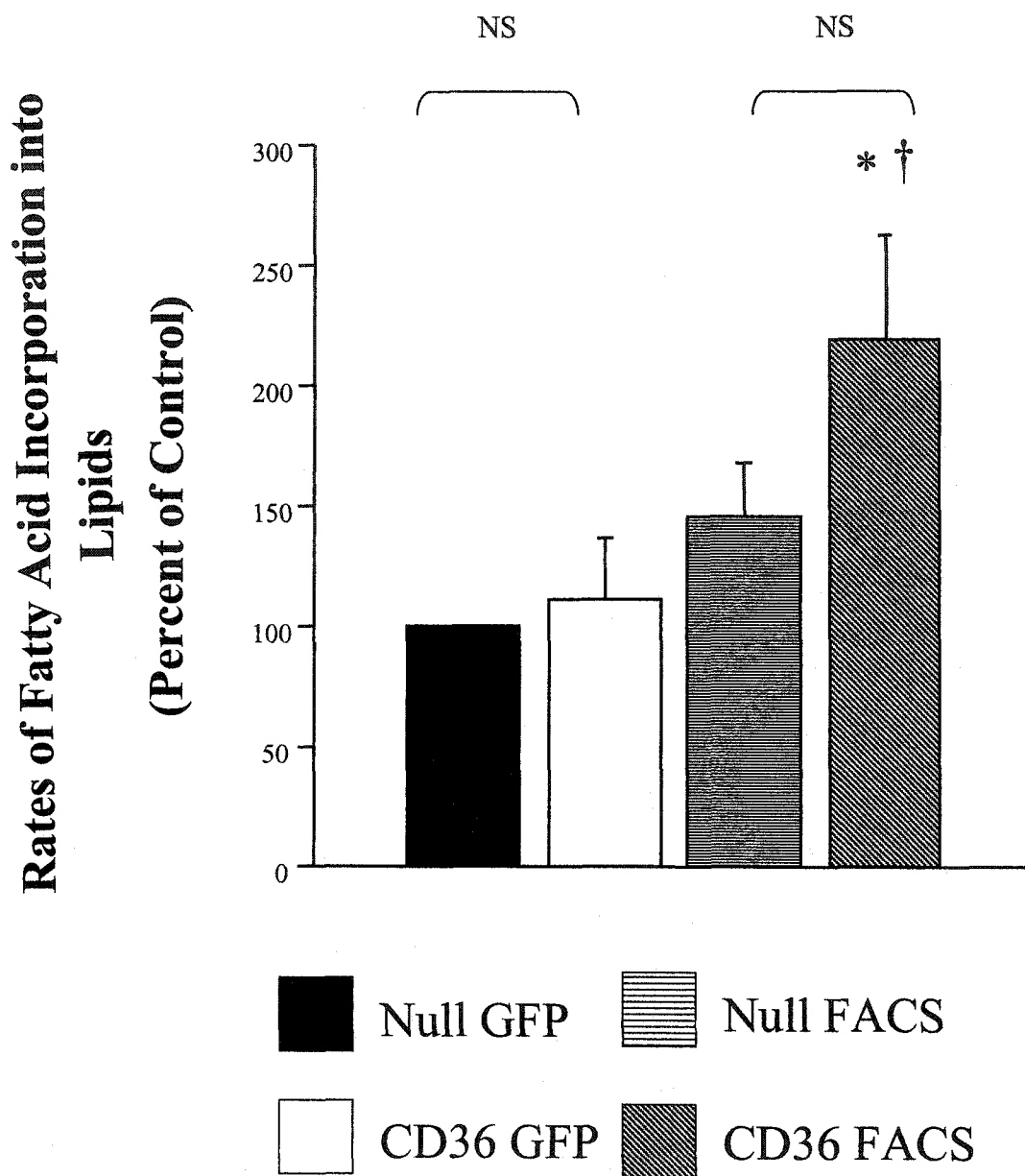


Fig. 4-6. **Rates of palmitate incorporation into lipids in neonatal rat cardiac myocytes.** Palmitate incorporation was calculated as a function of the amount of palmitate oxidized per gram cell mass per minute and expressed as a percent of control (Null GFP). Cell mass was calculated as a mean of eighteen pellets from neonatal cardiac rat myocyte cell homogenates. Data are means  $\pm$  S.E. of six experiments carried out with six different cardiomyocyte cell preparations. \*, signifies significantly different from Null GFP infected cardiac myocytes,  $p < 0.05$ . †, signifies significantly different from Ad.CD36 GFP infected cardiac myocytes,  $p < 0.05$ . NS, signifies not significant.

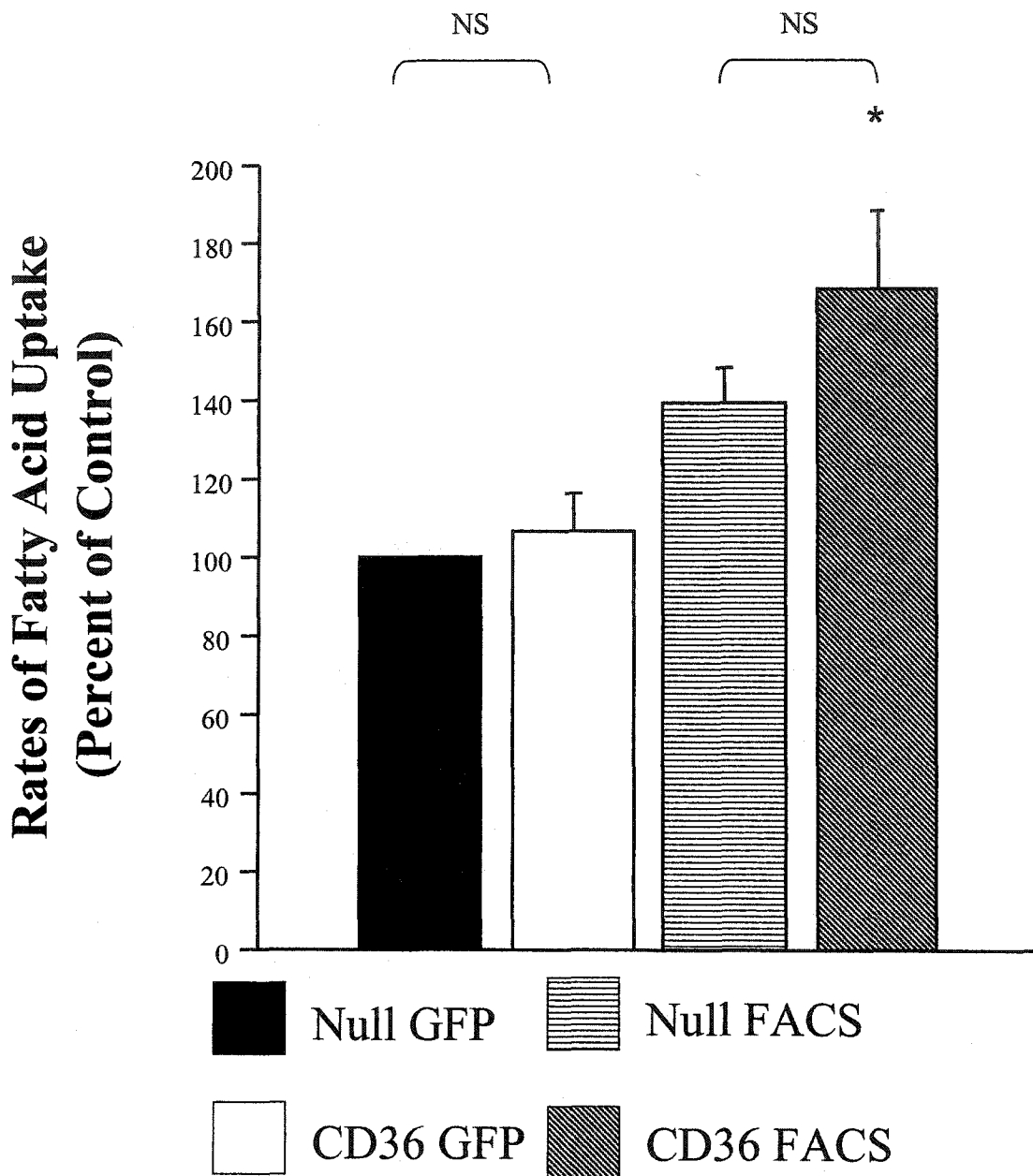


Fig. 4-7. **Rates of palmitate uptake in neonatal rat cardiac myocytes.** Palmitate uptake was calculated as the sum of fatty acid oxidation, palmitate incorporation into triglycerides and palmitate incorporation into neutral lipids. Data are means  $\pm$  S.E. of six experiments carried out with six different cardiomyocyte cell preparations. \*, signifies significantly different from Null GFP infected cardiac myocytes,  $p < 0.05$ . NS, signifies not significant.

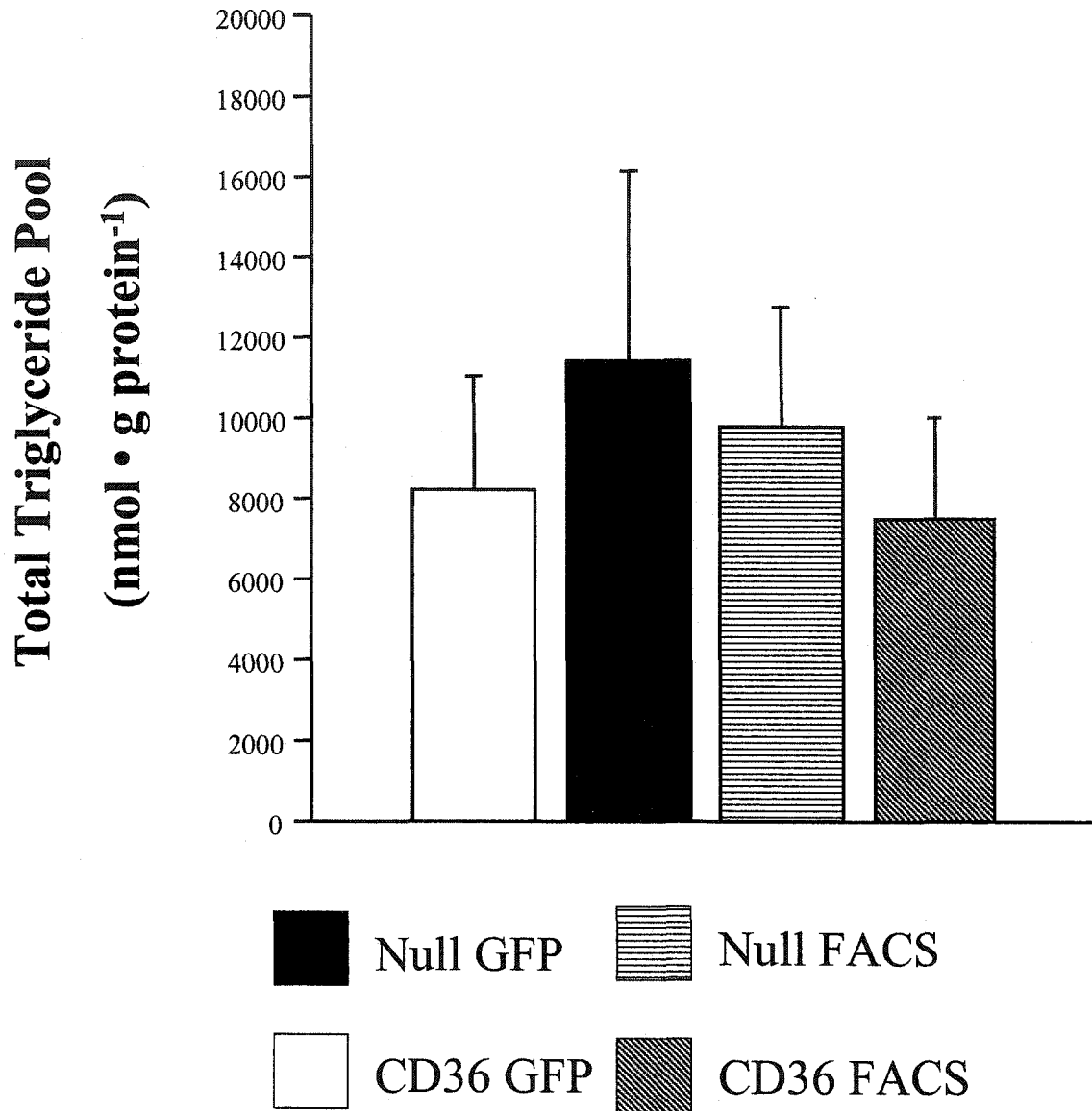
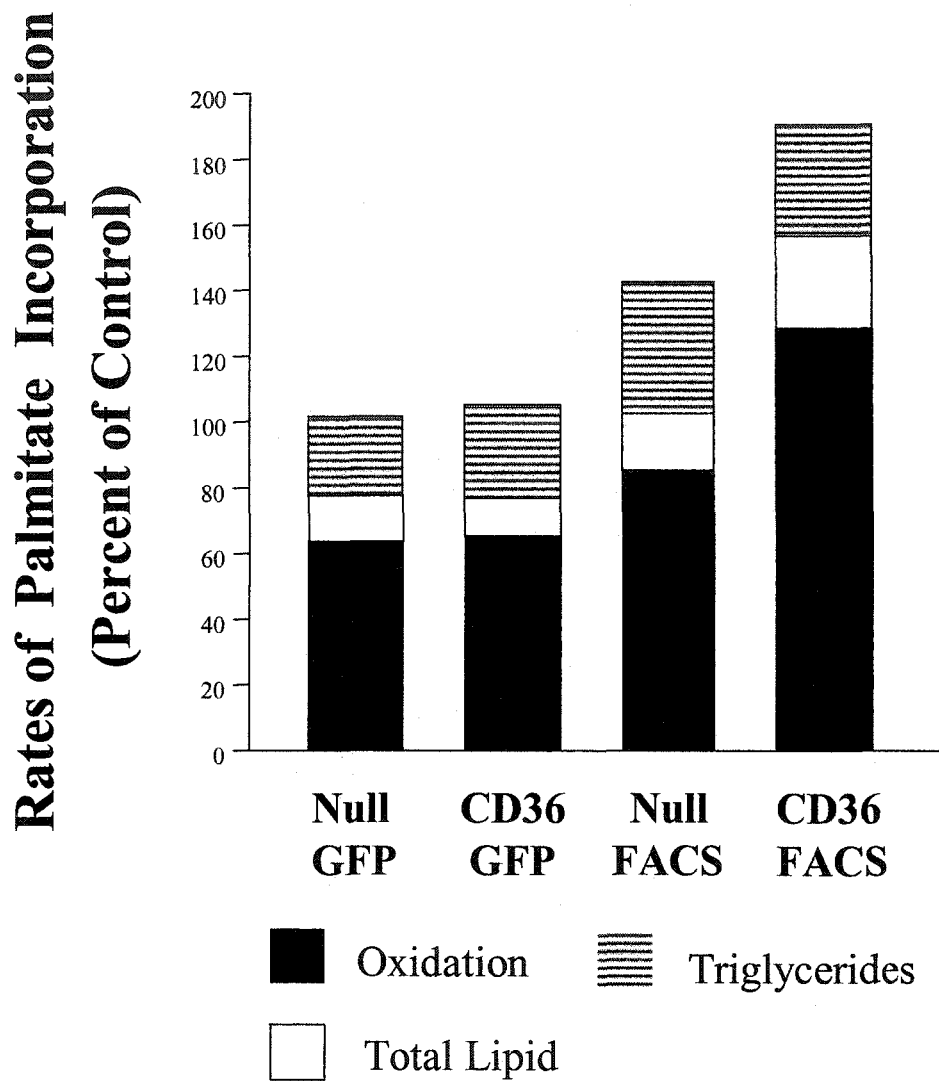


Fig. 4-8. Total triglyceride levels in neonatal rat cardiac myocytes. Data are means  $\pm$  S.E. of six experiments carried out with six different cardiomyocyte cell preparations.



**Fig. 4-9. Rates of palmitate incorporation in neonatal rat cardiac myocytes.** Rates of palmitate incorporation into cardiac myocytes were calculated as a percent of control of each lipid fate. Each lipid fate in the Null GFP group was set a 100% and every other compared was compared to this control group. Data are means of six experiments carried out with six different cardiac myocyte preparations.

## **Chapter 5**

# **Alterations in the AMPK-ACC-Malonyl CoA Signaling Axis in the FAT/CD36 Deficient Mouse**

**Acknowledgements:** Heart perfusions were performed by Cory Wagg and HPLC was conducted by Kenneth Strynadka

## Introduction

Our previous study (Chapter 3) showed that the FAT/CD36 KO mouse hearts exhibit significantly lower rates of palmitate oxidation during pre- and post-ischemic periods. In the present study, we sought to determine if the FAT/CD36 KO hearts attempt to restore rates of fatty acid oxidation during times deficient fatty acid oxidation. We have already shown that the FAT/CD36 KO hearts do not compensate for the loss in fatty acid oxidation. However, there may be signaling pathways that are altered in order to increase rates of fatty acid oxidation which may account for some of the palmitate oxidized in the in the FAT/CD36 KO mouse heart.

Since AMPK activation has been shown to accelerate fatty acid oxidation in the heart<sup>1</sup>, it is possible that AMPK is activated in response to decreased rates of fatty acid oxidation in the FAT/CD36 KO heart. In addition, since AMPK is activated during ischemia<sup>1</sup>, it is not unreasonable to hypothesize that AMPK is more highly active in the FAT/CD36 KO mouse heart when subjected to ischemia. This would result in an increase in phosphorylation and inhibition of ACC, subsequently leading to decreased malonyl CoA levels in the heart. Therefore, we also examined phospho-ACC 280 kDa (since the 280 kDa isoform is dominant in the heart compared to the 265 kDa isoform) and whether the FAT/CD36 KO hearts exhibited lower levels of malonyl CoA, as a compensatory mechanism to drive fatty acid oxidation in times of high energy demand and decreased rates of fatty acid oxidation. We also examined direct changes in MCD, as decreases in MCD levels could also compensate for the decreased rates of fatty acid oxidation observed in the FAT/CD36 deficient mice. We also examined levels of PPAR $\alpha$ , which

are a family of receptors that have been shown to be activated by fatty acids, to induce gene transcription (see <sup>2</sup> for review). A study utilizing PPAR $\alpha$  KO mice indicated that MCD expression is controlled by PPAR $\alpha$ <sup>3</sup>, much like other genes involved in fatty acid oxidation, such as FACS, FAT/CD36 and FABP.

## **Hypothesis**

We hypothesize that FAT/CD36 KO mouse hearts will exhibit compensatory intracellular mechanisms in response to the decrease in fatty acid oxidation. Specifically, the FAT/CD36 KO hearts will demonstrate higher levels of phospho-AMPK (Thr172), phospho-ACC (Ser79) and total MCD protein. These molecular changes will ultimately result in significantly lower levels of malonyl CoA, as compared to the wildtype hearts, which would normally accelerate fatty acid oxidation.

## **Materials and Methods**

*Western Blot Analysis.* As described in the Methods and Materials section.

*PCA Extraction of Acetyl CoA and Malonyl CoA.* Approximately 25 mg of powdered heart tissue from ischemic FAT/CD36 KO and wildtype mice were weighed out into cryovials. The heart tissue was transferred to Dounce homogenizers and homogenized in 6% perchloric acid. The homogenate was centrifuged at 3500 RPM for 10 min at 4°C. The samples were then analyzed with HPLC. Separation was performed on a Beckman System Gold with a UV detector 167. Each sample was run through a precolumn cartridge and a microsorb short-one column. A gradient was set up using buffer A, consisting of 0.2 M NaH<sub>2</sub>PO<sub>4</sub>, pH 5.0, and buffer B, consisting of 0.25 M NaH<sub>2</sub>PO<sub>4</sub> and

acetonitrile, pH 5.0, at a ratio of 80:20 (v/v). Both buffers were filtered using Nylon-66 filter membrane (Pierce). Buffers were initially mixed at 97% buffer A and 3% buffer B and maintained for 2.5 min, and changed to 18% B for 5 min. The gradient was changed to 37% buffer B for 3 min and to 90% buffer B for 17 min. At 42 min, buffer B was returned to 3% over 0.5 min and at 50 min, equilibration was completed. Peaks were integrated by Beckman System Gold.

*Statistical Analysis*- Data is expressed as mean  $\pm$  S.E. Comparisons between wild type and FAT/CD36 deficient hearts were performed using the unpaired Student's two-tailed t-test. Differences were judged to be significant when  $p < 0.05$ .

## **Results**

### *Phospho-AMPK (Thr172) levels in reperfused FAT/CD36 KO and wildtype mouse hearts*

– Phospho- $\alpha$ -AMPK levels (Thr172) were determined in order to examine whether there was an increase in AMPK activity in the FAT/CD36 KO hearts as compared to the wildtype hearts following ischemia and reperfusion. The FAT/CD36 KO hearts exhibited significantly higher levels of phospho- $\alpha$ -AMPK as compared to the wildtype hearts when normalized to total  $\alpha$ -AMPK (Figure 5-1A). Densitometric analysis also showed that P-AMPK levels were significantly elevated in FAT/CD36 deficient hearts when normalized to total  $\alpha$ -AMPK (Figure 5-1B). Moreover, when total  $\alpha$ -AMPK blots were normalized to actin levels in the tissue, we found that there was no significant difference between wildtype and FAT/CD36 KO hearts (Figure 5-2A). Densitometric analysis also showed

that there was no difference in actin between wildtype and FAT/CD36 deficient hearts (Figure 5-2B).

*ACC levels in reperfused FAT/CD36 KO and wildtype mouse hearts* – We examined phospho-ACC as a measure of ACC activity and also of AMPK activity, since the Ser79 residue of ACC is phosphorylated by AMPK. The phosphorylated form of the 280 kDa isoform of ACC was used to determine if ACC was more active in FAT/CD36 KO hearts as compared to wildtype controls. We found that the FAT/CD36 KO hearts exhibited significantly higher levels of phospho-ACC (280 kDa) as compared to wildtype heart tissue, when normalized to the amount of total ACC (280 kDa) in the tissue (Figure 5-3A).

*MCD levels in reperfused FAT/CD36 KO and wildtype mouse hearts* – We examined MCD levels in the heart tissues in order to determine if FAT/CD36 KO hearts exhibited altered levels of MCD as compared to the wildtype controls. We found that FAT/CD36 KO heart tissue exhibited significantly lower levels of MCD as compared to wildtype controls, when normalized to actin levels (Figure 5-4A).

*Malonyl CoA levels in reperfused FAT/CD36 KO and wildtype mouse hearts* – Since FAT/CD36 KO hearts exhibited higher levels of phospho-AMPK, the corresponding increased levels of phospho-ACC and decreased levels of MCD, we examined whether the FAT/CD36 KO hearts demonstrated changes in malonyl CoA levels. We found that

both sets of hearts exhibited similar levels of malonyl CoA after reperfusion (Figure 5-5A).

*Acetyl CoA levels in reperfused FAT/CD36 KO and wildtype mouse hearts* – Our previous study showed that the FAT/CD36 KO hearts are not energetically compromised since they compensate for the loss in fatty acid oxidation by increasing glucose oxidation. We calculated the amount of acetyl CoA theoretically produced in both sets of hearts and found that they produce similar amounts of acetyl CoA. In the current study, we also demonstrated that both sets of hearts produce similar amounts of acetyl CoA, following ischemia and reperfusion, confirming that FAT/CD36 KO hearts are not energetically compromised (Figure 5-5B). Acetyl CoA was calculated as a product of the rate of oxidation and number of acetyl CoA molecules produced from palmitate and glucose.

*Peroxisome proliferator-activated receptor alpha (PPAR $\alpha$ ) levels in FAT/CD36 KO and wildtype mouse hearts* – We attempted to examine PPAR $\alpha$  levels in FAT/CD36 KO and wildtype hearts in order to determine if the low MCD levels observed in FAT/CD36 KO mouse hearts were due to decreased levels of PPAR $\alpha$ . The results are inconclusive as the antibodies used failed to result in a clear band signifying PPAR $\alpha$ . In Figure 5-6A, we show that perfused hearts overexpressing PPAR $\alpha$  (lane 1) and hearts from a PPAR $\alpha$  knockout mouse (lane 2), exhibit no observable differences in immunoreactive bands. Therefore, we concluded that the PPAR $\alpha$  antibody was nonfunctional. Another possibility for the failed Western blot could be unsuccessful lysis of the nucleus, which would hinder the ability of the antibody to bind with PPAR $\alpha$ . In order to eliminate this as

a possibility, we probed the tissue homogenate for the nuclear protein, poly(ADP-ribose) polymerase (PARP). Figure 5-6B depicts a Western blot demonstrating the presence of PARP, which confirms that the nucleus was lysed. This data suggests that the PPAR $\alpha$  antibody used was nonfunctional and could not detect the presence of PPAR $\alpha$ .

## **Discussion**

In the current study, we hypothesized that the FAT/CD36 KO mouse hearts would exhibit altered signaling mechanisms to compensate for the decrease in rates of fatty acid oxidation. First we examined levels phospho-AMPK (Thr172), which is a surrogate of AMPK activity. We found that levels of phospho-AMPK were significantly higher in the FAT/CD36 KO mouse hearts, as compared to wildtype hearts. This suggests that AMPK activity is significantly higher in the FAT/CD36 KO hearts. Second, we examined levels of phospho-ACC, which is indicative of AMPK and ACC activity<sup>4</sup>. We found that levels of phospho-ACC were significantly increased in FAT/CD36 KO hearts as compared to controls, which also confirms that the activity of AMPK is increased. In addition, increased phospho-ACC will decrease ACC activity, decrease malonyl CoA production, thereby relieve inhibition of CPT 1 and increase rates of fatty acid oxidation. However, when malonyl CoA levels were examined in the FAT/CD36 KO hearts, we found that both the FAT/CD36 KO and wildtype hearts exhibited similar levels of malonyl CoA. This may be due to the fact that measurements of total cellular malonyl CoA also include mitochondrial malonyl CoA levels, which may mask changes in cytosolic malonyl CoA levels. Although we believe this to be the most likely scenario, the higher than expected levels of malonyl CoA in the FAT/CD36 KO hearts may also be explained by the

significantly lower levels of MCD found in these hearts, as compared to wildtype controls. If the FAT/CD36 KO hearts produce less malonyl CoA, due to increased phospho-ACC, this could be counteracted by a decrease in the amount of malonyl CoA degraded. This would explain why both the FAT/CD36 KO and wildtype hearts contain similar levels of malonyl CoA. The decreased levels of MCD may be explained by its regulation via peroxisome proliferator-activated receptor alpha (PPAR $\alpha$ ). Indeed, in situations where fatty acids are limiting, such as FAT/CD36 deficiency, PPAR $\alpha$  would not be activated leading to a decrease in expression of MCD. Thus, the reduction in MCD in FAT/CD36 KO hearts maybe due to the decreased concentration of intracellular fatty acids, which would reduce the activation of PPAR $\alpha$  to induce MCD expression. However, the inability to detect PPAR $\alpha$  using Western blot analysis precluded us from confirming if decreased levels of PPAR $\alpha$  also contributed to these effects (Figure 5-6).

The present study suggests that the amount of malonyl CoA in the FAT/CD36 KO hearts are regulated by the activity of AMPK and the amount of MCD. Although the FAT/CD36 KO heart may attempt to compensate for the decrease in fatty acid oxidation by activating AMPK and lowering levels of malonyl CoA, the rate of malonyl CoA degradation is limited by decreased levels of MCD. Although the precise reasons for decreased MCD expression in the FAT/CD36 KO hearts are not known, it may be due to a decrease in intracellular fatty acids and a subsequent decrease in PPAR $\alpha$  activation.

Our previous study (Chapter 3) showed that functional recovery during reperfusion of ischemic FAT/CD36 KO hearts was similar to recovery of the wildtype hearts. In the current study, we suggest that the FAT/CD36 KO hearts do not recover better than the wildtype hearts because FAT/CD36 KO hearts exhibit higher levels of

phospho-AMPK. It is well known that ischemic injury arises, in part, due to an uncoupling of glycolysis from glucose oxidation<sup>5</sup>. Moreover, it has been shown by several studies that inhibition of glycolysis has a beneficial effect on contractile recovery after ischemia<sup>6,7</sup>. Upon examination of reperfused FAT/CD36 KO hearts, we found that these hearts exhibited higher levels of phospho- $\alpha$ -AMPK, when normalized to total  $\alpha$ -AMPK, as compared to wildtype hearts. It has been shown in several studies that AMPK can stimulate glycolysis through activation of PFK-2<sup>8,9</sup>. Thus, an increase in AMPK activity, which has been shown to be indicative of AMPK (Thr172) phosphorylation<sup>10</sup>, would lead to an increase in PFK-2 flux, followed by an increase in PFK-1 activity and ultimately glycolysis. Therefore, we suggest that the FAT/CD36 KO hearts exhibited significantly higher rates of glycolysis, as compared to wildtype hearts, leading to further uncoupling of glycolysis from glucose oxidation and tissue damage. Obviously, these experiments would have to be performed before we can make these conclusions.

## **Conclusion**

These data suggest that the increase in AMPK phosphorylation may be a compensatory mechanism to increase rates of fatty acid oxidation in the FAT/CD36 KO heart. The increase in AMPK phosphorylation leads to higher levels of phospho-ACC, which confirms that AMPK is more active in the FAT/CD36 KO and suggests that malonyl CoA levels may be decreased. However, the latter is not the case as malonyl CoA levels in the FAT/CD36 KO and wildtype hearts were found to be similar. This is due to the fact that MCD levels in the FAT/CD36 KO hearts were significantly decreased, which is likely due to diminished PPAR $\alpha$  levels, as compared to the wildtype heart. Thus, the decrease in malonyl CoA production is balanced with a decrease in

malonyl CoA degradation, which resulted in no change in malonyl CoA levels, as compared to wildtype levels. In addition, the FAT/CD36 KO ischemic heart may not recover better than its wildtype counterpart because the KO heart exhibits enhanced levels of phospho- $\alpha$ -AMPK. Although glycolysis was not measured in our study, increased AMPK phosphorylation suggests that glycolytic rates were increased in the reperfused FAT/CD36 KO heart.

In conclusion, the deficiency in fatty acid uptake in the FAT/CD36 KO heart may oppose a compensatory decrease in malonyl CoA, which would attempt increase rates of fatty oxidation. Specifically, the lack of fatty acids as activators of PPAR $\alpha$ , would lead to decreased levels of MCD and malonyl CoA degradation. Therefore, no compensatory mechanism exists in the malonyl CoA axis because fatty acid supply is limited due to the absence of FAT/CD36.

## References

1. Kudo N, Gillespie JG, Kung L, Witters LA, Schulz R, Clanachan AS, Lopaschuk GD. Characterization of 5'AMP-activated protein kinase activity in the heart and its role in inhibiting acetyl-CoA carboxylase during reperfusion following ischemia. *Biochim Biophys Acta*. 1996;1301:67-75.
2. Auwerx J. Regulation of gene expression by fatty acids and fibric acid derivatives: an integrative role for peroxisome proliferator activated receptors. The Belgian Endocrine Society Lecture 1992. *Horm Res*. 1992;38:269-77.
3. Campbell FM, Kozak R, Wagner A, Altarejos JY, Dyck JR, Belke DD, Severson DL, Kelly DP, Lopaschuk GD. A role for peroxisome proliferator-activated receptor alpha (PPARalpha ) in the control of cardiac malonyl-CoA levels: reduced fatty acid oxidation rates and increased glucose oxidation rates in the hearts of mice lacking PPARalpha are associated with higher concentrations of malonyl-CoA and reduced expression of malonyl-CoA decarboxylase. *J Biol Chem*. 2002;277:4098-103.
4. Dyck JR, Kudo N, Barr AJ, Davies SP, Hardie DG, Lopaschuk GD. Phosphorylation control of cardiac acetyl-CoA carboxylase by cAMP-dependent protein kinase and 5'-AMP activated protein kinase. *Eur J Biochem*. 1999;262:184-90.
5. Liu B, el Alaoui-Talibi Z, Clanachan AS, Schulz R, Lopaschuk GD. Uncoupling of contractile function from mitochondrial TCA cycle activity and MVO<sub>2</sub> during reperfusion of ischemic hearts. *Am J Physiol*. 1996;270:H72-80.

6. Finegan BA, Lopaschuk GD, Gandhi M, Clanachan AS. Inhibition of glycolysis and enhanced mechanical function of working rat hearts as a result of adenosine A1 receptor stimulation during reperfusion following ischaemia. *Br J Pharmacol.* 1996;118:355-63.
7. Finegan BA, Gandhi M, Lopaschuk GD, Clanachan AS. Antecedent ischemia reverses effects of adenosine on glycolysis and mechanical function of working hearts. *Am J Physiol.* 1996;271:H2116-25.
8. Marsin AS, Bouzin C, Bertrand L, Hue L. The stimulation of glycolysis by hypoxia in activated monocytes is mediated by AMP-activated protein kinase and inducible 6-phosphofructo-2-kinase. *J Biol Chem.* 2002;277:30778-83.
9. Marsin AS, Bertrand L, Rider MH, Deprez J, Beauloye C, Vincent MF, Van den Berghe G, Carling D, Hue L. Phosphorylation and activation of heart PFK-2 by AMPK has a role in the stimulation of glycolysis during ischaemia. *Curr Biol.* 2000;10:1247-55.
10. Stein SC, Woods A, Jones NA, Davison MD, Carling D. The regulation of AMP-activated protein kinase by phosphorylation. *Biochem J.* 2000;345 Pt 3:437-43.

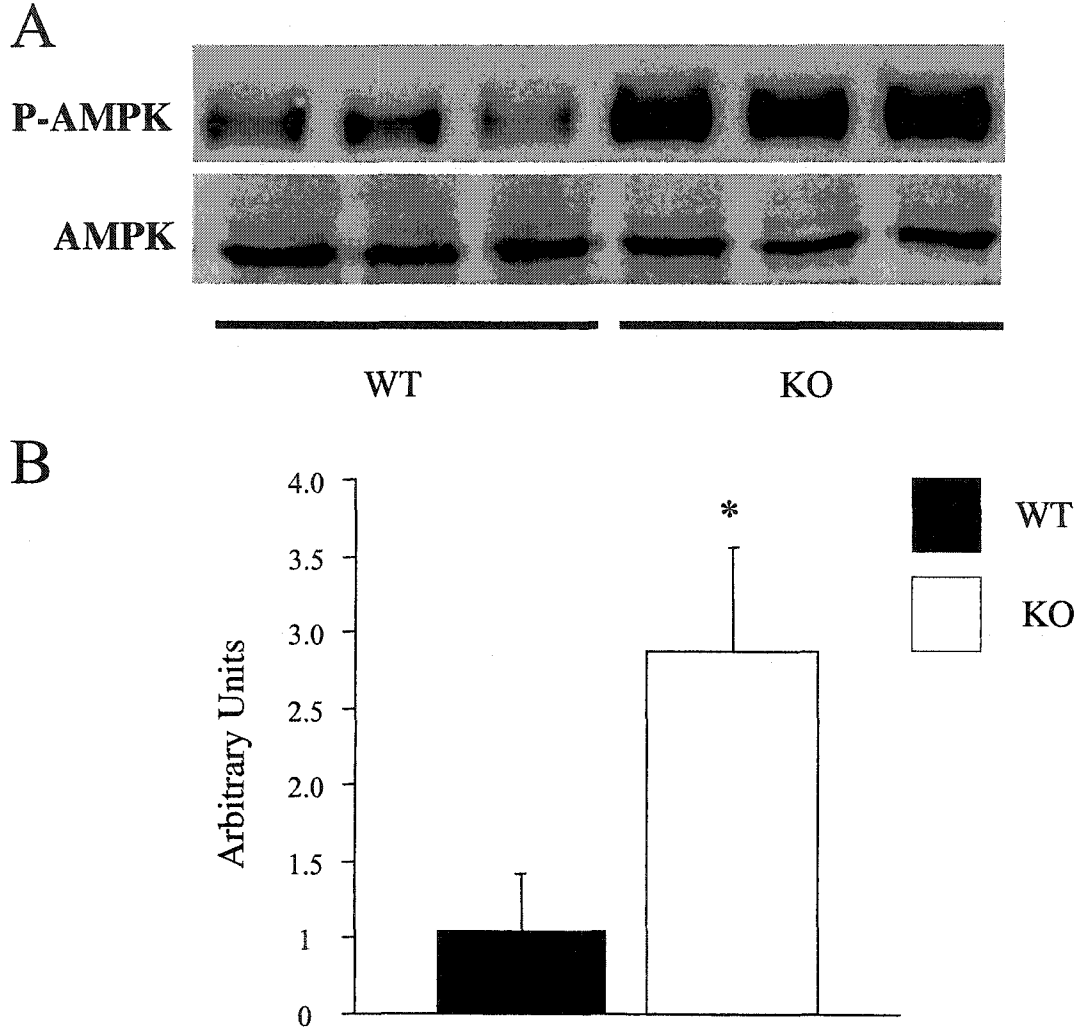


**Figure. 5-1. Western blot analysis of tissue homogenates from FAT/CD36 KO and wildtype reperfed mouse hearts.** Hearts were homogenized and subjected to SDS-PAGE followed by Western blot analysis using the phospho-AMPK (Thr172) and AMPK antibodies (A). Western blots were then subjected to densitometric analysis and the p-AMPK/AMPK ratio was graphed (B).  $n = 5$  for both the FAT/CD36 KO and wildtype hearts. \*, significantly different from wildtype,  $p < 0.05$ .

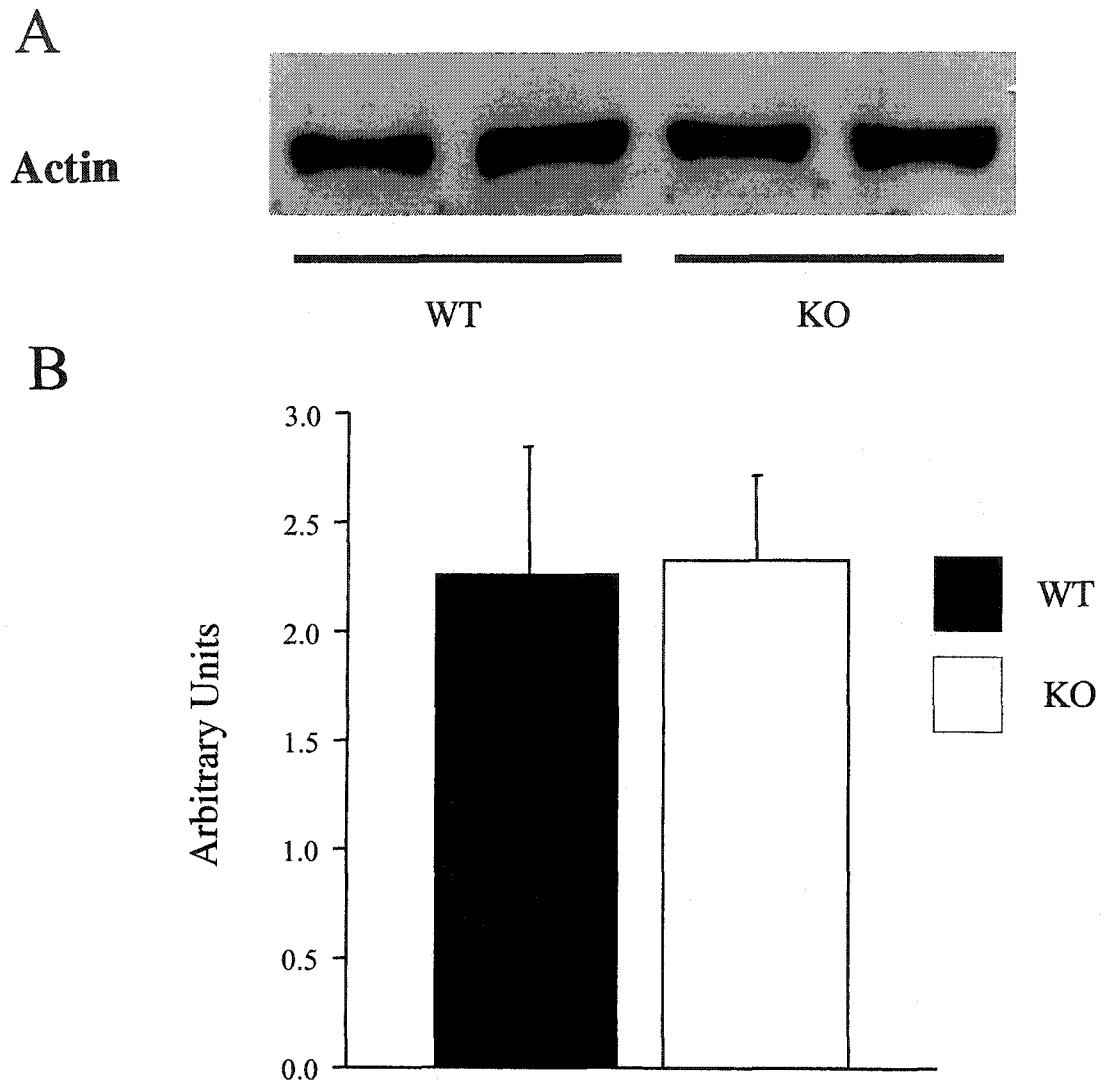


**Figure 5-2. Western blot analysis of tissue homogenates from FAT/CD36 KO and wildtype reperfused mouse hearts.** Hearts were homogenized and subjected to SDS-PAGE followed by Western blot analysis using the actin antibody (A). Western blots were then subjected to densitometric analysis and the AMPK/Actin ratio was graphed (B). n = 5 for both the FAT/CD36 KO and wildtype hearts.

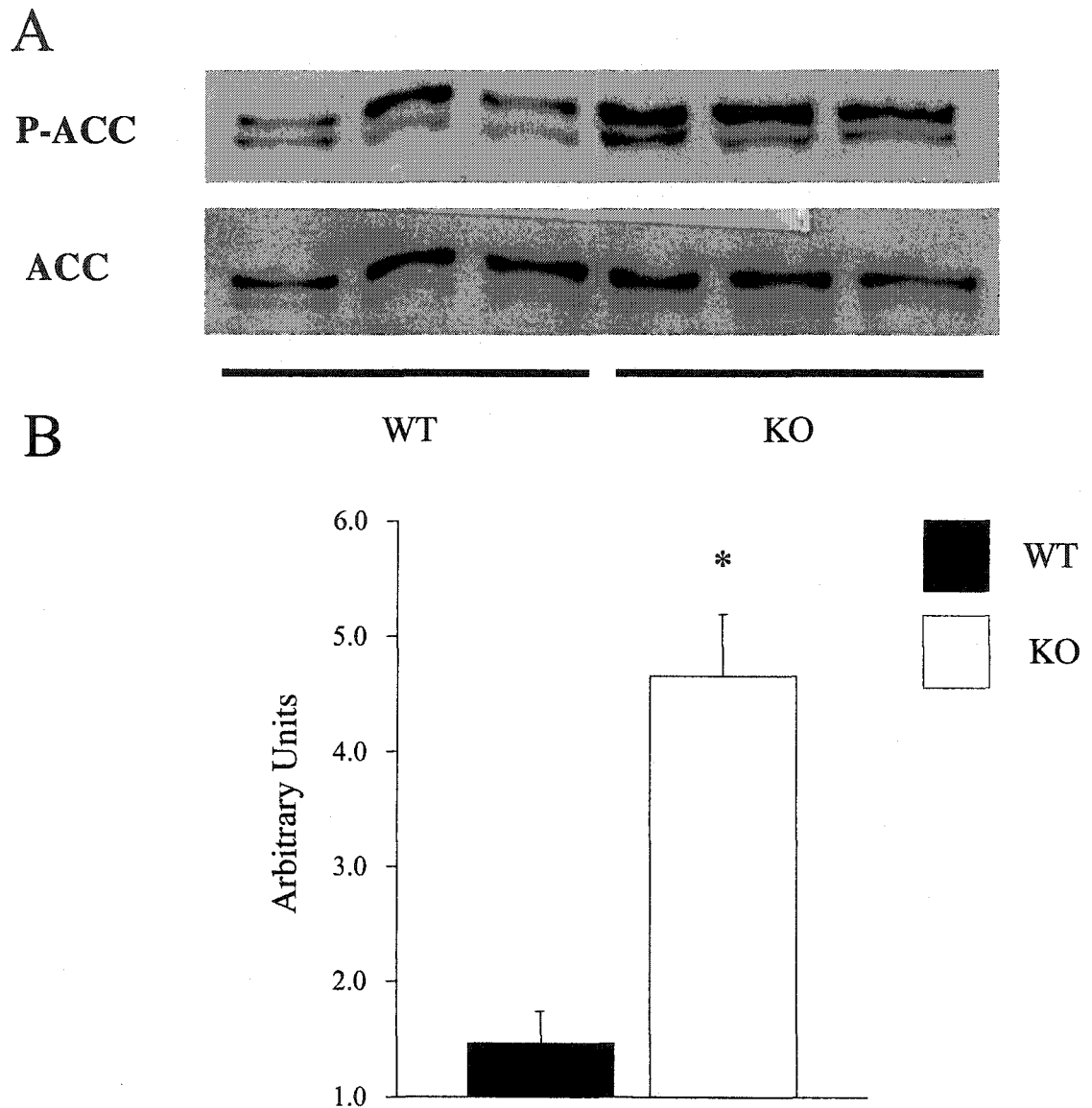


**Figure 5-3. Western blot analysis of tissue homogenates from FAT/CD36 KO and wildtype reperused mouse hearts.** Hearts were homogenized and subjected to SDS-PAGE followed by Western blot analysis using the Phospho-ACC antibody and streptavidin labeled peroxidase for ACC quantification (A). Western blots were then subjected to densitometric analysis and the p-ACC/ACC ratio was graphed (B).  $n = 5$  for both the FAT/CD36 KO and wildtype hearts. \*, significantly different from wildtype,  $p < 0.05$ .

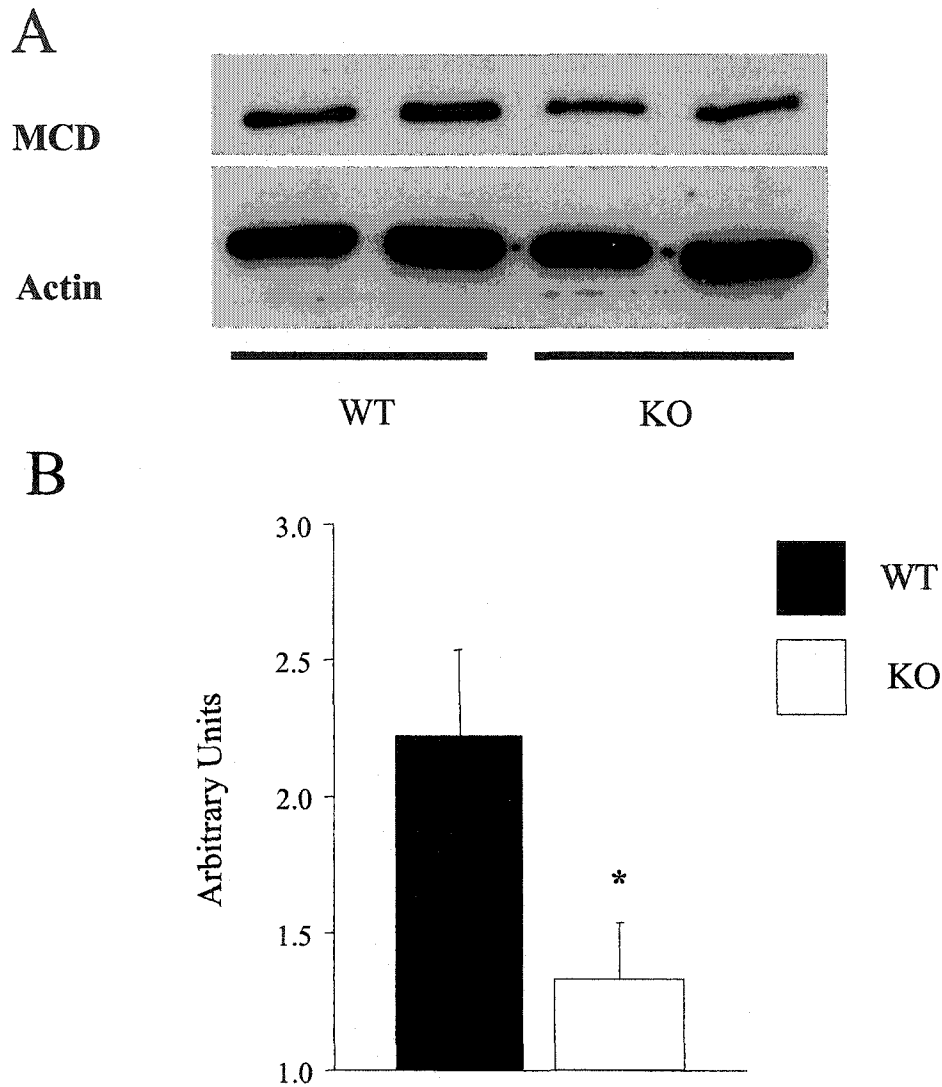


**Figure 5-4. Western blot analysis of tissue homogenates from FAT/CD36 KO and wildtype reperused mouse hearts.** Hearts were homogenized and subjected to SDS-PAGE followed by Western blot analysis using the MCD and actin antibodies (A). Western blots were then subjected to densitometric analysis and the MCD/Actin ratio was graphed (B).  $n = 5$  for both the FAT/CD36 KO and wildtype hearts. \*, significantly different from wildtype,  $p < 0.05$ .

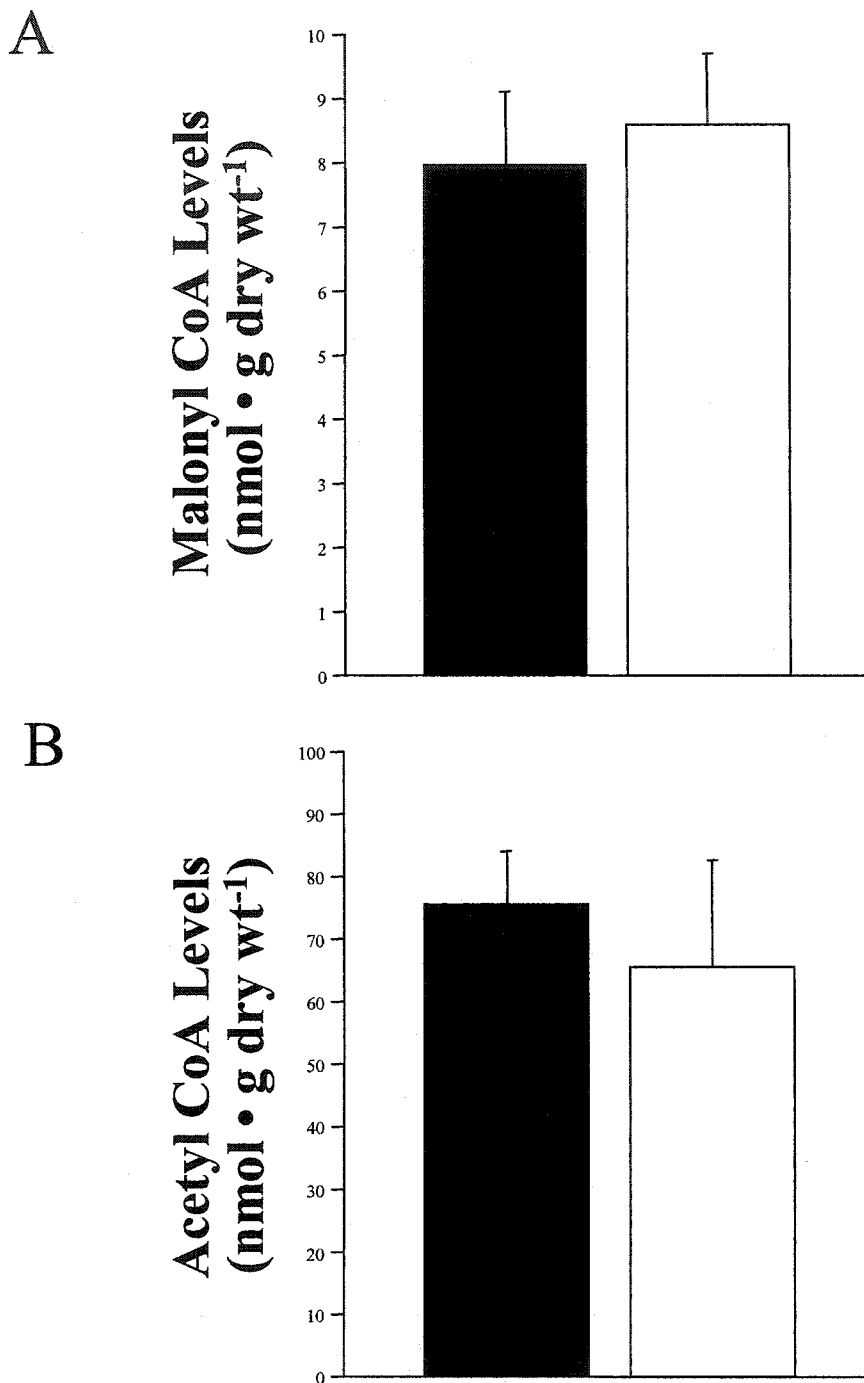


**Fig. 5-5. Malonyl CoA (A) and acetyl CoA (B) levels in FAT/CD36 KO and wildtype reperfused hearts.** Heart samples were homogenized with a 6% perchloric acid solution. Heart homogenates were cleared using centrifugation and the resulting supernatant was subjected to high performance liquid chromatography. n = 8 for wildtype hearts and n = 7 for FAT/CD36 KO hearts.

■ = Wildtype □ = FAT/CD36 KO

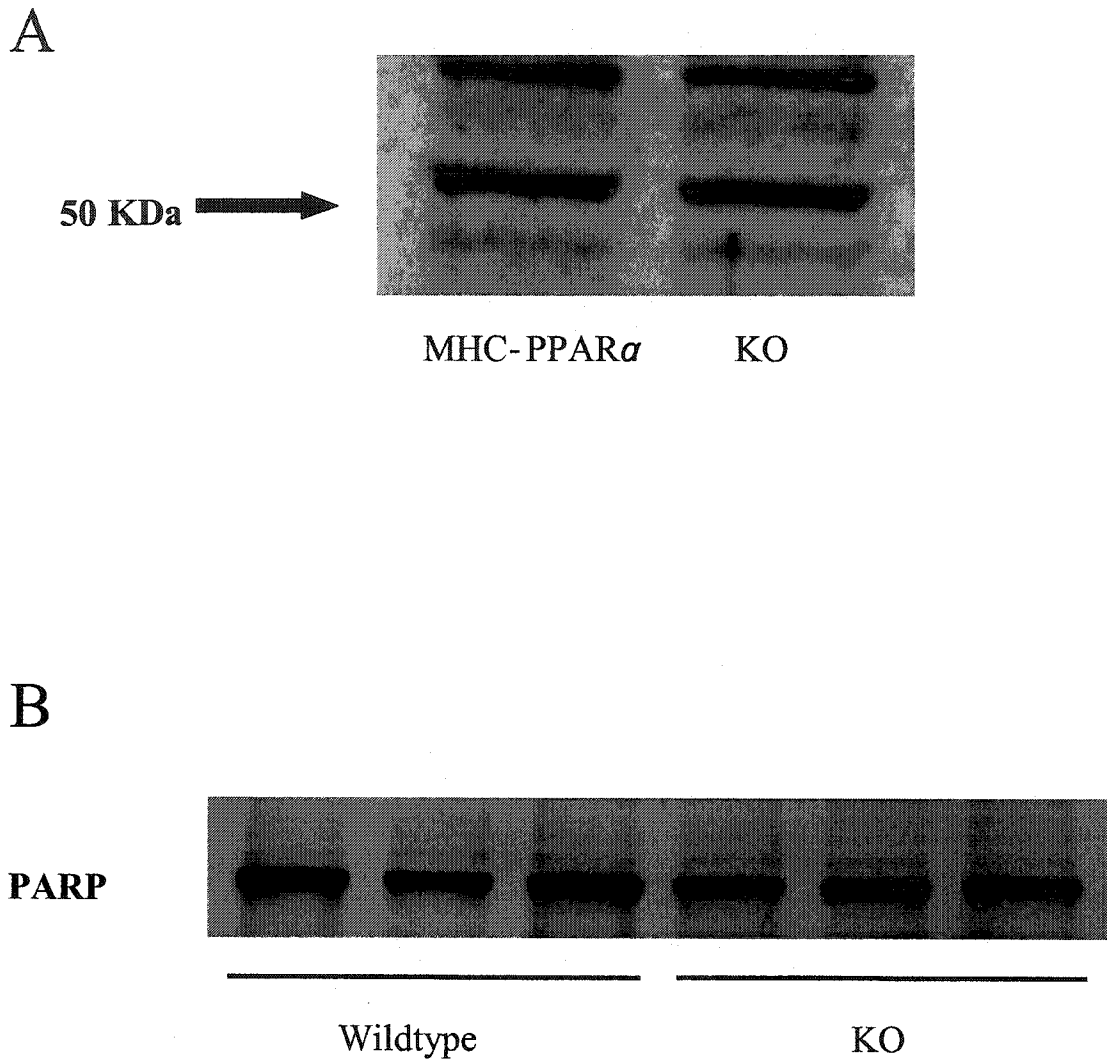


**Figure 5-6. Western blot analysis of MHC-PPAR and PPAR KO mouse hearts (A) and FAT/CD36 KO and wildtype reperused mouse hearts (B).** Hearts were homogenized and subjected to SDS-PAGE followed by Western blot analysis using the PPAR $\alpha$  antibody (A). FAT/CD36 KO and wildtype hearts were homogenized and subjected to SDS-PAGE followed by Western blot analysis using the PARP antibody (B).  $n = 5$  for both the FAT/CD36 KO and wildtype hearts.

## Chapter 6

### Development of a New Model to Study Localization and Translocation of FAT/CD36

**Acknowledgements:** Neonatal rat cardiac myocytes were isolated by Suzanne Kovacic, aid was given by Jennifer Douglas in the construction of the FAT/CD36-DsRed2 construct and aid was given by Honey Chan with the confocal microscope.

## Introduction

FAT/CD36 is an 88 kDa ditopic glycosylated protein that belongs to the class B family of scavenger receptors. This family also includes scavenger receptor class B type I (SR-BI), the receptor for selective cholesteryl ester uptake and lysosomal integral membrane protein II (LIMP-II) (see <sup>1</sup> for review). FAT/CD36 has been found to localize to intracellular microsomal vesicles<sup>2</sup> and caveolae membrane domains in the plasma membrane<sup>3</sup> of skeletal muscle cells.

It has been shown that FAT/CD36 is localized to the intracellular microsomal vesicles<sup>2</sup>, which is homologous to the distribution of the glucose transporter GLUT4<sup>4</sup>. Therefore it has been suggested that FAT/CD36 may colocalize with GLUT4 in intracellular compartments and share similar cellular machinery involved in their recruitment to the plasma membrane. Although it may be reasonable to propose that FAT/CD36 and GLUT4 are colocalized, there is contradictory evidence demonstrating FAT/CD36 and GLUT4 are not colocalized in skeletal muscle<sup>5</sup>. Due to this controversy, the question of whether FAT/CD36 and GLUT 4 are colocalized in the microsomal compartment remains unanswered.

In addition, FAT/CD36 has recently been shown to localize in the mitochondria of skeletal muscle, where it is thought to aid CPT-1 in facilitating movement of long chain fatty acids into the mitochondria<sup>6</sup>. Specifically, it has been suggested that FAT/CD36 acts as a long chain fatty acid acceptor and is involved in the transfer of fatty acids to CPT-1, which are subsequently transported into the mitochondrial matrix. The recruitment of FAT/CD36 from the endosomal compartment to the mitochondria would

provide a mechanism by which energy supply could be enhanced in response to increased energy demand. Therefore, the translocation process may be an important mechanism by which metabolism is regulated.

The translocation process has not been visualized nor is it well understood in the heart. Therefore, we have created a FAT/CD36 – [pDsRed2-N1] (Clontech) fusion protein in order to visualize and study FAT/CD36 intracellular localization and translocation. The pDsRed2-N1 plasmid encodes DsRed2, a red fluorescent protein, which can be detected using fluorescence microscopy. Large insoluble aggregates of protein, often observed in bacterial and mammalian cell systems expressing DsRed1, are dramatically reduced in cells expressing DsRed2, making FAT/CD36–DsRed2 an effective molecular tool in order to investigate properties of FAT/CD36.

## **Hypothesis**

With the transfection of the FAT/CD36-DsRed2 DNA into COS-7 cells and cardiac myocytes, we hypothesize that the FAT/CD36-DsRed2 protein will localize in the plasma membrane and intracellular compartments. Addition of insulin and AICAR, will stimulate the insulin signaling and AMPK cascades, respectively. This will result in the translocation of FAT/CD36-DsRed2 from the intracellular compartment to the plasma membrane. We also hypothesize that FAT/CD36-DsRed2 can colocalize with the mitochondria, which may provide a mechanism by which fatty acids are transported into the mitochondria.

## Materials and Methods

*Cell Culture.* As described in the Methods and Materials section.

*Construction of CD36/DsRed2 Fusion Protein.* Cloned mouse FAT/CD36 cDNA (kindly provided by Maria Febbraio) was cut at the multiple cloning sites surrounding mouse FAT/CD36 cDNA by restriction enzymes EcoR1 and BamH1. This reaction yielded a linear 1.7 kb fragment, which coded for mouse FAT/CD36. The FAT/CD36 fragment was gel purified using a 1% agarose gel, and amplified by PCR using primers derived from the fragment. The antisense primer contained a BamH1 restriction site which was used for directional cloning. The 4.7 kb pDsRed2-N1 vector (Clontech) was also digested with restriction enzymes EcoR1 and BamH1 to produce linear pDsRed2-N1. Both the linearized pDsRed2-N1 and FAT/CD36 PCR product were ligated together to produce a 6.4 kb plasmid. The new plasmid was transformed into supercompetent XL-1 Blue cells (Stratagene), plated and positive colonies cultured in large volumes (500 mL). DNA from the resulting cultures was extracted and purified using a Plasmid MAXI kit (Qiagen).

*Cell Transfection.* Both COS-7 cells and neonatal rat cardiac myocytes were used in transfection experiments. COS-7 cells were maintained in DMEM supplemented with 10% fetal bovine serum and cardiomyocytes were maintained in DMEM supplemented with ITS (SIGMA) and AraC (SIGMA). COS-7 cells were transfected with 1  $\mu$ g CD36/DsRed2 DNA using 3  $\mu$ L FuGENE 6 (ROCHE) and cardiomyocytes were transfected with 2  $\mu$ g CD36/DsRed2 DNA using 6  $\mu$ L FuGENE 6 according to the manufacturer's instructions. Cells were incubated in the transfection media for 24 hours,

after which media was changed and cells were incubated for 24 hours in serum free media.

*Mitochondrial Staining.* For cardiac myocyte staining, MitoTracker Green was diluted to a working concentration of 25 nM in 1 mL of prewarmed serum free DMEM. Neonatal rat cardiac myocytes were incubated for 30 min with the stain and replaced with prewarmed serum free DMEM after incubation.

*Confocal Laser Scanning Microscopy (CLSM).* Localization of FAT/CD36, GLUT4 and mitochondria in COS-7 and neonatal rat cardiac myocytes were studied using CLSM (Zeiss LSM 510). For excitation of the green fluoresin (MitoTracker Green and GLUT4-GFP), a 488 nm argon laser was used. For excitation of the DsRed2 fluoresin a 543 nm helium-neon (HeNe) laser was used to visualize. The multi track option of the microscope was used to scan each laser line separately for individual excitation of the dyes, to exclude cross-excitation between detection channels.

## **Results**

*Transfection with DsRed2*– Cells transfected with the DsRed2 vector appeared a solid red color, with no signs of punctuates (Figure 6-1). However, cells transfected with the FAT/CD36-DsRed2 fusion protein displayed red punctuates, suggesting that intracellular endosomes carry FAT/CD36 (Figure 6-2).

*Translocation of FAT/CD36-DsRed2 in response to insulin and AMPK stimulation* – Live COS-7 cells were transfected with the FAT/CD36-DsRed2 expression plasmid and

allowed to express the protein for 48 hours. Cells were subsequently treated with 1 nM insulin (Figure 6-3) or 1 mM AICAR (Figure 6-4) for 20 min and 30 min, respectively, in order to investigate translocation of FAT/CD36. Appearance of transfected COS-7 cells treated with insulin for 30 min differed from the COS-7 cells at time zero (before insulin treatment). Specifically, the punctuates containing FAT/CD36-DsRed2 fusion proteins appeared to translocate from the intracellular compartment to the plasma membrane. No change in punctuates, containing FAT/CD36 fusion proteins, localization was observed in those cells treated with 1mM AICAR at 30 min or time zero.

*Colocalization of FAT/CD36 with the mitochondria* – Live cells were transfected with FAT/CD36–DsRed2 expression plasmid and allowed to express the protein for 48 hours. Cells were subsequently stained with MitoTracker Green in order to examine possible FAT/CD36 localization in the mitochondria. Confocal images depicting cells transfected with FAT/CD36-DsRed2 and stained with MitoTracker green are shown in Figure 6-5 and Figure 6-6. Figure 6-5 depicts cells that express FAT/CD36-DsRed2 which do not colocalize with mitochondria. Figure 6-6 depicts cells that express FAT/CD36-DsRed2 which colocalize with mitochondria.

*Colocalization of FAT/CD36 with GLUT 4* – Live cells were transfected with both FAT/CD36–DsRed2 expression plasmid and GLUT 4-GFP expression plasmid in order to examine colocalization of FAT/CD36 and GLUT 4 (Figure 6-7). Confocal images show that GLUT 4 and FAT/CD36-DsRed2 are present in the intracellular compartments (A, B) and (C,D), respectively. Confocal images demonstrate that red punctuates,

containing the FAT/CD36-DsRed2 fusion protein, do not colocalize with the green punctuates of the GLUT4-GFP construct (E, F).

## **Discussion**

In the present study, we have created a novel research tool in order to investigate localization and translocation of FAT/CD36. Using membrane fractionations and palmitate uptake studies Luiken et al<sup>4,7</sup> have shown that insulin and AMPK result in translocation of FAT/CD36 from an intracellular compartment to the plasma membrane. However, the localization and translocation has not been visualized within the cardiac myocyte. Therefore, we have created a FAT/CD36-DsRed2 fusion protein that can be studied in live cells using fluorescent microscopy. Although this is an effective method in the examination of FAT/CD36 localization and translocation, there are several limitations to this study that warrant further discussion.

Although the data clearly show that the FAT/CD36-DsRed2 fusion protein does not colocalize with the mitochondria or GLUT4, we cannot conclude that endogenous FAT/CD36 behaves in the same manner. This is because the DsRed2 fluorescent protein may interfere with normal function and localization of FAT/CD36. Despite this potential drawback, the confocal images suggest that FAT/CD36 localizes to intracellular compartments in the cardiac myocyte, may localize to the mitochondria, and does not colocalize with GLUT4.

Another interesting finding is that the FAT/CD36-DsRed2 fusion protein appears to localize in the nuclear membrane of cardiac myocytes, suggesting that FAT/CD36 may

be involved in the transport of fatty acids into the nucleus. It is not unreasonable to hypothesize that nuclear membrane bound FAT/CD36 transports long chain fatty acid into the nucleus, where they can act as ligands for PPAR $\alpha$ . It has been shown that long chain fatty acids trans-activate PPAR $\alpha$ <sup>8</sup>, but the mechanism by which fatty acids are presented to PPAR $\alpha$  remains unknown. Although there is some evidence which suggests that FABP is involved in the transfer of fatty acids to PPAR $\alpha$ <sup>9</sup>, we cannot exclude the possible role of FAT/CD36 in the transfer of fatty acids to PPARs. In order to investigate this hypothesis, several studies need to be conducted. Purification of the nuclear membrane fraction of cardiac myocytes would have to be done, followed by the probing of this fraction with a FAT/CD36 antibody. This would determine if FAT/CD36 is present in the nuclear membrane. Second, the transfer of fatty acids from FAT/CD36 to PPAR $\alpha$  would have to be established. This could be accomplished by the addition of labeled fatty acids to wildtype neonatal rat cardiac myocytes and those overexpressing FAT/CD36. The nucleus of the cells would need to be isolated, and the PPAR $\alpha$  could then be immunoprecipitated and counted for radioactivity. This would determine whether labeled fatty acids, from FAT/CD36, were transferred to PPAR $\alpha$ . Third, the association of FAT/CD36 and PPAR $\alpha$  would have to be determined. This could be accomplished by the use of immunohistochemistry, utilizing antibodies against FAT/CD36 and PPAR $\alpha$ . These studies would have to be conducted, in conjunction with the current confocal imagery, in order to conclude that FAT/CD36 is localized to the nuclear membrane in order to transfer fatty acids to PPAR $\alpha$ .

The confocal images depicting the translocation of FAT/CD36-DsRed2 fusion proteins from the intracellular compartment to the plasma membrane are inconclusive

without further study. Although there are definite changes in the location of the fluorescent punctuates, without a phase contrast image of cells prior to insulin addition, we are not able to determine whether the punctates reside on the plasma membrane prior to insulin treatment. Changes in cell morphology or membrane blebbing could be the cause of the changes in location of the fluorescent punctuates during the time of incubation with insulin. In order to determine whether the FAT/CD36-DsRed2 fusion protein functions as previously described<sup>4,7</sup>, membrane fractionations must be conducted in cells prior to and after addition of insulin, in order to separate the plasma membrane and endosomal fractions. These fractions can then be probed with the DsRed antibody in order to determine if the amount of DsRed, which equates to the amount of FAT/CD36, in the fractions.

In summary, no definitive conclusion can be made from the current study because of the limitations of the model. Although it appears that FAT/CD36-DsRed2 fusion protein does not colocalize with the mitochondria or GLUT4, more studies have to be conducted in order to determine whether the present results are representative of the true cellular function of FAT/CD36. Moreover, the functional aspect of the construct must also be determined. Although there are limits to the current study, the FAT/CD36-DsRed2 construct may be an effective molecular tool that can be used in conjunction with other studies in order to characterize the localization and translocation of FAT/CD36.

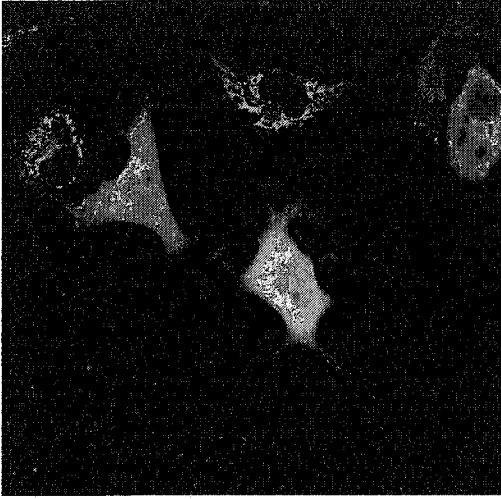
## References

1. Febbraio M, Hajjar DP, Silverstein RL. CD36: a class B scavenger receptor involved in angiogenesis, atherosclerosis, inflammation, and lipid metabolism. *J Clin Invest.* 2001;108:785-91.
2. Luiken JJ, Koonen DP, Willems J, Zorzano A, Becker C, Fischer Y, Tandon NN, Van Der Vusse GJ, Bonen A, Glatz JF. Insulin stimulates long-chain fatty acid utilization by rat cardiac myocytes through cellular redistribution of FAT/CD36. *Diabetes.* 2002;51:3113-9.
3. Lisanti MP, Scherer PE, Vidugiriene J, Tang Z, Hermanowski-Vosatka A, Tu YH, Cook RF, Sargiacomo M. Characterization of caveolin-rich membrane domains isolated from an endothelial-rich source: implications for human disease. *J Cell Biol.* 1994;126:111-26.
4. Luiken JJ, Dyck DJ, Han XX, Tandon NN, Arumugam Y, Glatz JF, Bonen A. Insulin induces the translocation of the fatty acid transporter FAT/CD36 to the plasma membrane. *Am J Physiol Endocrinol Metab.* 2002;282:E491-5.
5. Muller H, Deckers K, Eckel J. The fatty acid translocase (FAT)/CD36 and the glucose transporter GLUT4 are localized in different cellular compartments in rat cardiac muscle. *Biochem Biophys Res Commun.* 2002;293:665-9.
6. Campbell SE, Tandon NN, Woldegiorgis G, Luiken JJ, Glatz JF, Bonen A. A novel function for FAT/CD36: Involvement in long chain fatty acid transfer into the mitochondria. *J Biol Chem.* 2004.
7. Luiken JJ, Coort SL, Willems J, Coumans WA, Bonen A, van der Vusse GJ, Glatz JF. Contraction-induced fatty acid translocase/CD36 translocation in rat

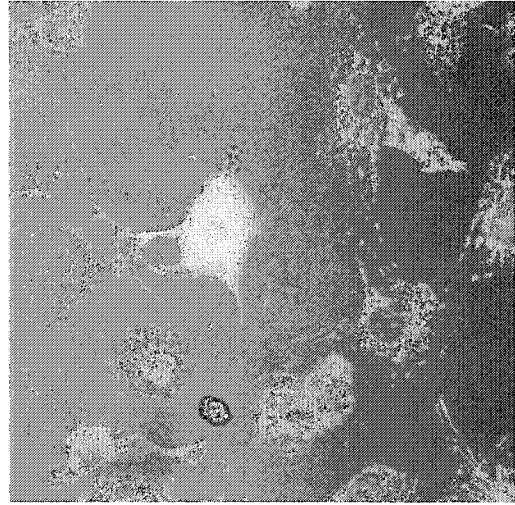
cardiac myocytes is mediated through AMP-activated protein kinase signaling. *Diabetes*. 2003;52:1627-34.

8. Gottlicher M, Widmark E, Li Q, Gustafsson JA. Fatty acids activate a chimera of the clofibric acid-activated receptor and the glucocorticoid receptor. *Proc Natl Acad Sci U S A*. 1992;89:4653-7.
9. Wolfrum C, Borrmann CM, Borchers T, Spener F. Fatty acids and hypolipidemic drugs regulate peroxisome proliferator-activated receptors alpha - and gamma-mediated gene expression via liver fatty acid binding protein: a signaling path to the nucleus. *Proc Natl Acad Sci U S A*. 2001;98:2323-8.

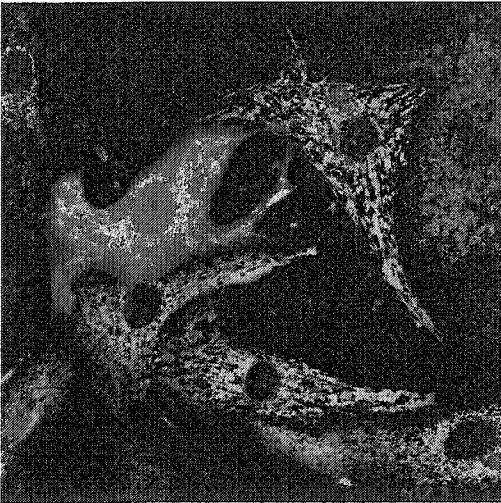
A



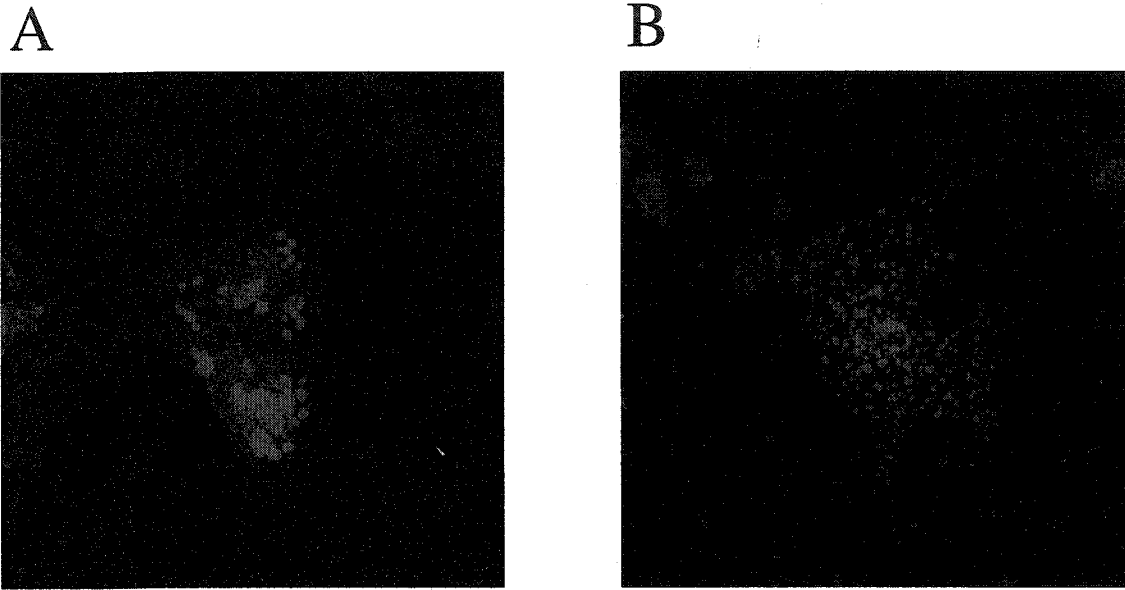
B



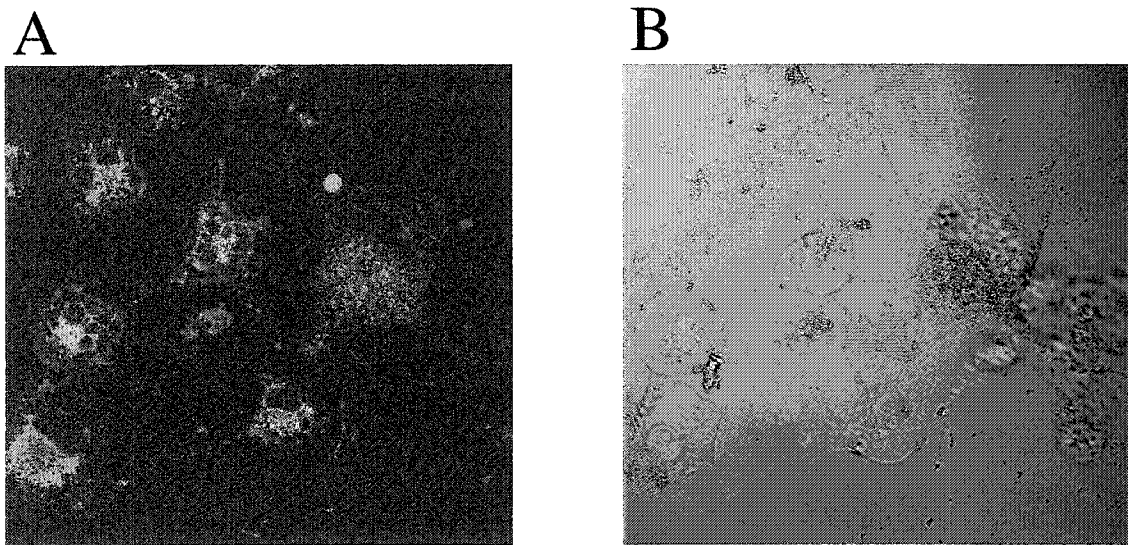
C



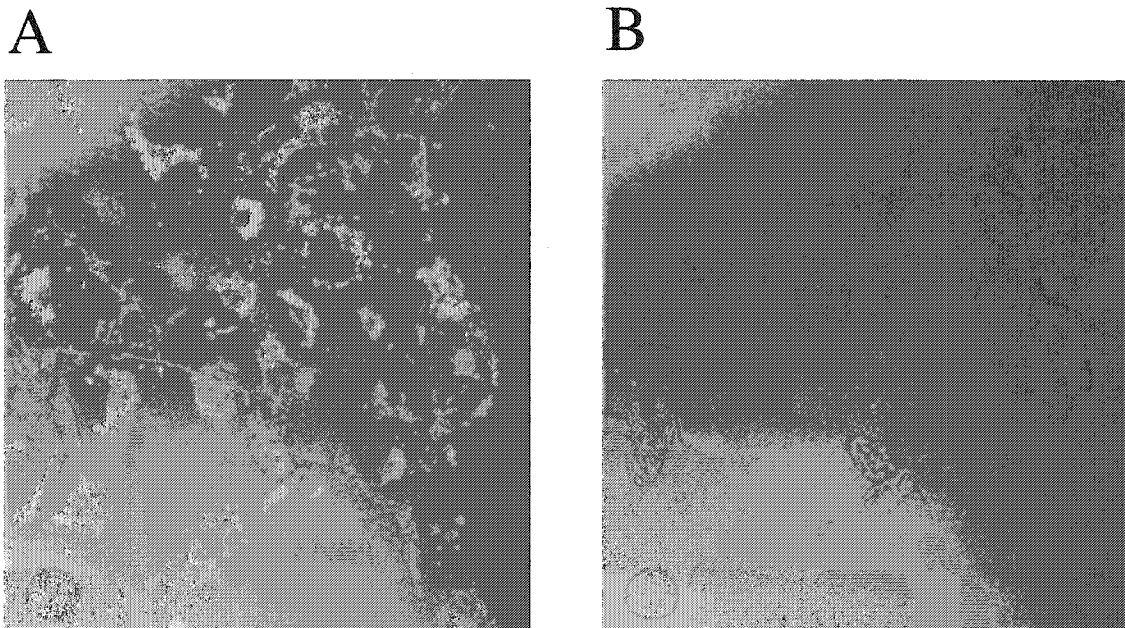
**Fig. 6-1. Confocal images of DsRed2 transfection in COS-7 and neonatal rat cardiac myocytes.** The DsRed2 vector was transfected COS-7 cells (A,B) and neonatal rat cardiac myocytes. Cells were then stained with MitoTracker Green FM dye, for 30 min and visualized. The 488 nm argon laser was used to excite the MitoTracker Green. n =1 for all experiments.



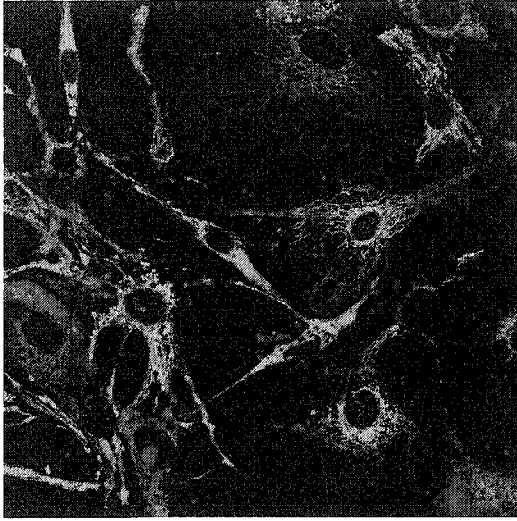
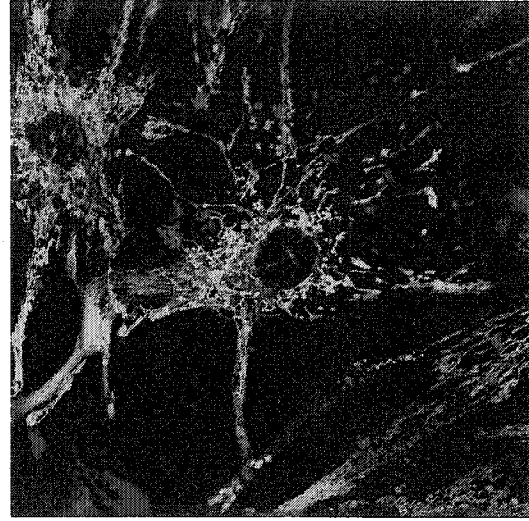
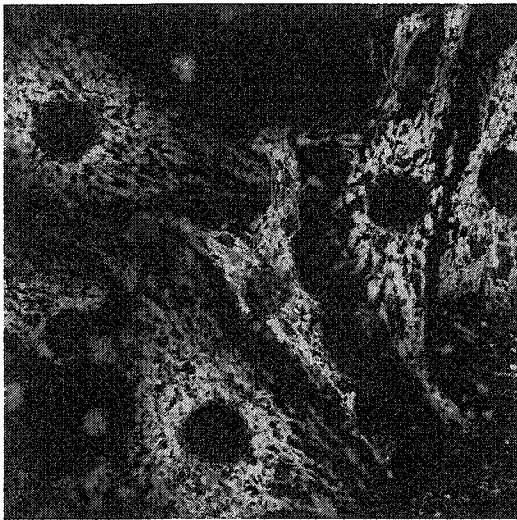
**Fig. 6-2. Confocal images of FAT/CD36-DsRed2 transfection in COS-7 and neonatal rat cardiac myocytes.** The FAT/CD36-DsRed2 plasmid was transfected into COS-7 cells (A) and neonatal rat cardiac myocytes (B). The 488 nm argon laser was used to excite the DsRed2 fluorophore. n =1 for all experiments.



**Fig. 6-3. Confocal images of FAT/CD36-DsRed2 transfection in COS-7 Cells and FAT/CD36 translocation.** The FAT/CD36-DsRed2 plasmid was transfected into COS-7 cells and allowed to express for 48 hours. Cells were subsequently treated with 1 nM insulin for 20 min. Cells were then stained with MitoTracker Green FM dye for 30 min and visualized. The 488 nm argon laser was used to excite the DsRed2 fluorophore and the 543 HeNe laser was used to excite the MitoTracker Green. Confocal images were taken at time zero, before insulin addition (A) and 20 min after insulin addition, which is shown in phase contrast (B). n =1 for all experiments.

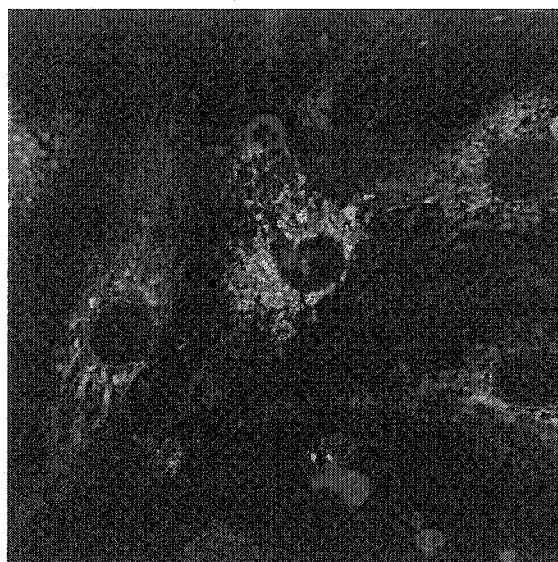


**Fig. 6-4. Confocal images of FAT/CD36-DsRed2 transfection in neonatal rat cardiac myocytes and FAT/CD36 translocation.** The FAT/CD36-DsRed2 plasmid was transfected into cardiac myocytes and allowed to express for 48 hours. Cells were subsequently treated with 1 mM AICAR for 30 min. Cells were then stained with MitoTracker Green FM dye for 30 min and visualized. The 488 nm argon laser was used to excite the DsRed2 fluorophore and the 543 HeNe laser was used to excite the MitoTracker Green. Confocal images were taken at time 30 min (A) and in phase contrast (B). n =1 for all experiments.

**A****B****C**

**Fig. 6-5. Confocal images of FAT/CD36-DsRed2 transfection in neonatal rat cardiac myocytes stained with MitoTracker Green.** The FAT/CD36-DsRed2 plasmid was transfected into neonatal cardiac myocytes and allowed to express for 48 hours. Cells were subsequently stained with MitoTracker Green for 30 min (A,B,C). The 488 nm argon laser was used to excite the DsRed2 fluorophore and the 543 HeNe laser was used to excite the MitoTracker Green. n =1

A



B

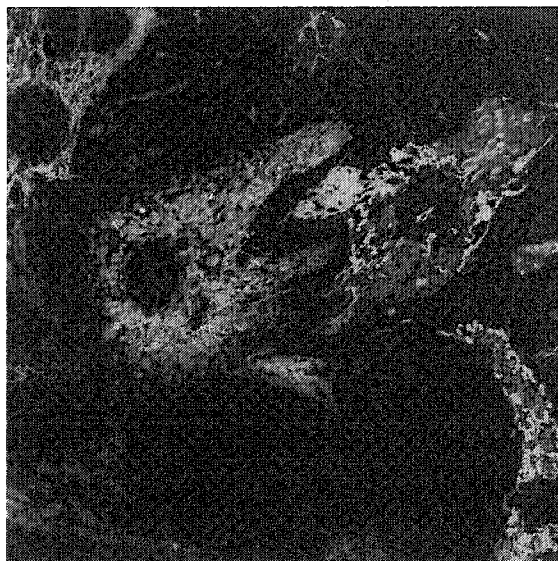


**Fig. 6-6. Confocal images of FAT/CD36-DsRed2 transfection in neonatal rat cardiac myocytes stained with MitoTracker Green.** The FAT/CD36-DsRed2 plasmid was transfected into neonatal cardiac myocytes and allowed to express for 48 hours. Cells were subsequently stained with MitoTracker Green for 30 min (A,B). The 488 nm argon laser was used to excite the DsRed2 fluorophore and the 543 HeNe laser was used to excite the MitoTracker Green. n = 1 for all experiments.

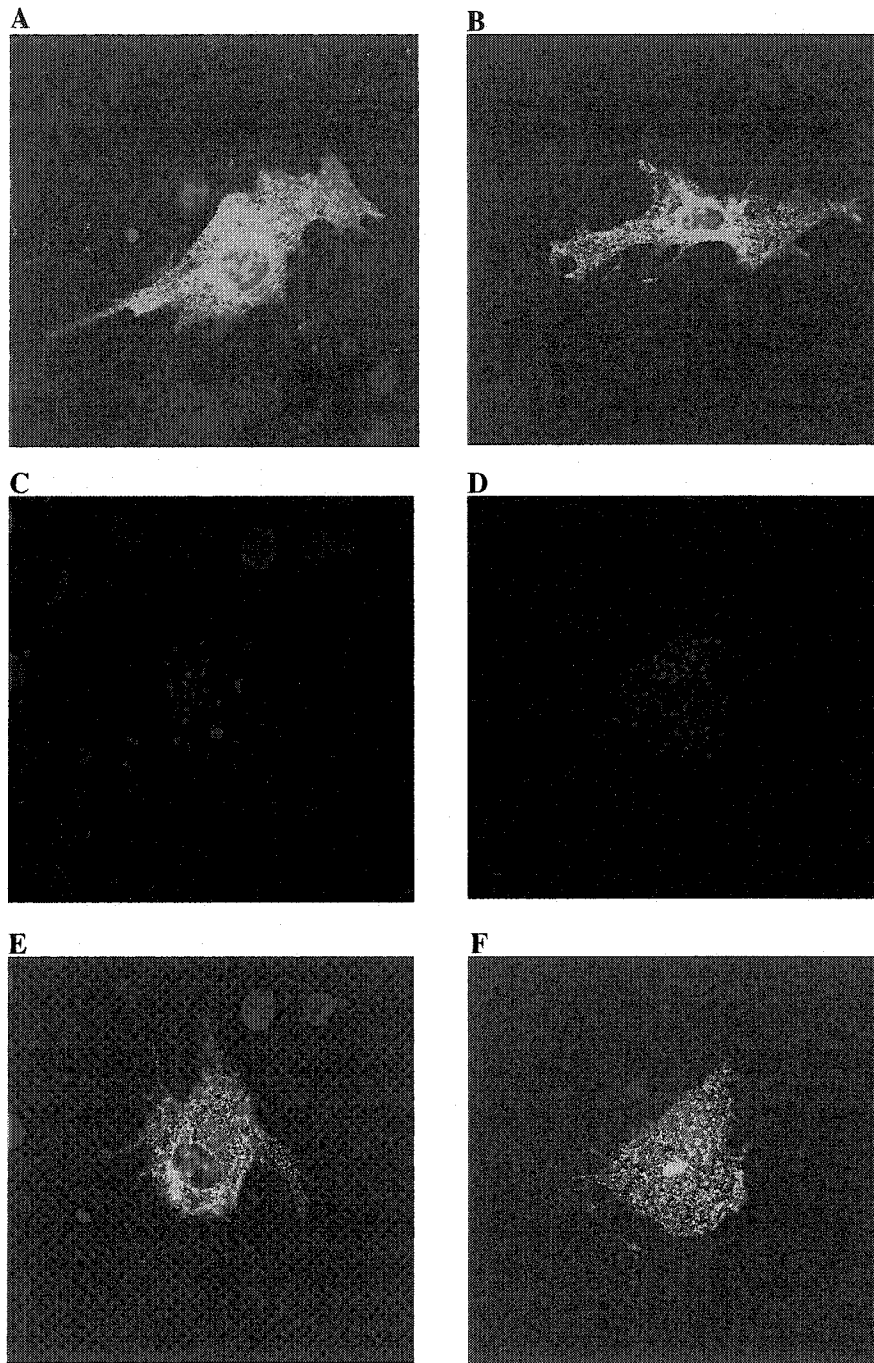


**Fig. 6-7. Confocal images of FAT/CD36-DsRed2 and GLUT4-GFP transfection in neonatal rat cardiac myocytes.** The GLUT4-GFP and FAT/CD36-DsRed2 expression plasmids were transfected into neonatal cardiac myocytes and allowed to express for 48 hours. Cells expressing GLUT4 are shown in (A,B). Cells expressing FAT/CD36-DsRed2 fusion proteins are shown in (C,D). Cells from (C,D) coexpressing GLUT4 and FAT/CD36-DsRed2 fusion proteins are shown in (E,F). The 488 nm argon laser was used to excite the DsRed2 fluorophore and the 543 HeNe laser was used to excite the GFP fluorophore. n =1 for all experiments.

## **Chapter 7**

### **Conclusions and Future Directions**

In this thesis, evidence has been presented to suggest that FAT/CD36 is an important regulator of fatty acid oxidation in the heart. Although several studies have examined the effect of FAT/CD36 deficiency on lipid metabolism in skeletal muscle and isolated cell lines, the effect of FAT/CD36 deficiency on fatty acid oxidation in the intact heart was unknown. Our studies conducted on the isolated perfused mouse heart showed that FAT/CD36 deficiency results in significantly lower rates of fatty acid oxidation, which is compensated for by an increase in glucose oxidation. Due to this increase in glucose oxidation, FAT/CD36 deficient hearts were not energetically compromised, as previously suggested<sup>1</sup>. Since the FAT/CD36 deficient heart exhibits an increase in glucose oxidation, it would be interesting to examine whether rates of glucose uptake are correspondingly increased. Moreover, the activities and expression of GLUT 1 and GLUT 4 at the plasma membrane remains unknown. The FAT/CD36 deficient mouse heart also exhibited similar levels of cardiac function before and after ischemia as compared to the wildtype heart. Therefore, the current study demonstrates that FAT/CD36 deficiency does not result in energetically or functionally compromised hearts, as was previously proposed<sup>1</sup>.

Since rates of glucose oxidation are significantly enhanced in the FAT/CD36 deficient hearts and rates of fatty acid oxidation are significantly decreased, it would be expected that these hearts would recover better than wildtype hearts. As shown by the perfusion data, this is not the case. Therefore we also sought to elucidate the cause of this discrepancy. The current study demonstrates that there are alterations in signaling mechanisms in the FAT/CD36 deficient ischemic heart. Specifically, levels and/or activities of proteins involved in the AMPK-ACC-malonyl CoA axis are significantly

altered. We found that levels of P-AMPK, which is indicative of activity, are significantly enhanced in FAT/CD36 deficient hearts. Therefore, it is possible that the enhanced activity of AMPK increases glycolytic rates in the FAT/CD36 deficient hearts during reperfusion. This would negate the beneficial effect of increased rates of glucose oxidation by further uncoupling glycolysis from glucose oxidation, resulting in proton accumulation and poor functional recovery. Although this may be a potential rationale for the poorer than expected functional recovery of the knockout hearts, this must be examined further.

One study that could be conducted would be to perfuse FAT/CD36 deficient and wildtype hearts and measure rates of glycolysis to confirm that rates of glycolysis are elevated in the knockout hearts. Another study that could be conducted would be to subject FAT/CD36 deficient and wildtype hearts to ischemia/reperfusion in the presence or absence of cyclohexyladenosine (CHA), which has been shown to inhibit glycolysis in the perfused heart<sup>2</sup>. If the FAT/CD36 deficient hearts exhibit higher rates of glycolysis, CHA would improve the coupling between glycolysis and glucose oxidation and improve functional recovery during reperfusion.

Another reason why contractile recovery of ischemic FAT/CD36 KO is lower than expected, is that there could also be other signaling mechanisms in the FAT/CD36 deficient heart. FAT/CD36 is a surface receptor and is involved in intracellular signaling (see <sup>3</sup> for review). Therefore a null mutation in FAT/CD36 could lead to an alteration and/or aberration in intracellular signaling, which could have a negative impact on the heart. Currently, there are only a limited number of studies examining the signaling pathways to which FAT/CD36 is involved. It has been shown that scavenger receptor

type B1 is involved in activation of the mitogen-activated protein kinase (MAPK) pathway<sup>4</sup> and p38 MAPK activation has been shown to be detrimental to recovery of the ischemic heart<sup>5</sup>. Therefore, the FAT/CD36 deficient heart could also exhibit alterations in the MAPK signaling pathway, which could alter cardiovascular function. Currently, the role of FAT/CD36 in the activation of MAPKs is unknown.

The current study also demonstrates that FAT/CD36 expression, by itself, is not sufficient to increase rates of fatty acid transport and oxidation. However, the overexpression of FACS and FAT/CD36 resulted in a significant increase in fatty acid metabolism in neonatal rat cardiac myocytes. This suggests that FAT/CD36 does not function as a lone entity to transport fatty acids across the membrane, but works in cooperation with other proteins, such as FACS, to increase fatty acid uptake in the myocyte. It has been suggested by other studies that FAT/CD36 and FACS work in coordination<sup>6</sup>, but this is the first report that presents functional data which demonstrates cooperation. Other studies that must be conducted to elucidate further the function of FAT/CD36 would be the expression of combinations of FAT/CD36, FACS, FATP and H-FABP in cardiac myocytes. This would determine whether FAT/CD36 works in cooperation with these proposed fatty acid transport proteins. Also, these coexpression studies would demonstrate whether FAT/CD36 has a preference for either FACS or H-FABP in maintaining a fatty acid concentration gradient across the sarcolemmal membrane.

Taken together, the research presented in this thesis demonstrates that FAT/CD36 is important in fatty acid metabolism and may be rate limiting for fatty acid oxidation. Moreover, FAT/CD36 deficiency also leads to alterations in signaling within the AMPK-

ACC-malonyl CoA axis. This suggests that the FAT/CD36 KO mouse attempts to compensate for the decrease in fatty acid oxidation, but the limited uptake of fatty acids lowers the expression of MCD, thereby eliminating a potential compensatory effect. Also, FAT/CD36 may work in cooperation with other proteins involved in fatty acid uptake into the cardiac myocytes. Finally, the study provides advances towards a new cellular model that can be used to examine the regulation of FAT/CD36. The DsRed2-FAT/CD36 fusion protein, if found to be functional, could be a very useful tool in order to examine translocation and colocalization. Although the current study sheds some light on the role and regulation of FAT/CD36, more research must be conducted in order to further examine FAT/CD36.

## References

1. Irie H, Krukenkamp IB, Brinkmann JF, Gaudette GR, Saltman AE, Jou W, Glatz JF, Abumrad NA, Ibrahimi A. Myocardial recovery from ischemia is impaired in CD36-null mice and restored by myocyte CD36 expression or medium-chain fatty acids. *Proc Natl Acad Sci U S A*. 2003;100:6819-24.
2. Fraser H, Lopaschuk GD, Clanachan AS. Alteration of glycogen and glucose metabolism in ischaemic and post-ischaemic working rat hearts by adenosine A1 receptor stimulation. *Br J Pharmacol*. 1999;128:197-205.
3. Husemann J, Loike JD, Anankov R, Febbraio M, Silverstein SC. Scavenger receptors in neurobiology and neuropathology: their role on microglia and other cells of the nervous system. *Glia*. 2002;40:195-205.
4. Grewal T, de Diego I, Kirchhoff MF, Tebar F, Heeren J, Rinninger F, Enrich C. High density lipoprotein-induced signaling of the MAPK pathway involves scavenger receptor type BI-mediated activation of Ras. *J Biol Chem*. 2003;278:16478-81.
5. Clanachan AS, Jaswal JS, Gandhi M, Bottorff DA, Coughlin J, Finegan BA, Stone JC. Effects of inhibition of myocardial extracellular-responsive kinase and P38 mitogen-activated protein kinase on mechanical function of rat hearts after prolonged hypothermic ischemia. *Transplantation*. 2003;75:173-80.
6. Luiken JJ, Han XX, Dyck DJ, Bonen A. Coordinately regulated expression of FAT/CD36 and FACS1 in rat skeletal muscle. *Mol Cell Biochem*. 2001;223:61-9.